

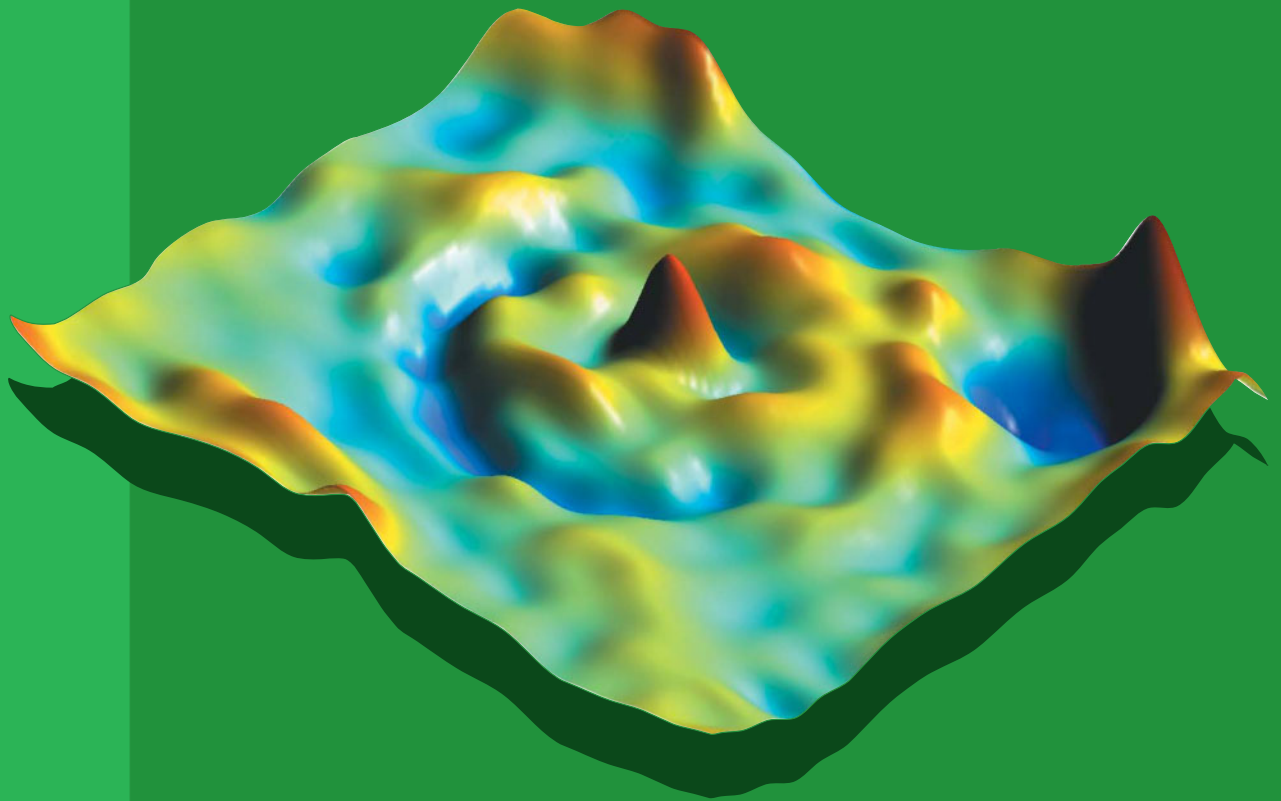
**REPORT  
79**



**GOVERNMENT OF  
WESTERN AUSTRALIA**

# **THE GEOPHYSICAL INTERPRETATION OF THE WOODLEIGH IMPACT STRUCTURE SOUTHERN CARNARVON BASIN WESTERN AUSTRALIA**

**by R. P. Iasky, A. J. Mory, and K. A. Blundell**



**GEOLOGICAL SURVEY OF WESTERN AUSTRALIA**



**DEPARTMENT OF MINERALS AND ENERGY**



**GEOLOGICAL SURVEY OF WESTERN AUSTRALIA**

**REPORT 79**

**THE GEOPHYSICAL INTERPRETATION OF  
THE WOODLEIGH IMPACT STRUCTURE,  
SOUTHERN CARNARVON BASIN,  
WESTERN AUSTRALIA**

by  
**R. P. Iasky, A. J. Mory, and K. A. Blundell**

**Perth 2001**

**MINISTER FOR STATE DEVELOPMENT; TOURISM;  
SMALL BUSINESS; GOLDFIELDS–ESPERANCE  
The Hon. Clive Brown MLA**

**DIRECTOR GENERAL  
L. C. Ranford**

**DIRECTOR, GEOLOGICAL SURVEY OF WESTERN AUSTRALIA  
Tim Griffin**

**Copy editor: D. P. Reddy**

**REFERENCE**

**The recommended reference for this publication is:**

IASKY, R. P., MORY, A. J., and BLUNDELL, K. A., 2001, The geophysical interpretation of the Woodleigh impact structure, Southern Carnarvon Basin, Western Australia: Western Australia Geological Survey, Report 79, 41p.

**National Library of Australia  
Cataloguing-in-publication entry**

Iasky, R. P. (Robert Paul), 1956–  
The geophysical interpretation of the Woodleigh impact structure, Southern Carnarvon Basin, Western Australia

**Bibliography.**

**ISBN 0 7307 5680 7**

1. Geomorphology — Western Australia — Carnarvon Basin.
2. Seismic reflection method.
3. Seismic prospecting — Western Australia — Carnarvon Basin.
  - I. Mory, A. J. (Arthur John), 1953–.
  - II. Blundell, K. A. (Kelvin Ashley), 1966–.
  - III. Geological Survey of Western Australia.
  - IV. Title. (Series: Report (Geological Survey of Western Australia); 79).

622.153099413

**ISSN 0508–4741**

Printed by Haymarket, Perth, Western Australia

**Copies available from:  
Information Centre  
Department of Minerals and Energy  
100 Plain Street  
EAST PERTH, WESTERN AUSTRALIA 6004  
Telephone: (08) 9222 3459 Facsimile: (08) 9222 3444  
www.dme.wa.gov.au**

**Cover photograph:**

**Oblique view from the southwest of the first vertical derivative of the Bouguer gravity for the Woodleigh area.**

## Contents

Abstract .....	1
Introduction .....	1
History of investigation .....	3
Previous exploration .....	3
GSWA studies .....	4
Geomorphology .....	4
Regional geology and stratigraphy .....	5
Ordovician succession .....	7
Silurian succession .....	10
Lower Devonian succession .....	10
Middle–Upper Devonian succession .....	11
Carboniferous to Triassic succession .....	11
Jurassic succession .....	11
Cretaceous and Tertiary succession .....	11
Age of the impact .....	12
Geophysics .....	14
Gravity surveys .....	14
Gravity modelling .....	16
Magnetic surveys .....	24
Airborne magnetic surveys .....	24
Ground magnetic surveys .....	24
Magnetic modelling .....	26
Seismic interpretation .....	30
Discussion .....	34
Conclusions .....	35
Acknowledgements .....	37
References .....	38

## Appendices

1. Summary of wells and bores that penetrated below the Cretaceous horizon in the Woodleigh area .....	40
2. Acquisition and processing of ground magnetic data .....	41

## Plate

1. Geophysical profiles across the Woodleigh impact structure (digital file only)

## Figures

1. Location of the Woodleigh impact structure in the Southern Carnarvon Basin .....	2
2. Landsat image of the Woodleigh region .....	3
3. Gravity coverage for the Woodleigh impact structure .....	5
4. Digital elevation model of the Woodleigh region with superimposed drainage .....	6
5. Physiography and palaeodrainage of the Woodleigh region .....	7
6. Stratigraphy of the Southern Carnarvon Basin .....	8
7. Pre-Cretaceous geology of the Woodleigh area .....	9
8. Correlation of shallow stratigraphic horizons from Yaringa 1 to GSWA Woodleigh 1 .....	12
9. Location of seismic lines, bores, and wells within the Woodleigh impact structure .....	13
10. Potential-field images of selected Australian impact structures .....	14
11. Bouguer gravity image of the Southern Carnarvon Basin .....	16
12. Bouguer gravity image of the Woodleigh impact structure, showing northwest–southwest gravity profile .....	17
13. Image of first vertical derivative of Bouguer gravity over the Woodleigh impact structure .....	18
14. Comparison of potential-field signature of the Woodleigh and Gosses Bluff impact structures .....	19
15. East–west two-dimensional gravity model and cross section of the Woodleigh impact structure .....	20
16. North–south two-dimensional gravity model and cross section of the Woodleigh impact structure .....	21

17. Northwest–southeast two-dimensional gravity model and cross section of the Woodleigh impact structure .....	22
18. Total magnetic intensity image of the Southern Carnarvon Basin .....	24
19. Total magnetic intensity image of the Woodleigh impact structure .....	25
20. Drainage pattern superimposed on a grey-scale total magnetic intensity image of the Woodleigh impact structure .....	26
21. Image of the reconnaissance ground magnetic data over the centre of the Woodleigh impact structure .....	27
22. Regional ground magnetic traverse and magnetic model of the centre of the Woodleigh impact structure .....	28
23. Magnetic model of arcuate anomaly on the eastern margin of the Woodleigh impact structure .....	28
24. Magnetic model for a central magnetic dipole anomaly of the Woodleigh impact structure .....	29
25. East–west seismic section (line YY65T-014) across the northwestern margin of the Woodleigh impact structure .....	31
26. North–south seismic section (line W65G-002) across the northern half of the Woodleigh impact structure .....	32
27. East–west seismic section (lines W65G-003, and W65T-003) across the Woodleigh impact structure .....	33
28. East–west seismic section (line YY65T-015) in the western part of the Woodleigh impact structure .....	34
29. Evolution of the Woodleigh impact structure .....	36

## Tables

1. Log-derived densities (in g/cm <sup>3</sup> ) from wells in the southern Gascoyne Platform .....	10
2. Density measurements of cores from GSWA Woodleigh 1 and 2A .....	23

# The geophysical interpretation of the Woodleigh impact structure, Southern Carnarvon Basin, Western Australia

by

R. P. Iasky, A. J. Mory, and K. A. Blundell

## Abstract

The diameter of the Woodleigh impact structure within the Gascoyne Platform, on the Southern Carnarvon Basin in Western Australia, is estimated at 120 km from gravity and magnetic data, making it the largest impact structure discovered on the Australian continent. The structure has its centre at 26°03'25"S and 114°39'50"E, about 50 km east of Hamelin Pool. The structure is evident only from geophysical data because it is buried by up to 600 m of Jurassic–Tertiary sedimentary rock. The age of the impact is best constrained between the Middle Devonian and Early Jurassic by the regional stratigraphy.

Gravity data indicate a multi-ring feature with an inner ring anomaly about 25 km in diameter, which is interpreted as the central uplift of a complex impact structure. There is good coincidence between the concentric annular gravity lows and highs and the troughs and ridges on seismic data. The outermost diameter corresponds to the abrupt truncation of the northerly trending Wandagee and Ajana Ridges. The eastern margin of the structure is defined by an arcuate magnetic anomaly, coincident with a drainage divide, implying recent reactivation along a bounding ring fault. The southeast–northwest asymmetry of gravity anomalies within the structure is interpreted as the combined effect of different rock types within the impact site and post-impact tectonism during the Early Cretaceous. The latter reactivated faults along the Wandagee–Ajana Ridges, producing a regional tilt to the northwest and probably allowing the southeastern side of the structure to be eroded.

A ground magnetic survey over the centre of the structure detected a magnetic dipole anomaly sourced from a shallow part of the central uplift. Modelling of this anomaly is too poorly constrained to provide an independent age for the structure. Seismic data show intense deformation up to 25 km from the centre and only minor deformation to the outer rim — a pattern of deformation consistent with other impact structures in which the inner third to one half has undergone intense deformation.

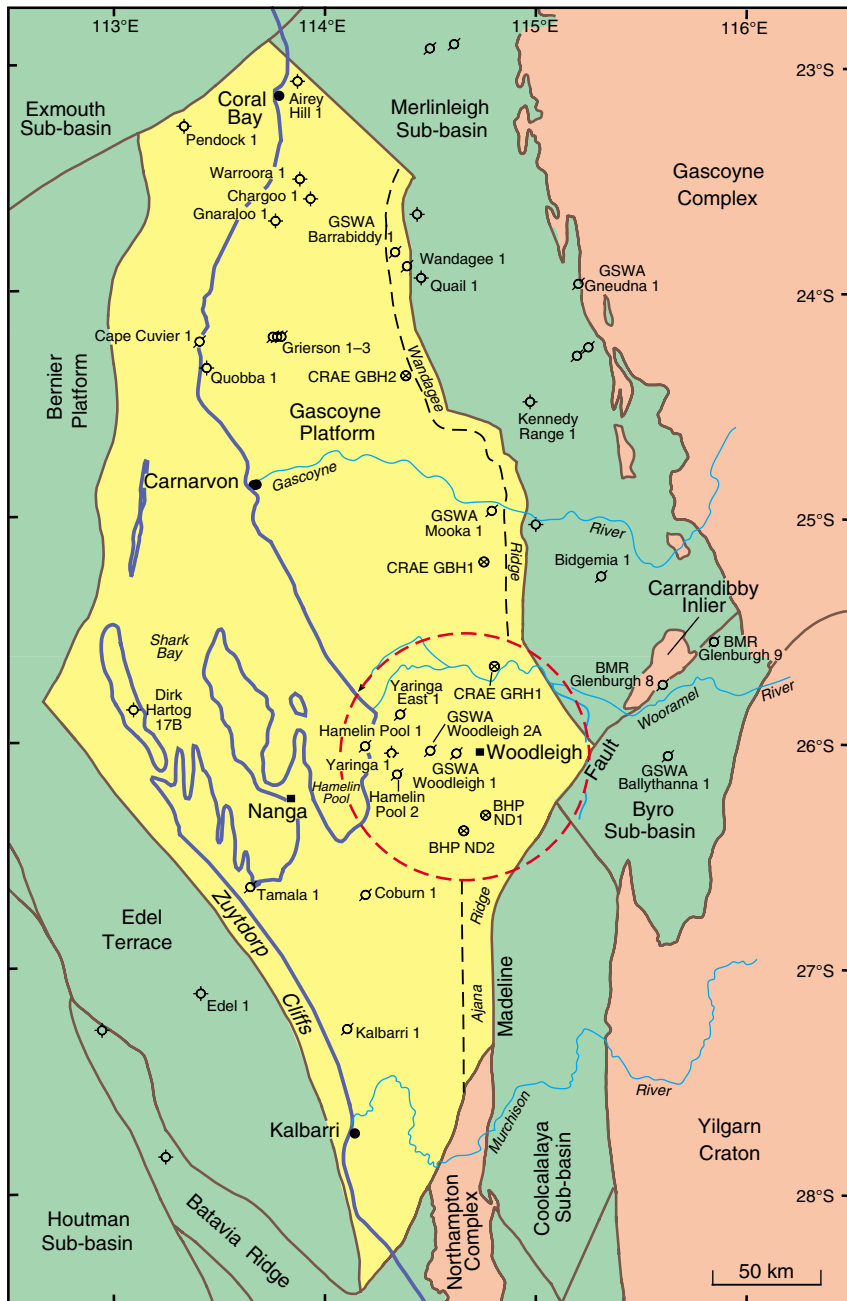
**KEYWORDS:** impact structures, gravity, magnetic anomalies, seismic reflection surveys, remanent magnetism, palaeomagnetism, magnetic susceptibility, density.

## Introduction

The Woodleigh impact structure is a recently discovered, buried, multi-ring feature on the Gascoyne Platform of the Southern Carnarvon Basin, Western Australia (Mory et al., 2000). The centre of the structure is at latitude 26°03'25"S, longitude 114°39'50"E, on Woodleigh Station (after which it is named), approximately 160 km south-southeast of Carnarvon and about 50 km east of Hamelin Pool (Fig. 1). The impact origin of the structure is demonstrated by shock-metamorphic features in core samples of granitoid basement from drillhole GSWA Woodleigh 1 at the centre of the structure (Mory et al., 2000). These features include shock-induced planar

deformation features (PDFs) in quartz, feldspar, and zircon, together with pervasive diaplectic vitrification of feldspar and penetrative pseudotachylite veining. This aspect of the structure is not discussed further in this Report, but is covered in more detail by Glikson et al. (in prep.) and Mory et al. (in prep.). The Woodleigh impact structure is not obvious from the present-day landscape (Fig. 2) and was identified from geophysical data.

Although there has been little exploration in the Woodleigh area compared to other parts of the Southern Carnarvon Basin, there are sufficient geophysical and well data for a preliminary interpretation of the structure. This Report focuses mainly on the interpretation of the



RPI157a

05.06.01

- ◇ Petroleum exploration well, dry
- ⊙ Stratigraphic well
- ⊗ Mineral exploration drillhole
- Town
- Homestead
- 2 Australian impact structure mentioned in text

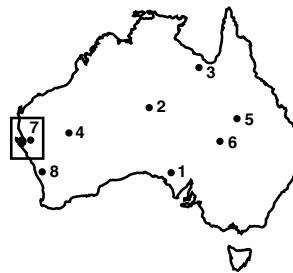


**Figure 1.** Tectonic subdivisions of the Southern Carnarvon Basin and location of the Woodleigh impact structure. Also shown is the distribution of drillholes. Australian impact structures referred to in the text are labelled as: 1 — Acraman (Gawler Craton, South Australia); 2 — Gosses Bluff (Amadeus Basin, Northern Territory); 3 — Lawn Hill (Lawn Hill Platform, Queensland); 4 — Shoemaker (Earaheedy Basin, Western Australia); 5 — Talundilly (Eromanga Basin, Queensland); 6 — Tookanooka (Eromanga Basin, Queensland); 7 — Woodleigh (Southern Carnarvon Basin, Western Australia); and 8 — Yallalie (Perth Basin, Western Australia)

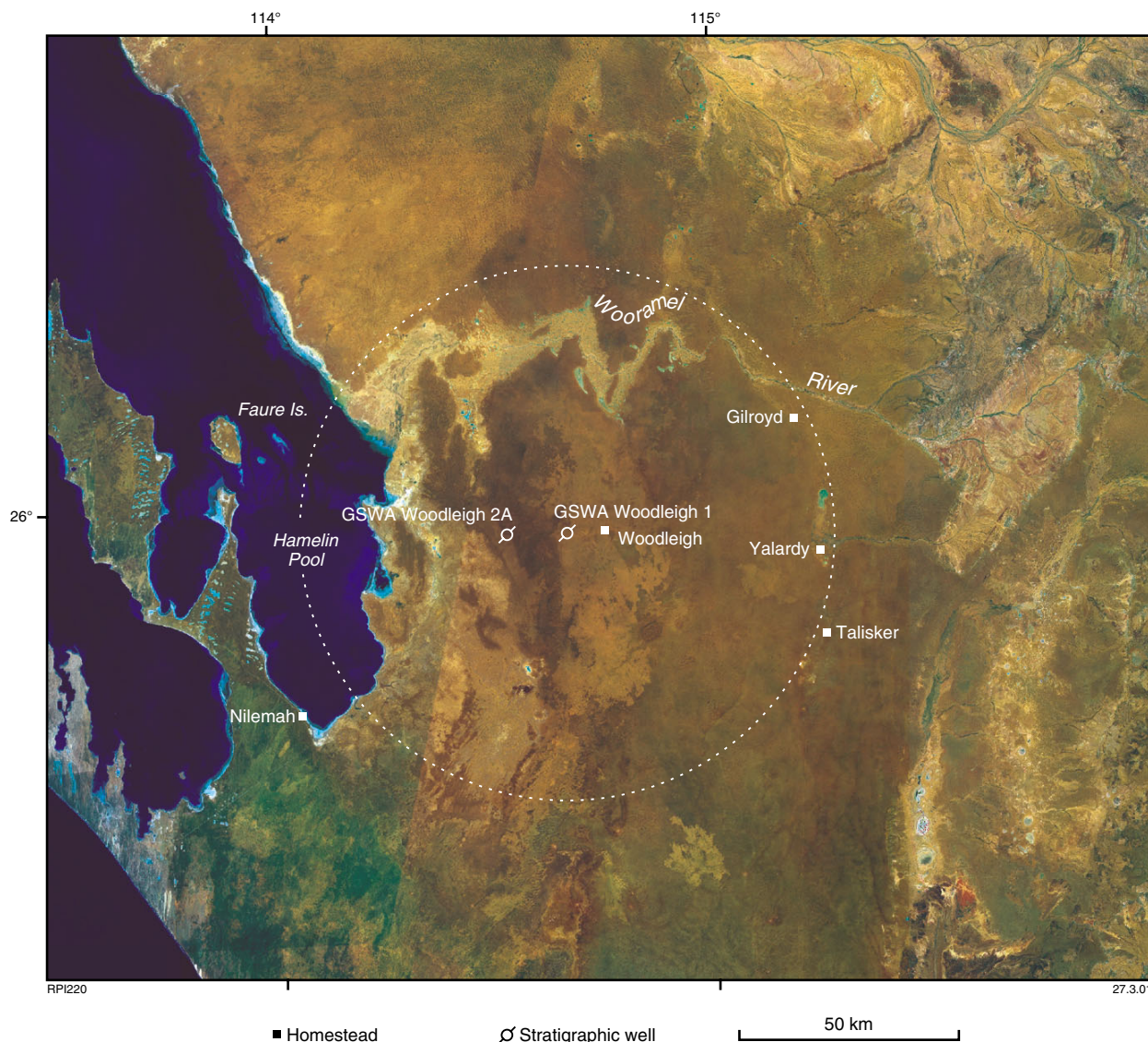


**Figure 2. Landsat image of the Woodleigh region, showing the lack of surface expression of the Woodleigh impact structure**

gravity, magnetic, and seismic data to determine the morphology of the structure. The geophysical modelling is constrained by well data, summarized in **Regional geology and stratigraphy**. More complete details of drillholes GSWA Woodleigh 1 and 2A are provided by Mory et al. (in prep.).

## History of investigation

### Previous exploration

The oldest data within the Woodleigh impact structure are from shallow water bores drilled across the Gascoyne Platform as early as 1902 (Playford and Chase, 1955), from which the Lower Jurassic Woodleigh Formation was defined (McWhae et al., 1958).

Between 1956 and 1959, the Bureau of Mineral Resources (BMR, now the Australian Geological Survey

Organisation — AGSO) conducted regional airborne magnetic and radiometric surveys over the Gascoyne Platform, including the Woodleigh area. In the late 1960s, BMR also carried out regional helicopter-assisted gravity surveys over most of the Southern Carnarvon Basin. Continental Oil Company (Conoco) carried out a regional seismic survey of the Woodleigh area in 1965 and drilled Yaringa 1 in 1966, 30 km west of the centre of the Woodleigh impact structure (Fig. 1). In 1968, Magellan Petroleum drilled Hamelin Pool 1 and 2, about 45 and 32 km west of the centre of the Woodleigh impact structure respectively (Fig. 1), to evaluate evaporite rocks and the petroleum potential of the Dirk Hartog Group. Regional seismic and gravity surveys conducted by West Australian Petroleum Pty Ltd (WAPET), Conoco, and Oceania Ventures Pty Ltd in the early 1970s covered the Woodleigh impact structure.

In the late 1970s to early 1980s the main exploration target in the region were Permian coal measures. During



this period, CRA Exploration (CRAE) and Utah Development focused on the Merlinleigh, Byro, and Coolcalalaya Sub-basins, but also tested the eastern margin of the Gascoyne Platform. At the same time, Eagle Corporation was exploring for petroleum on the Gascoyne Platform. The company postulated the 'Woodleigh Graben' (on the western side of the Woodleigh impact structure as defined here) based on gravity data and the presence of Jurassic sedimentary rocks in several water bores, as well as poor-quality seismic data recorded by Conoco in 1965. Upon discovering the prominent circular gravity anomaly at the centre of the Woodleigh impact structure, the company diverted its attention from petroleum to mineral exploration and drilled two holes over this anomaly to test for mineralization within Silurian carbonates and possible shallow Permian coal (Layton and Associates, 1981). The second of these drillholes, Woodleigh 1981/2, penetrated shallow granitic rocks at 171 m, immediately below Cretaceous cover. The petrographic report on granite cuttings samples identified unusual fine deformation lamellae in the quartz, which were interpreted as a possible result of the drill action (Layton and Associates, 1981, appendix 3). A further hole (Woodleigh 1982/1), drilled 37 km to the southeast in the following year, failed to find the desired Permian coal measures (Layton and Associates, 1982) and the company relinquished its tenements shortly thereafter.

BHP Minerals Pty Ltd resumed its interest in the region in the 1990s and drilled three holes for copper-lead mineralization (Edgar, 1994), two of which were within the Woodleigh impact structure. In 1997, Pace Petroleum drilled a stratigraphic well (Yaringa East 1) to investigate the petroleum potential of the region (Yasin and Mory, 1999b), at first not realizing the nature of the structure. In 1999, this hole was deepened by Britannia Gold in an unsuccessful attempt to find potash in the Silurian Yaringa Formation.

## GSWA studies

An impact origin for the Woodleigh structure was first postulated in late 1997 while modelling gravity data for a Geological Survey of Western Australia (GSWA) review of the Gascoyne Platform, although the structure was first thought to be about 18 km across (Iasky et al., 1998b; Iasky and Mory, 1999). Image processing of existing data clearly shows the circular nature of the gravity anomaly (Fig. 3). Only the central gravity peak can be identified on older gravity contour maps. Initial modelling of an east-west gravity traverse across the structure showed that the granite in Woodleigh 1981/2 (Layton and Associates, 1981) had lower density than the average crystalline basement ( $2.67 \text{ g/cm}^3$ ). This prompted the reinterpretation of the unusual deformation in the granite, illustrated in photomicrographs of cuttings samples in the well completion report (Layton and Associates, 1981), as PDFs typical of shock metamorphism. Unfortunately, the original cutting samples and thin sections from Woodleigh 1981/2 could not be located, and GSWA deepened the original hole in March 1999 (GSWA Woodleigh 1) to test the impact hypothesis. The new drillcore samples show

extremely well preserved shock-metamorphic features, including thin veins of melted glass (pseudotachylite), breccia, and PDFs, thereby providing clear evidence of an impact origin for the structure (Mory et al., 2000). Immediately following the completion of the first drillhole, GSWA Woodleigh 2 and 2A were drilled 14 km to the west to investigate the crater fill and underlying section. At the same time, GSWA staff recorded 600 new gravity stations to fill gaps in the existing gravity coverage (coloured red in Figure 3) and improve the resolution of the images. In addition, five short ground magnetic traverses (4 to 13 km in length) were recorded across the centre of the structure in an attempt to locate a central magnetic anomaly not resolved by the 1956–1959 BMR aeromagnetic data.

## Geomorphology

The region is characterized by subdued topography (Figs 4 and 5), with the most obvious features being areas of sandplain, low-lying Cretaceous–Cainozoic outcrop, thin duricrust, and Quaternary coastal sediments along the edge of Shark Bay and the Wooramel River. Although the Woodleigh impact structure and the overlying Jurassic strata are buried beneath 50–200 m of flat-lying Cretaceous and younger sediments, there are a few subtle arcuate drainage patterns about 60 km from the centre of the structure (Fig. 4). These drainage features are all unnamed and, apart from those to the northwest and the claypans associated with the eastern drainage, have previously been depicted only on the WOORAMEL\* and YARINGA 1:250 000 geological maps (Denman et al., 1985; van de Graaff et al., 1983). The best defined drainage feature extends in an  $83^\circ$  arc relative to the centre of the structure, from a prominent bend of the Wooramel River south to near Talisker Homestead (Fig. 4). This drainage course runs via a series of claypans past the Gilroyd, Yalardy, and Talisker homesteads and, according to Denman et al. (1985, fig. 2), is the former course of the Wooramel River in the Pliocene or perhaps somewhat earlier (Fig. 5). A weakly defined drainage divide extends farther south from Talisker Homestead to cover a  $60^\circ$  arc, ending about due south of the centre of the structure. To the northwest, drainage channels along the contact of the Wooramel delta and Carnarvon coastal plain are distinctly parallel to the interpreted outer limit of the Woodleigh impact structure over an arc of about  $20^\circ$ . In total, these drainage features extend through an arc of  $160^\circ$  along the margin of the structure (see **Geophysical surveys**).

Another arcuate topographic feature centred approximately on GSWA Woodleigh 1 is the western shore of Hamelin Pool between Faure Island and the now abandoned Nilemah Homestead (extending along an arc of  $60^\circ$  measured from the centre of the structure; Figs 2 and 4). This feature extends onshore at the western edge of a topographically low region, which probably marks the limit of a brief marine transgression in the Holocene (Fig. 4). A duricrust terrain (Carbla Plateau of

\* Capitalized names refer to standard 1:250 000 map sheets.

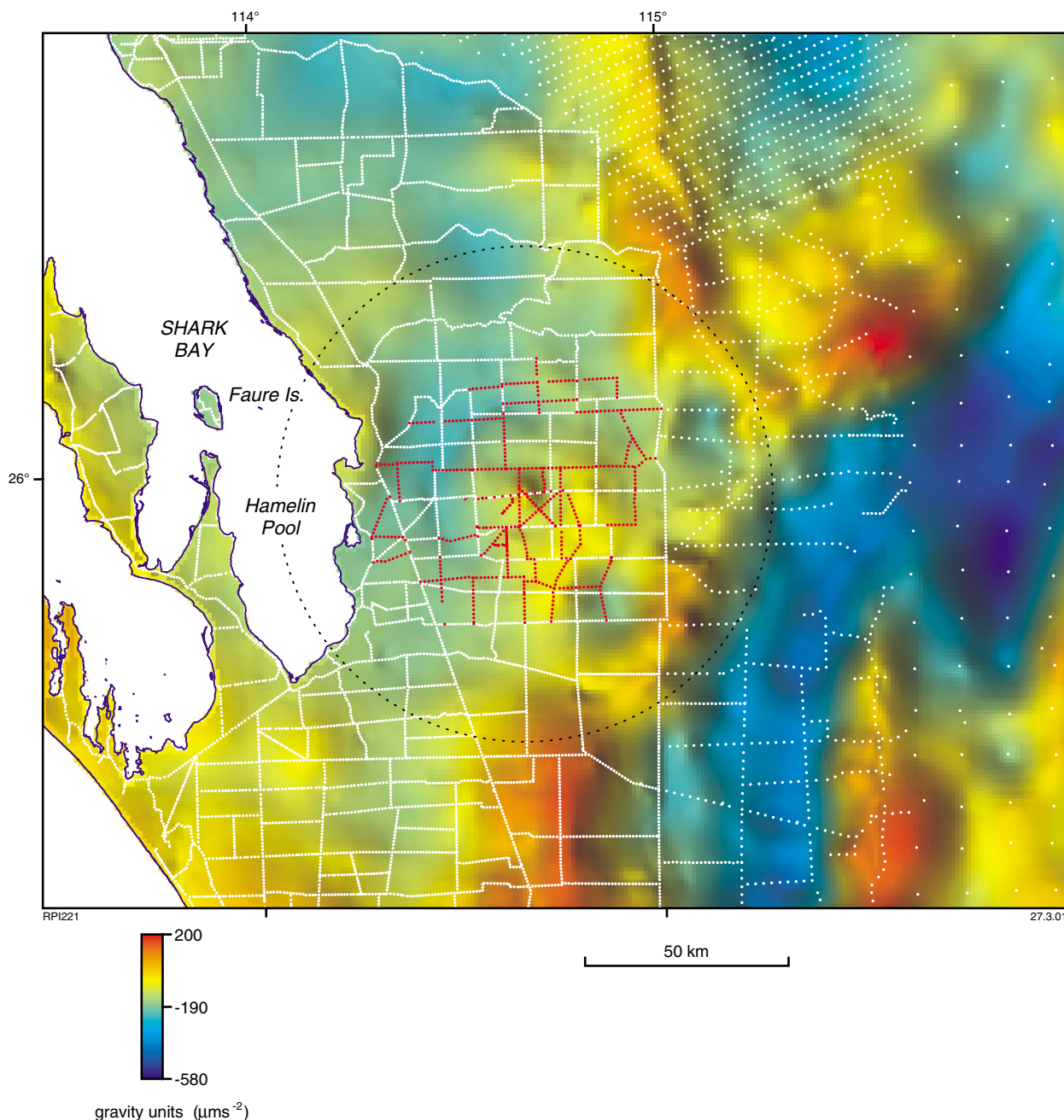


**Figure 3. Gravity coverage for the Woodleigh impact structure, displayed over a Bouguer gravity image. White stations represent pre-1999 data and red stations show the 1999 GSWA infill survey**

van de Graaff et al., 1983; Denman et al., 1983; Fig. 5) covers the relatively elevated parts of this topographic low. Another distinct topographic feature evident in Figure 4 is a series of low north-northeasterly and northerly oriented scarps in the more elevated region east of the Carbla Plateau.

The most obvious linear feature aligned with the centre of the structure is the westerly directed creek that debouches into the claypan next to Yalardy Homestead. In addition, the north-northeasterly oriented playa deposits associated with a prominent bend in the Wooramel River (Fig. 2), and possibly the southeasternmost shore of Hamelin Pool (Figs 2 and 4), are aligned with the centre of the structure.

## Regional geology and stratigraphy

The Woodleigh impact structure is in the southern part of the Gascoyne Platform, where deformed Ordovician to Upper Devonian strata underlie a local, flat-lying, Lower Jurassic lacustrine succession (Woodleigh Formation) and a regional, 60–200 m-thick, Cretaceous transgressive marine sequence (Winning Group and Toolonga Calcilutite; Fig. 6). The Jurassic succession is restricted to the central part of the structure (Appendix 1).

The Gascoyne Platform contains a northerly dipping Ordovician to lowermost Carboniferous succession up to

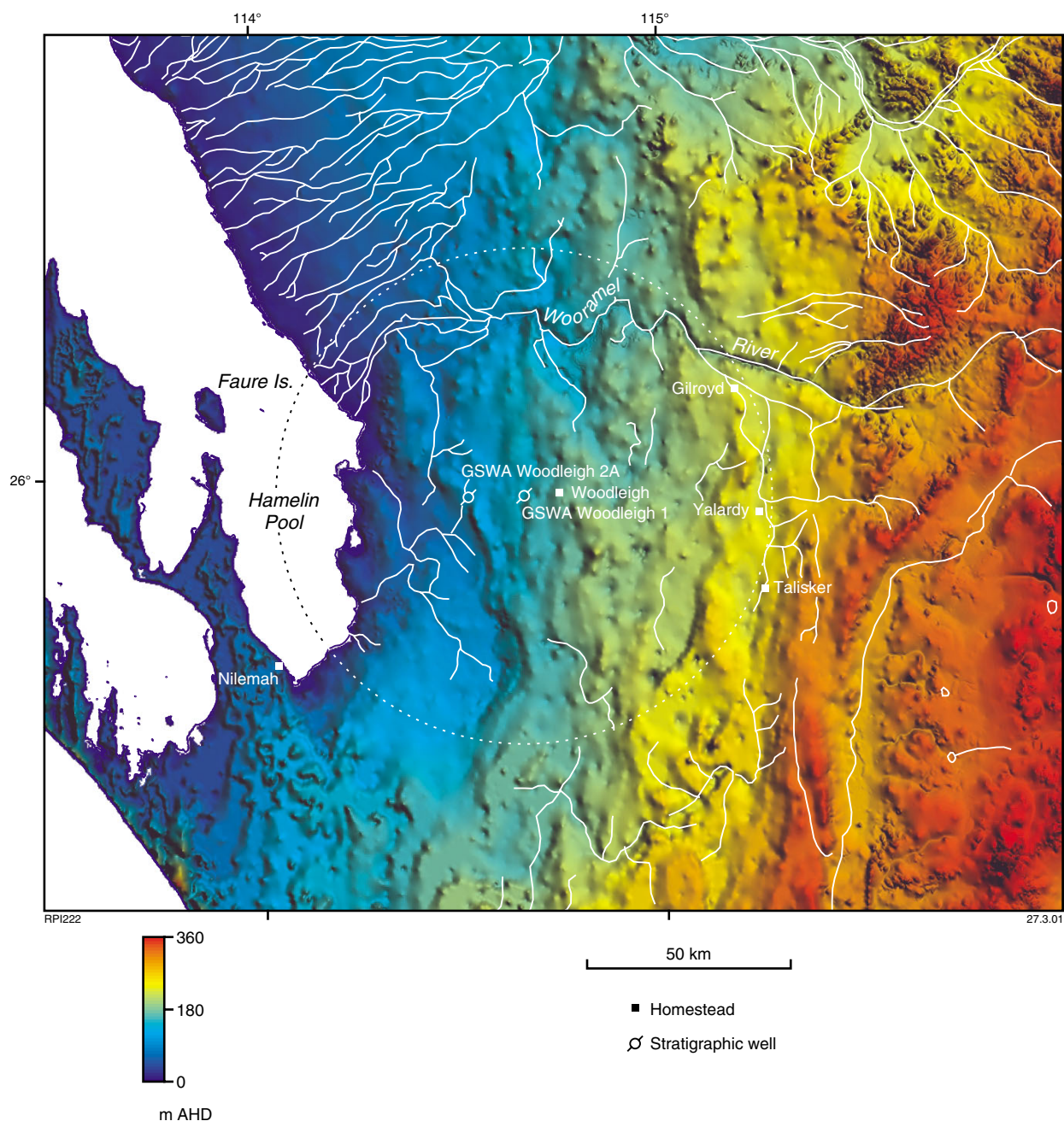


**Figure 4.** Digital elevation model of the Woodleigh region with superimposed drainage (after Denman et al., 1985, and van de Graaff et al., 1983)

5000 m thick, locally restricted Carboniferous–Permian and Lower Jurassic sedimentary sections, and widespread, mostly flat lying Cretaceous strata up to 400 m thick (Iasky et al., 1998b). Wells and bores that penetrate below the Cretaceous strata within the structure (Appendix 1) indicate progressively younger units to the northwest (Fig. 7). This is consistent with the northwesterly dip of Palaeozoic strata evident from seismic reflection data north of the Woodleigh impact structure (Iasky and Mory, 1999). To the east are the middle Carboniferous–Permian depocentres of the Merlinleigh and Byro–Coolcalalaya Sub-basins (Fig. 1; Iasky et al., 1998b;

Mory et al., 1998a), which are separated by the uppermost Archean to Palaeoproterozoic Carrandibby Inlier. Regionally, the absence of Permian strata on the southern Gascoyne Platform is interpreted as non-deposition (Iasky et al., 1998b), but it is unclear whether or not this is true along the entire eastern margin of the platform.

The following summary of the stratigraphic units relevant to the Woodleigh impact structure is based on Hocking et al. (1987), Mory et al. (1998b), and Iasky and Mory (1999).

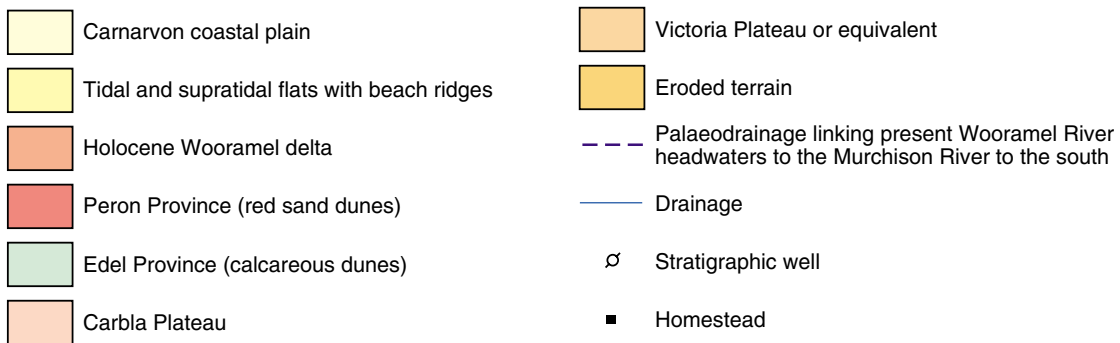
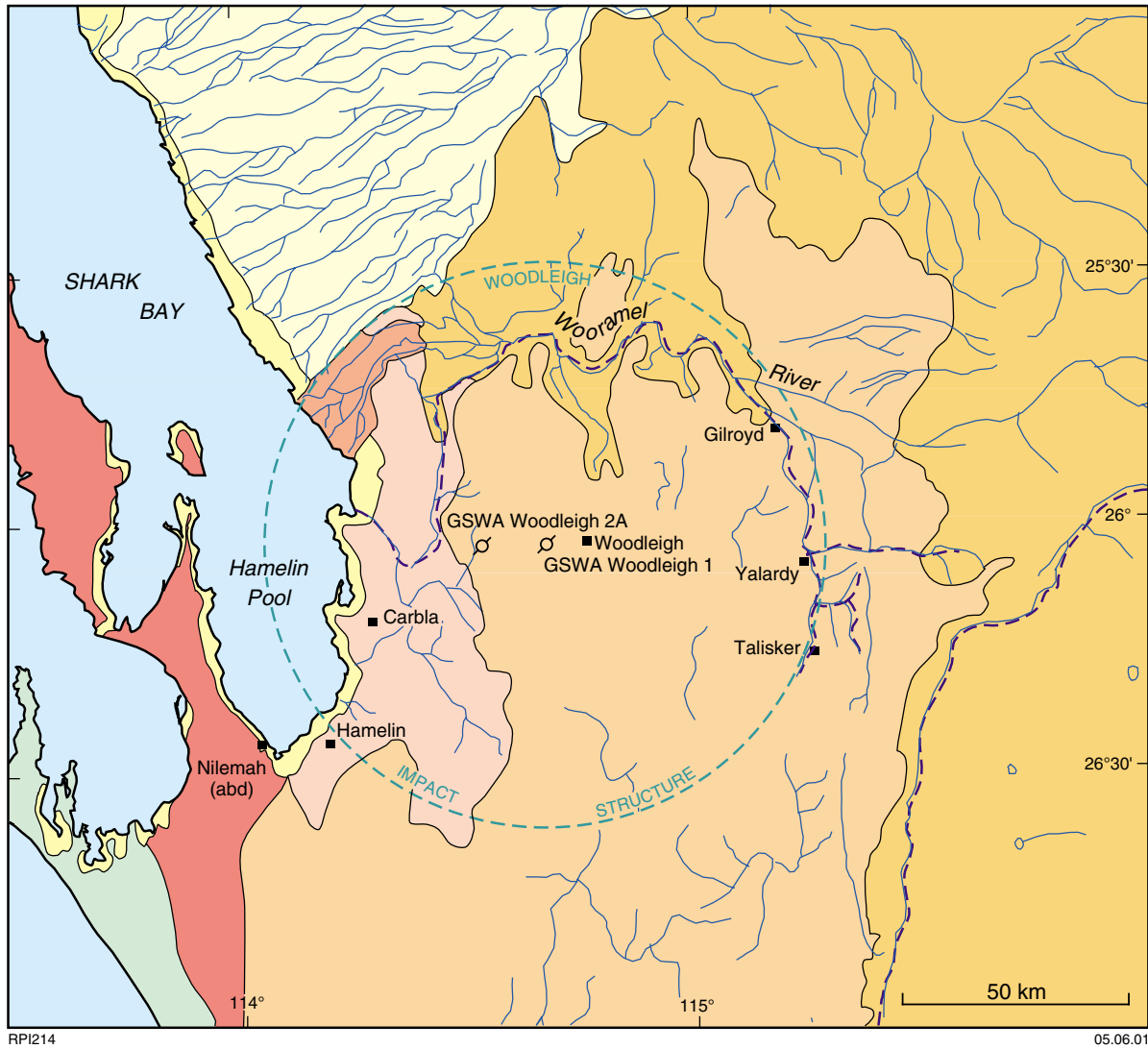


Figure 5. Physiography and palaeodrainage of the Woodleigh region (after Denman et al., 1985, fig. 2)

### Ordovician succession

The only unit of this age is the Tumblagooda Sandstone, which is the oldest Phanerozoic sedimentary unit on the Gascoyne Platform. The Tumblagooda Sandstone consists of red sandstone and minor conglomerate interpreted as deposited in a braided, fluvial, high-energy tidal and interdistributary environment (Hocking, 1991), or as mixed fluvial and eolian sand sheet deposits (Trewin,

1993a,b). The age of the Tumblagooda Sandstone is Middle to Late Ordovician on the basis of conodonts from the overlying Dirk Hartog Group (Mory et al., 1998b; Iasky and Mory, 1999). The unit is exposed only near the Murchison River and Northampton Complex (Figs 1 and 7; Hocking, 1991), but is penetrated by numerous drillholes on the Gascoyne Platform (Iasky and Mory, 1999). Drillhole and geophysical data indicate that the unit thickens to the southeast, reaching a

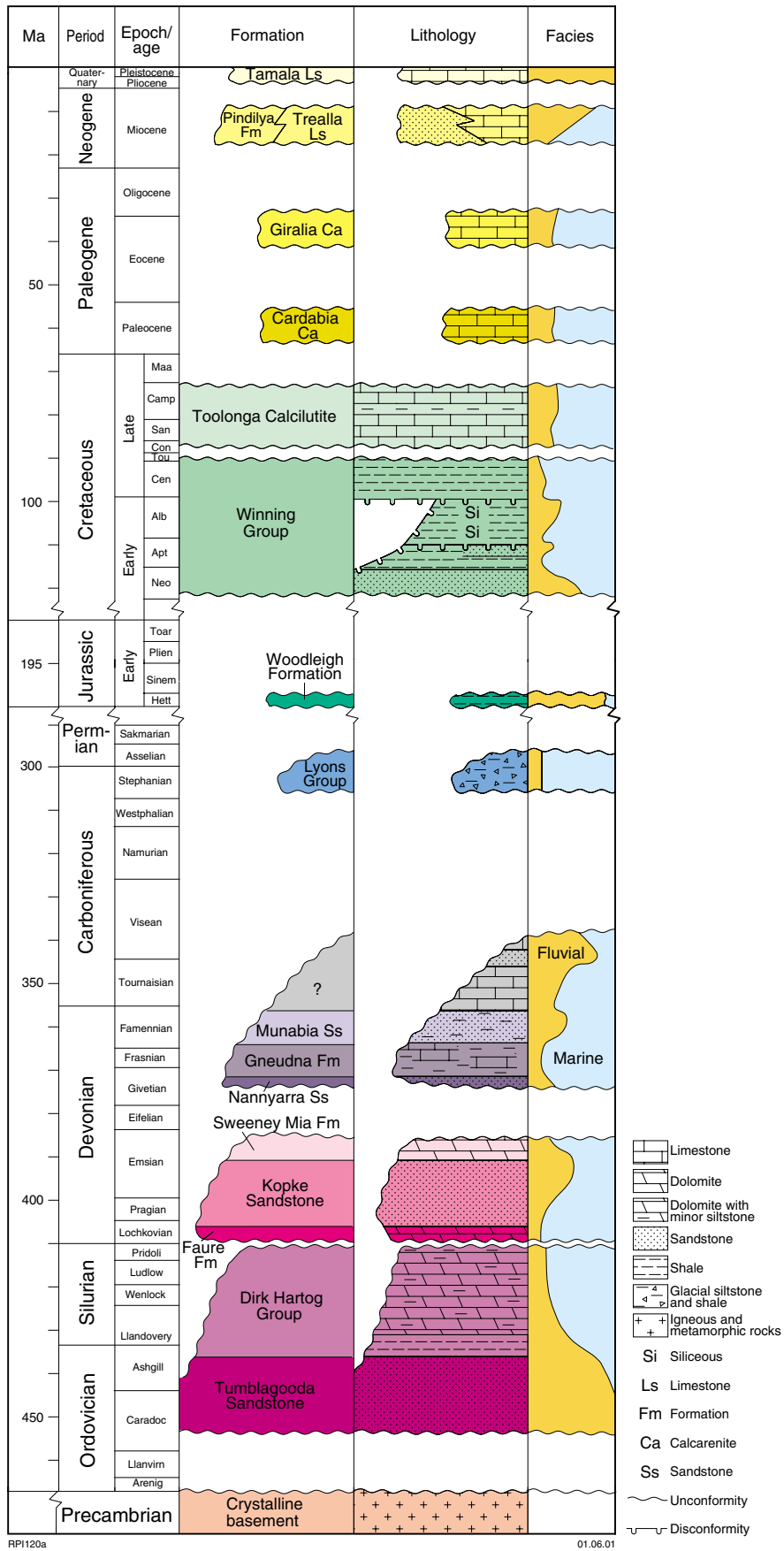


Figure 6. Stratigraphy of the Southern Carnarvon Basin

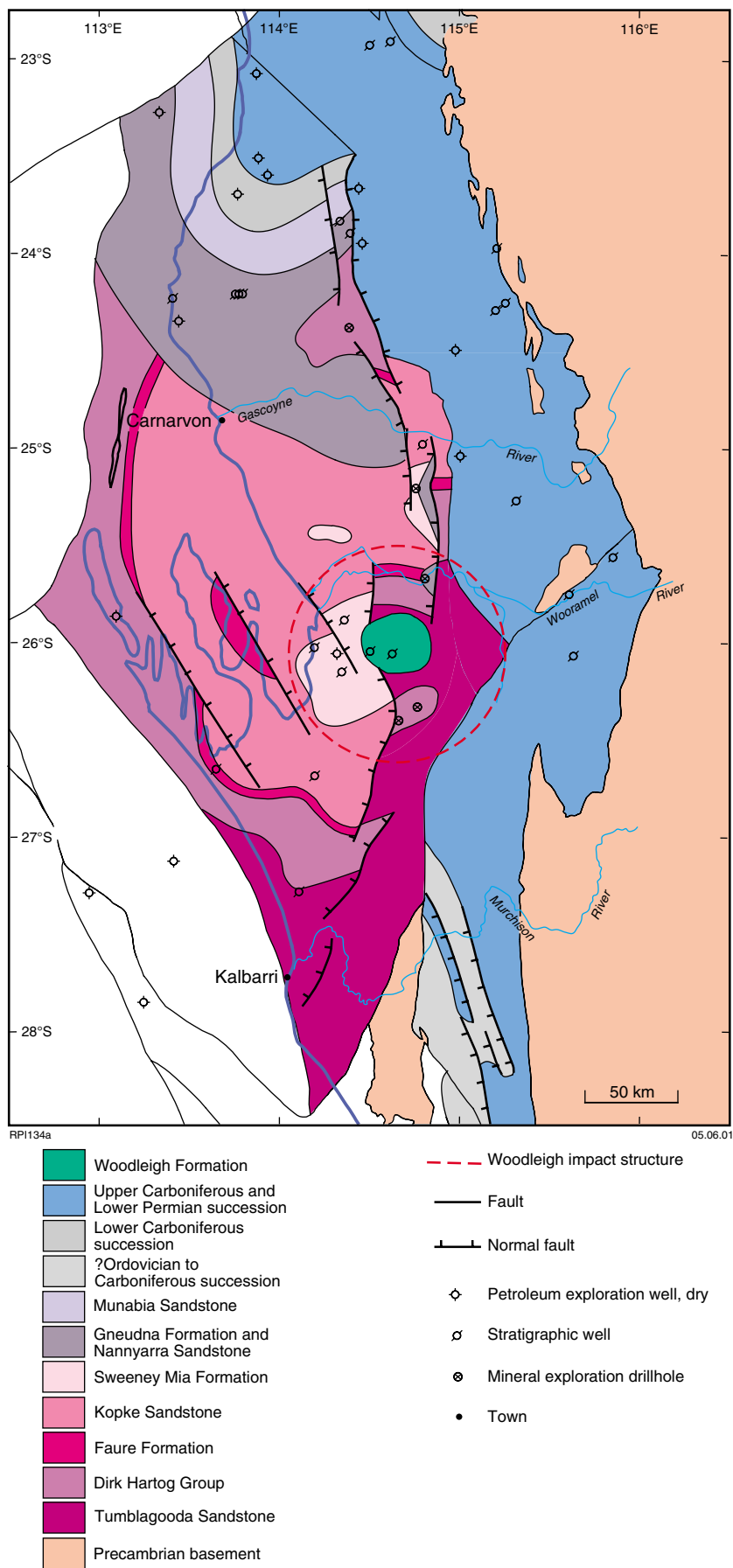


Figure 7. Pre-Cretaceous geology of the Woodleigh area

**Table 1. Log-derived densities (in g/cm<sup>3</sup>) from wells in the southern Gascoyne Platform**

Well	<i>K</i>	<i>Jw</i>	<i>Ds</i>	<i>Dk</i>	<i>SD</i>	<i>Ot</i>	<i>pCcu</i>
Coburn 1	2.42	–	–	2.35	2.77	2.41	–
Hamelin Pool 1	–	–	2.4	2.26	2.67	2.29	–
Kalbarri 1	2.03	–	–	–	2.41	2.36	–
Tamala 1	2.03	–	–	2.25	2.63	2.45	–
Yaringa 1	–	–	2.35	2.29	2.58	2.3	–
Yaringa East 1	–	–	2.5	2.41	–	–	–
GSWA Woodleigh 1	–	–	–	–	–	–	2.55
GSWA Woodleigh 2A	–	2.35	–	–	–	–	–

**NOTES:** Values represent weighted average densities  
*K*: Cretaceous undifferentiated  
*Jw*: Woodleigh Formation  
*Ds*: Sweeney Mia Formation  
*Dk*: Kopke Sandstone  
*SD*: Dirk Hartog Group, including Faure Formation  
*Ot*: Tumblagooda Sandstone  
*pCcu*: Precambrian basement of central uplift

Densities used in the gravity models for the Gascoyne Platform:  
 Cretaceous–Tertiary = 2.10 g/cm<sup>3</sup>  
 Sweeney Mia Formation = 2.5 g/cm<sup>3</sup>  
 Kopke Sandstone = 2.4 g/cm<sup>3</sup>  
 Dirk Hartog Group = 2.7 g/cm<sup>3</sup>  
 Salt within the Dirk Hartog Group = 2.2 g/cm<sup>3</sup>  
 Tumblagooda Sandstone = 2.37 g/cm<sup>3</sup>  
 Crystalline basement of central uplift = 2.55 g/cm<sup>3</sup>

maximum of about 3500 m near the Ajana Ridge. Electric logs show that the unit has a density of about 2.37 g/cm<sup>3</sup> (Table 1). The unit is inferred at shallow depths within the eastern part of the Woodleigh impact structure on the basis of cuttings of red sandstone described from shallow bores (summarized in Appendix 1).

## Silurian succession

The Dirk Hartog Group consists of carbonates deposited in restricted marine environments throughout the Silurian (Mory et al., 1998a). The relationship with the underlying Tumblagooda Sandstone appears to be conformable, although the apparent termination of small faults near this level implies a time break (Iasky and Mory, 1999). The group is widely distributed in the subsurface of the Gascoyne Platform, extending as far south as 27°30'S (Fig. 7), and thickens towards the west, with a maximum known thickness of 740 m in drillhole Dirk Hartog 17B (Fig. 1). The Dirk Hartog Group has at its base the Ajana Formation, which is an upward-shoaling carbonate unit (Gorter et al., 1994) with a distinctive basal siltstone and minor medium-grained sandstone (Marron Member). The formation thickens to the northwest and the greatest penetrated section is 435 m in Dirk Hartog 17B. Above the Ajana Formation lies the Yaringa Formation, which consists mainly of dolomite and evaporite rocks, but locally consists predominantly of sandstone. The formation is thickest (105 m) in Yaringa 1, which contains the greatest known proportion of evaporites. The Coburn Formation overlies the Yaringa Formation and consists mainly of dolomitic carbonate rocks. The unit thickens to the northwest, where the greatest thickness (335 m) is shown in Pendock 1.

The rock density of the Dirk Hartog Group is high because of the predominantly carbonate lithology, and averages 2.7 g/cm<sup>3</sup>, based on electric log data (Table 1). The Yaringa Formation, however, has an evaporite content

of significant thickness, which has been assigned a density of 2.2 g/cm<sup>3</sup> for gravity modelling.

## Lower Devonian succession

The Lower Devonian Faure Formation consists of mudstone, dolomite, and fine-grained sandstone, and disconformably overlies the Dirk Hartog Group (Gorter et al., 1994). The unit was deposited in a low-energy, saline to hypersaline, shallow-water environment in an arid climate in which body or trace fossils were either absent or not preserved (Yasin and Mory, 1999a). The formation is present in five drillholes in the southern Gascoyne Platform, and varies in thickness from 72 to 149 m. The Faure Formation has not been separated from the Dirk Hartog Group in the gravity modelling because the two units have similar lithologies and densities.

The Lower Devonian Kopke Sandstone conformably overlies the Faure Formation (Fig. 6), is up to 500 m thick, and consists predominantly of sandstone with minor dolomite and siltstone. The overall upward coarsening in the formation implies a largely wave influenced, deltaic setting. The upper part of the formation may have been deposited in a fluvial environment in which high-energy sheet floods were common (Yasin and Mory, 1999a,b). Electric log data indicate an average rock density of 2.4 g/cm<sup>3</sup> for the unit (Table 1).

The Sweeney Mia Formation consists of oxidized, mixed carbonate and siliciclastic rocks with minor evaporitic intervals, deposited in a reducing, shallow lagoonal to supratidal environment (Yasin and Mory, 1999b). The age of the formation is poorly constrained, but is likely to be Early Devonian based on the conformable relationship with the underlying Kopke Sandstone. The unit is known only in the central part of the Gascoyne Platform, where it reaches a maximum thickness of 192 m in Yaringa East 1. Well log data indicate a rock density of about 2.5 g/cm<sup>3</sup> (Table 1).

## Middle–Upper Devonian succession

The Middle–Upper Devonian succession is internally conformable and probably disconformably overlies Lower Devonian and older strata (Iasky and Mory, 1999, fig. 4). Only the Nannyarra Sandstone at the base of this succession has been identified within the Woodleigh impact structure (in Yaringa East 1).

The Nannyarra Sandstone comprises predominantly sandstone with minor siltstone, and was deposited in a low-energy, shallow-marine, intertidal environment, marking the base of a major marine transgression. In the central and southern parts of the Gascoyne Platform, the unit appears to progressively overstep older units (Fig. 7). The maximum known thickness of the Nannyarra Sandstone is 214 m in drillhole CRAE GBH 1, north of the Woodleigh impact structure.

The Gneudna Formation consists of interbedded carbonate and siltstone with minor evaporite, and was deposited in a nearshore to restricted shallow-marine environment. The unit is present in the northern part of the Gascoyne Platform, where it conformably overlies the Nannyarra Sandstone.

Conformably overlying the Gneudna Formation is the late Frasnian to early late Famennian Munabia Sandstone, which consists of sandstone with minor claystone, conglomerate, and dolomite deposited in a braided fluvial to alluvial-fan environment (Hocking et al., 1987).

## Carboniferous to Triassic succession

Although Carboniferous–Triassic rocks are not represented within the Woodleigh impact structure, they are present immediately to the west within the Permian depocentres, as well as within the northernmost part of the Gascoyne Platform.

The Carboniferous succession of limestone, sandstone, and claystone is unconformably overlain by the Upper Carboniferous – Lower Permian Lyons Group (Hocking et al., 1987), which consists predominantly of shale deposited in a glacially influenced marine environment. The relationship between the Carboniferous succession and underlying Munabia Sandstone, which is only seen in seismic sections, may be either conformable or disconformable.

In the Gascoyne Platform, the Triassic Kockatea Shale is present only in the coastal cliffs near Kalbarri, 130 km south of the Woodleigh impact structure, where it directly overlies the Tumblagooda Sandstone.

## Jurassic succession

The only named Jurassic unit in the region is the Woodleigh Formation, which is restricted to the vicinity of Woodleigh Station (Playford and Chase, 1955). The

unit consists of a weakly indurated, nonmarine, shaly succession that was deposited in a lake environment and dated as Early Jurassic from abundant spores and pollens (McWhae et al., 1958). This unit also contains Early Permian palynomorphs, which increase in abundance towards the base of the unit in GSWA Woodleigh 2A, but are probably reworked. The greatest known thickness of the formation is 298 m in GSWA Woodleigh 2A (Fig. 8). The farthest extent of the unit from the centre of the Woodleigh impact structure is uncertain, but it is present in Woodleigh water bore 9, 25 km east-southeast of the centre of the structure, and probably extends well into the gravity trough 24 km to the west. It is also possible that the thin shaly units between the Cretaceous and Lower Palaeozoic strata in Woodleigh 1982/1, 30 km to the southeast, and in the Carpentaria CB2 and 3 bores, 50 km to the south (Fig. 9, Appendix 1), belong to this unit. However, there are no samples available to confirm such an interpretation. The formation is notably absent in GSWA Woodleigh 1, in which the Cretaceous succession directly overlies basement rocks, and in Yaringa 1, 30 km to the west (Fig. 8).

The Woodleigh Formation provides the minimum possible age of the impact. The 66 m-thick unnamed paraconglomerate at the base of the Woodleigh Formation in GSWA Woodleigh 2A (Fig. 8) has not been dated satisfactorily, but contains shale clasts with Early Permian palynomorphs. This unit contains mainly sandstone clasts in an oxidized clayey medium-grained matrix, as well as sparse clasts of granite with shock-metamorphic features indicating that it postdates the impact. Below the paraconglomerate in GSWA Woodleigh 2A is an unnamed breccia (587–601 m) that consists of large blocks of Upper Silurian dolomite and shale. As no shock-metamorphic features are evident in this unit, it is unclear whether or not it is related to the impact, even though it is depicted as following the base of the Woodleigh Formation in Figure 8.

Apatite fission-track analyses of samples from the base of the Woodleigh Formation in GSWA Woodleigh 2A indicate an uplift in the order of 700 m (Gibson, 2000). This implies that the Woodleigh Formation may have been 1100 m thick at this location before uplift during the breakup of Australia from Greater India.

## Cretaceous and Tertiary succession

The breakup of Australia from Greater India in the Early Cretaceous was a major tectonic event in the region, and is commonly marked by an angular unconformity between the typically flat lying Cretaceous succession and underlying strata (Iasky and Mory, 1999).

The Lower Cretaceous Winning Group was deposited during a transgression that began in the Neocomian and continued to the end of the Cenomanian. The group thickens to the west, where it reaches a maximum known thickness of about 600 m. The succession consists of a basal transgressive sandstone (Birdrong Sandstone) overlain by low-energy, marine shale (Muderong Shale),



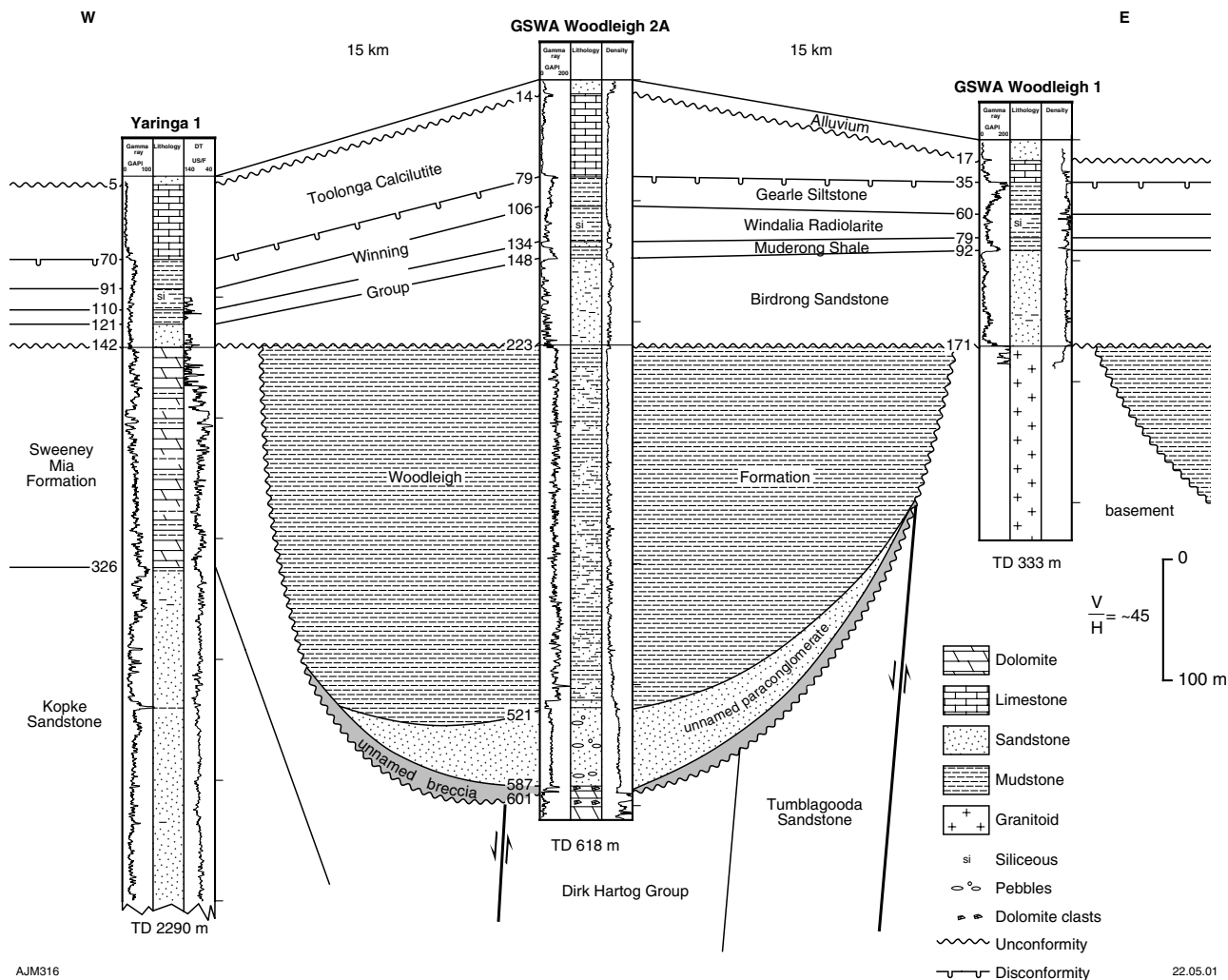


Figure 8. Correlation of shallow stratigraphic horizons from Yaringa 1 to GSWA Woodleigh 1

which may contain sand deposited in a moderate-energy, marine environment near normal wave base (Winalia Sandstone Member). The Winalia Radiolarite overlies the Muderong Shale and was deposited in a low-energy, shallow-marine environment with relatively low clastic-material input. These rocks are overlain by glauconitic siltstone (Gearle Siltstone) and coeval greensand (Alinga Formation) near Kalbarri.

Disconformably overlying the Winning Group is the Cretaceous Tooolonga Calcilutite, which consists of massive, fossiliferous calcilutite and calcisiltite deposited in a low-energy, inner- to middle-shelf marine environment. The unit is 273 m thick in Dirk Hartog 17B and thins to the east, where it is absent over parts of the Wandagee and Ajana Ridges. In the southern Gascoyne Platform, the Upper Cretaceous Miria Formation and Tertiary rocks unconformably overlie the Tooolonga Calcilutite.

Tertiary sedimentary rocks on the Gascoyne Platform are typically flat lying and consist of the shallow-marine Cardabia and Giralia Calcarenites and eolian Trealla Limestone (Hocking et al., 1987). The Cainozoic succession is unlikely to be thicker than 50 m in the

immediate vicinity of the Woodleigh impact structure. A veneer of Quaternary alluvium and colluvium deposits, usually less than 20 m thick, unconformably overlies the Tertiary rocks.

For the gravity model, Cretaceous and Tertiary rocks have been grouped and assigned an average rock density of 2.10 g/cm<sup>3</sup> (Table 1), based on well log data.

## Age of the impact

A pre-Early Jurassic age is indicated by Early Jurassic palynomorphs in the Woodleigh Formation, which overlies the Woodleigh impact structure. Early Permian (Sakmarian) palynomorphs from a shale clast in the unnamed paraconglomerate directly overlying deformed Silurian strata in GSWA Woodleigh 2A (drilled in the inner ring syncline) were taken by Mory et al. (2000) as indicating a maximum age for the impact.

Attempts were made to isotopically date biotite, zircon, and feldspar from granitic samples in GSWA Woodleigh 1, but these did not yield meaningful ages because of the instability of the zircon U–Pb ages and biotite K–Ar and

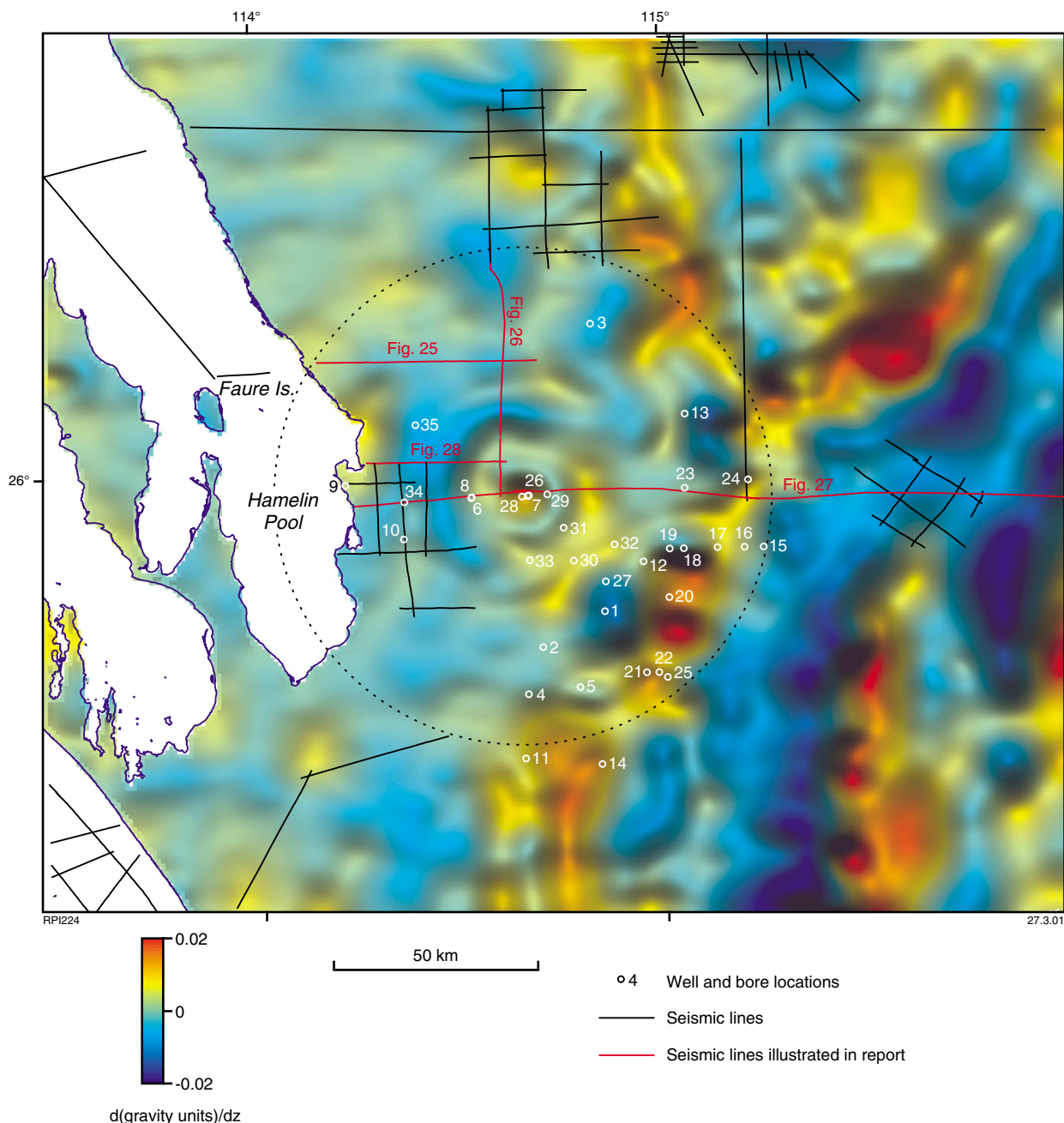


**Figure 9. Location of seismic lines, bores, and wells within the Woodleigh impact structure. Drillholes corresponding to the numbers are listed in Appendix 1. Background is the image of the first vertical derivative of the Bouguer gravity**

Rb–Sr age systematics. Furthermore, Ar–Ar and K–Ar ages of feldspar and pseudotachylite were reset after the Early Jurassic (Mory et al., 2000).

Recent K–Ar isotopic studies of illite and smectite from three samples of the clay matrix of the basal paraconglomerate in GSWA Woodleigh 2A yielded ages of  $364 \pm 8$  Ma,  $352 \pm 8$  Ma, and  $342 \pm 7$  Ma. In addition, two separates of a phyllosilicate mineral with some very fine grained smectite in a granite sample from GSWA Woodleigh 1 yielded ages of  $336 \pm 8$  Ma and  $364 \pm 8$  Ma (Mory et al., in prep.), ranging from Frasnian–Famennian (Late Devonian) to Early Carboniferous. The

younger K–Ar isotopic ages can be explained in terms of partial resetting of the K–Ar systematics in clay minerals during protracted post-impact hydrothermal activity. Although the isotopic systematics of zircon and biotite can be retained upon impact, the isotopic systematics of clay minerals would stabilize during post-impact hydrothermal activity around the central part of the structure.

If the K–Ar ages of the illite and smectite from GSWA Woodleigh 1 represent hydrothermal activity in the wake of the impact, the K–Ar clay systematics in the central uplift appear to constrain the age of the impact to no younger than Late Devonian. However, given the limited

and relatively wide ranging (28 m.y.) isotopic data and the inconsistency with the stratigraphic data, until new evidence is found the age of the structure is left as an open question constrained only by the regional stratigraphy (Middle Devonian to Early Jurassic).

## Geophysics

### Gravity surveys

Of all the data over the Woodleigh impact structure, gravity provides the best evidence for its morphology. This is in accord with many other large impact structures because the fracturing and brecciation caused by the

impact produces a negative gravity anomaly (Fig. 10; Pilkington and Grieve, 1992). However, post-impact tectonism and erosion can decrease the size of this negative gravity signature to the point where only the background gravity can be discerned (Plado et al., 1999). It is also possible, as in the case of the Yallalie structure in the Perth Basin, for an impact structure to have a positive gravity anomaly (Dentith et al., 1999). In the case of Yallalie, the positive anomaly is attributed to the complete erosion of the brecciated material, allowing deeper and denser rocks to dominate the gravity response (Dentith et al., 1999).

WAPET and Conoco originally collected the gravity data used in imaging the Woodleigh impact structure (Fig. 3) in the early 1970s. These data, together with data

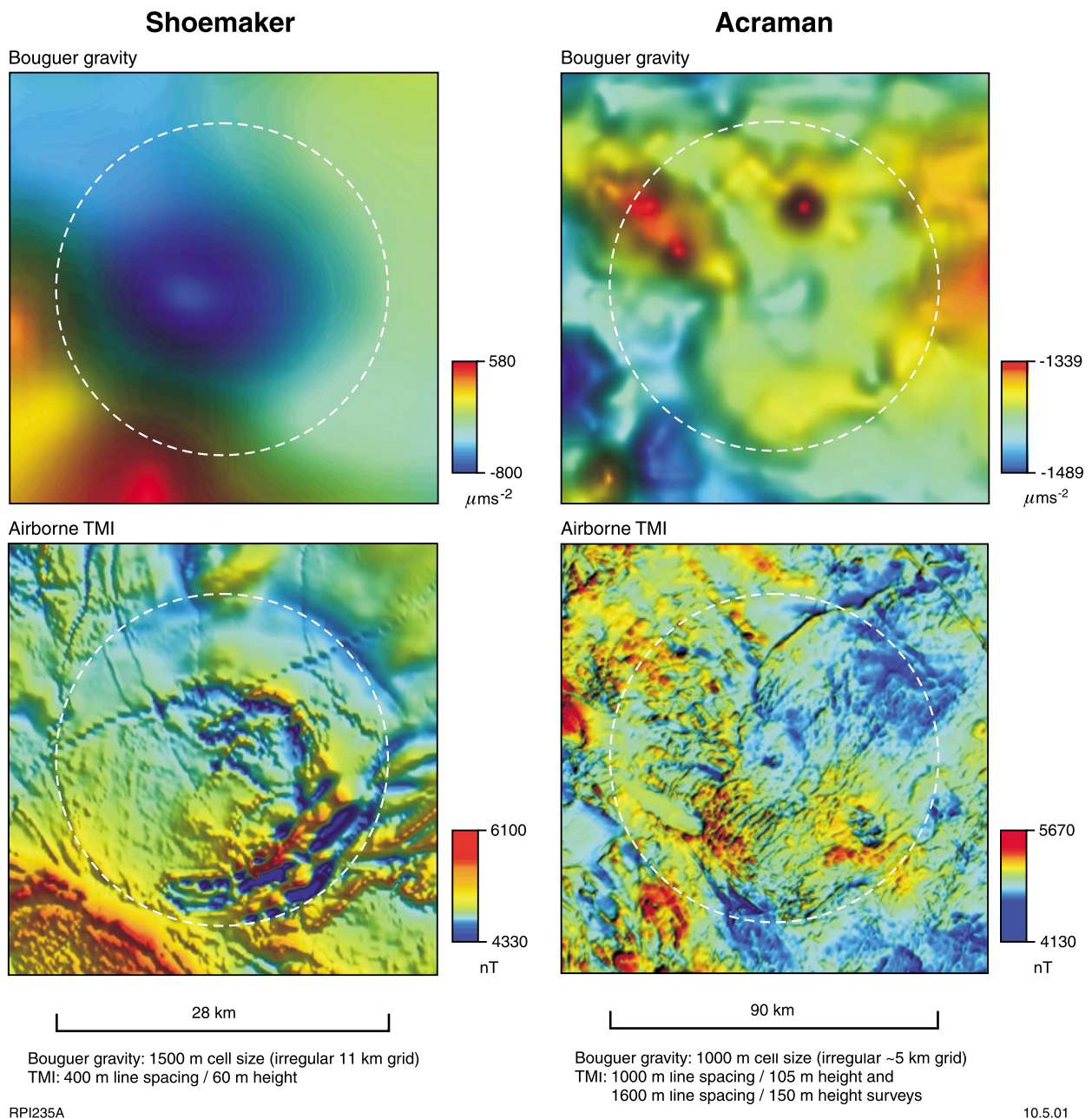


Figure 10. Potential-field images of selected Australian impact structures (data used with the permission of AGSO)

recorded from gravity stations by GSWA within 40 km of the centre of the Woodleigh impact structure, are now available from the AGSO national gravity database. The AGSO database includes measurements on a regional 11 km grid and stations are spaced 800–1000 m apart along available tracks and fence lines.

The regional Bouguer gravity image of the Southern Carnarvon Basin (Fig. 11) clearly displays three main basin subdivisions: the Gascoyne Platform, and the Permian depocentres of the Merlinleigh and Byro–Coolcalalaya Sub-basins to the east. Along the eastern edge of the Gascoyne Platform, the Wandagee and Ajana Ridges converge towards the Woodleigh impact structure. The eastern margin of the structure is coincident with the junction of the Byro and Merlinleigh Sub-basins with the

Gascoyne Platform, implying that the impact may have influenced the development of these Permian depocentres. The outer limit of the structure is interpreted from the abrupt truncation of the Wandagee and Ajana Ridges, 60 km northeast and 60 km southeast of the centre of the structure respectively. A north-northeasterly trending gravity lineament separating a broad gravity ‘high’ to the east from a gravity ‘low’ to the west across the middle of the structure (Fig. 12) implies that the Wandagee and Ajana Ridges were once a continuous ridge. This lineament is disrupted by a circular gravity high interpreted as a central uplift within the impact structure (Fig. 12). The magnitude of the anomaly is best illustrated along a northwesterly profile, with the central gravity high of  $160 \mu\text{ms}^{-2}$  superimposed on a broad saucer-shaped gravity ‘low’ of about  $240 \mu\text{ms}^{-2}$  (Fig. 12). The signature of the gravity

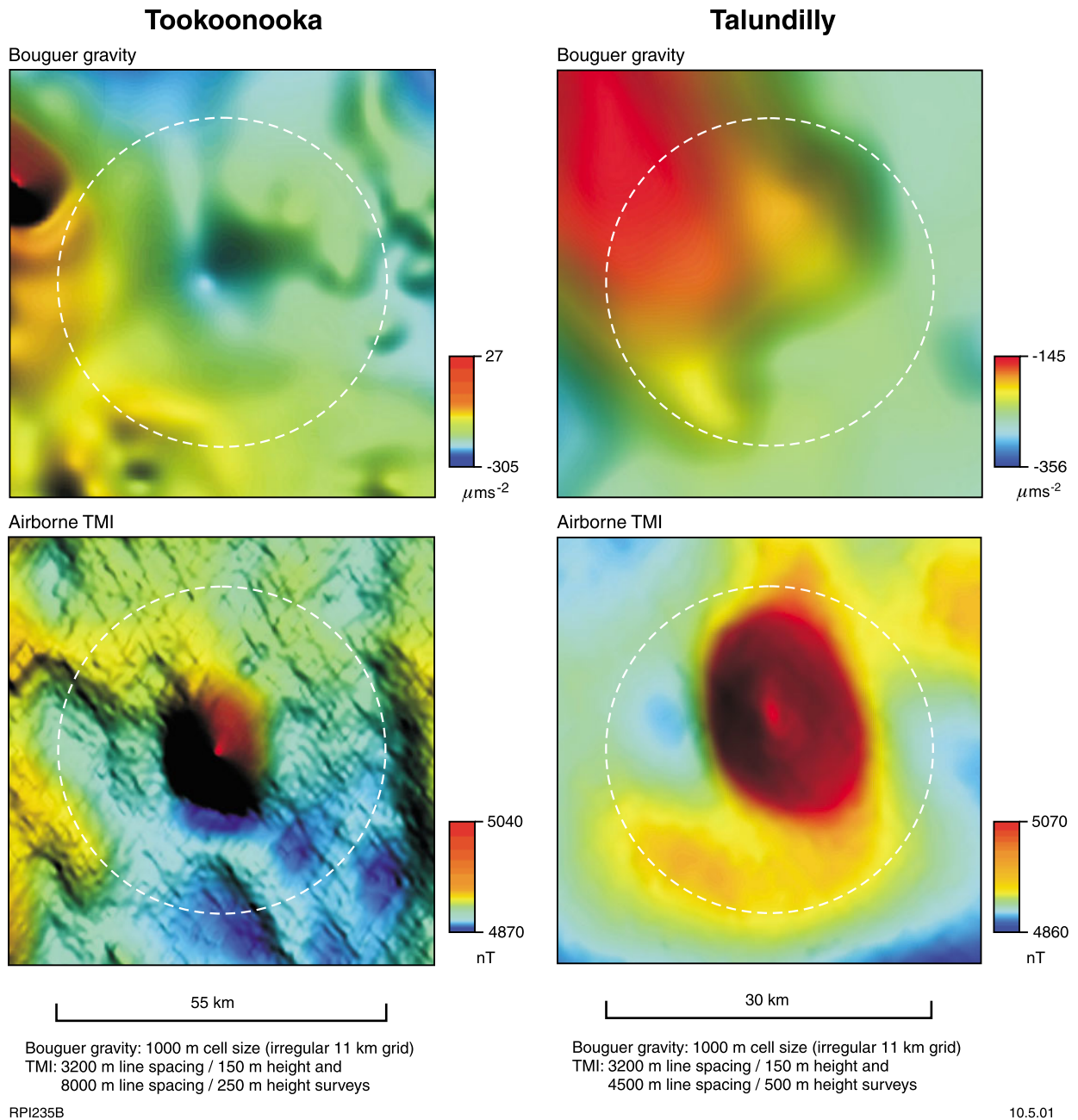
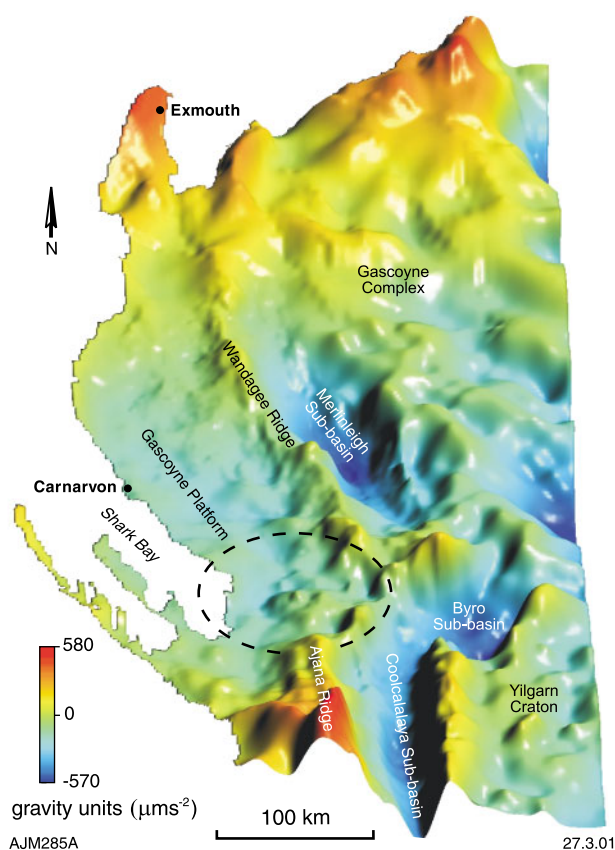


Figure 10. (continued)



**Figure 11. Oblique view from the south of the Bouguer gravity image of the Southern Carnarvon Basin**

anomaly along this profile resembles that of the 100 km-diameter Manicouagan impact structure in Canada (Pilkington and Grieve, 1992) and the Vredefort impact structure in South Africa (Henkel and Reimold, 1996).

The Woodleigh impact structure is most clearly shown as a series of annular ridges and troughs on the first vertical derivative of the Bouguer gravity image (Figs 13 and 14). The structure can be described as multi-ring with a central gravity ‘high’ about 25 km in diameter. This central ‘high’ can be subdivided into a central gravity peak about 8 km across (a on Fig. 13), an inner annular gravity trough at about 10 km radius (b), and an inner annular gravity ridge about 12 km from the centre (c). The adjacent annular gravity ‘trough’ (d) about 20 km from the centre probably represents a ring syncline filled with the Woodleigh Formation, and possibly also the underlying unnamed paraconglomerate and breccia units in GSWA Woodleigh 2A (Fig. 8; Mory et al., in prep.). About 30–35 km from the centre there is an outer circular gravity ridge (e), which delineates the minimum diameter of the structure because it is the farthest clearly identifiable circular feature. This outer ridge is adjacent to a poorly defined outermost annular gravity low that extends out to the interpreted crater rim (f) about 60 km from the centre of the structure. The limits of the impact-deformed aureole (f) are based on a broad arcuate gravity ridge crossing the coast 60 km from the centre in the north-western quadrant and the intersection of the regional structure by the outer-

most geophysical ‘ring’. This criterion is similar to that used to identify the outer limits of impact structures such as Chicxulub (Mexico; Morgan and Warner, 1999a; Sharpton et al., 1996), Shoemaker (Euraheedy Basin, Western Australia; Pirajno and Glikson, 1998; Glikson, 1996) and Lawn Hill (Lawn Hill Platform, northwest Queensland; Shoemaker and Shoemaker, 1996; Glikson, 1996). To the southeast the outermost ring is cut by the Madeline Fault, which marks the western margin of the Byro–Coolcalalaya Sub-basin. The structure is poorly defined to the west due to an absence of gravity data within Shark Bay.

A comparison of gravity signatures of significant Australian impact features (Figs 10 and 14; Glikson, 1996) shows that the Woodleigh and Gosses Bluff (Amadeus Basin, Northern Territory) structures (Fig. 14) have the best defined gravity signatures. The gravity signatures of the Shoemaker, Acraman (Gawler Craton, South Australia), Tookoonooka, and Talundilly (both in the Eromanga Basin, Queensland) impact structures are poorly resolved by the sparse gravity coverage over these structures, although broad gravity lows are clearly recognizable in the Shoemaker and Tookoonooka structures.

A direct comparison can be made between the gravity anomalies and underlying geometry of the Woodleigh and Gosses Bluff impact structures (Fig. 14). The gravity profiles of the two structures are very similar, from the inner rings of the central peaks to the diffuse troughs extending to the outer rims. Furthermore, the rocks in both structures consist of Devonian and Ordovician sedimentary successions. The Gosses Bluff crater provides a good model for complex impact structures because it is exposed (although only partially preserved). Even though the diameter of the Woodleigh Structure is five times larger, the ratios of the diameters of the inner gravity ridges (a on Fig. 14) to the diameter of the outer rim are very close for the two structures (~0.25). Furthermore, the ratios of the diameter of the outer circular gravity ridges (b on Fig. 14) to the diameter of the outer rim are very close for the two structures (~0.5).

Within the Woodleigh impact structure, BHP ND1 and ND2 (1 and 2 in Fig. 9) were drilled in the poorly defined, outermost annular gravity low. Both drillholes penetrated the Dirk Hartog Group and Tumblagooda Sandstone beneath the Cretaceous succession. Even though BHP ND1 intersected the Tumblagooda Sandstone just 93 m shallower than BHP ND2 (Iasky and Mory, 1999, appendix 4), it was drilled over a relative gravity low compared to BHP ND2. This variation of the gravity field indicates either large variations in the thickness of the Tumblagooda Sandstone or significant lateral changes in density within the structure. The latter explanation is probably more likely, given that the gravity low near CRAE GRH1 (3 in Fig. 9) has a lower amplitude than near BHP ND1, even though CRAE GRH1 penetrated a stratigraphically higher Devonian succession.

## Gravity modelling

The Woodleigh impact structure is completely buried beneath a cover of Cretaceous–Tertiary strata, which

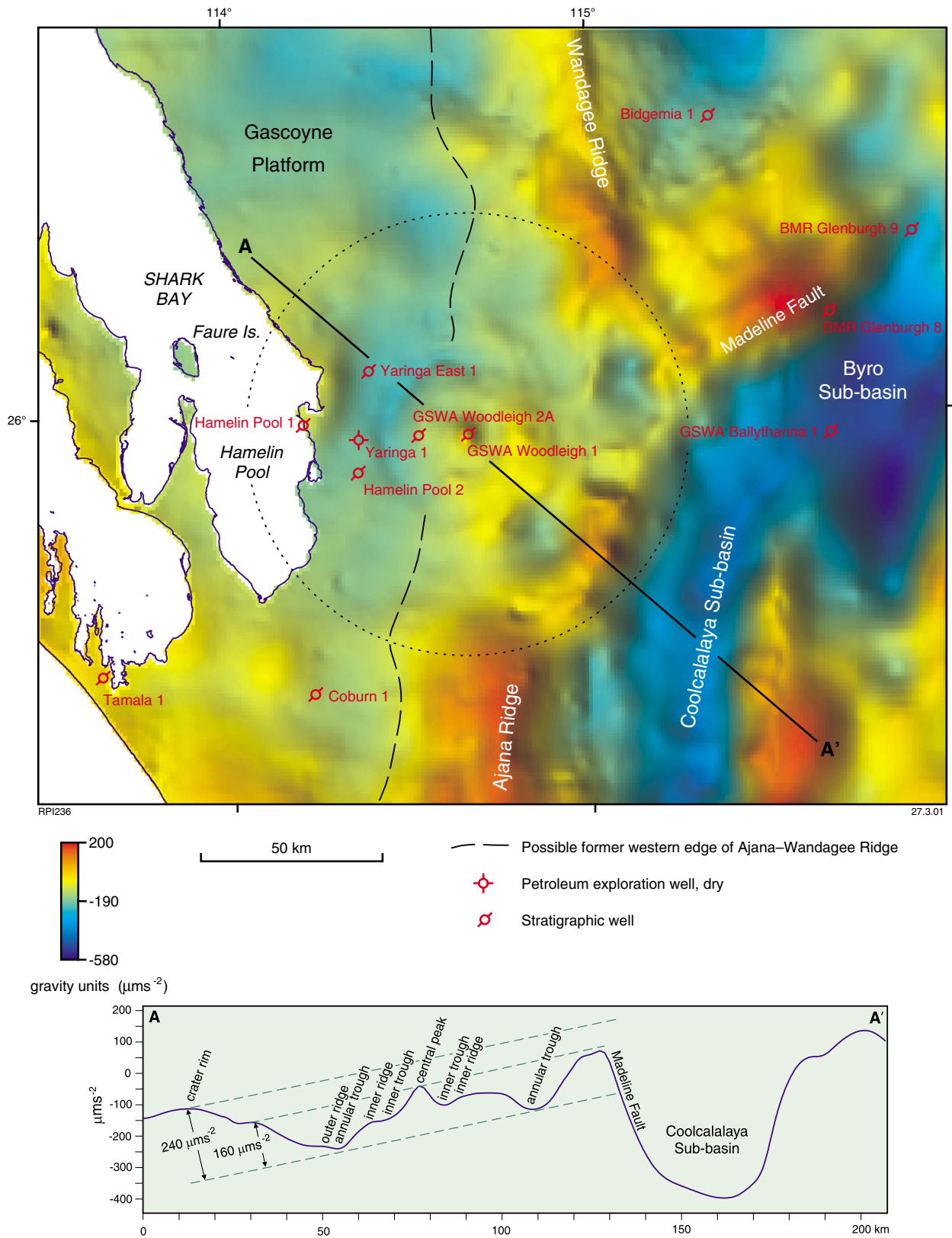
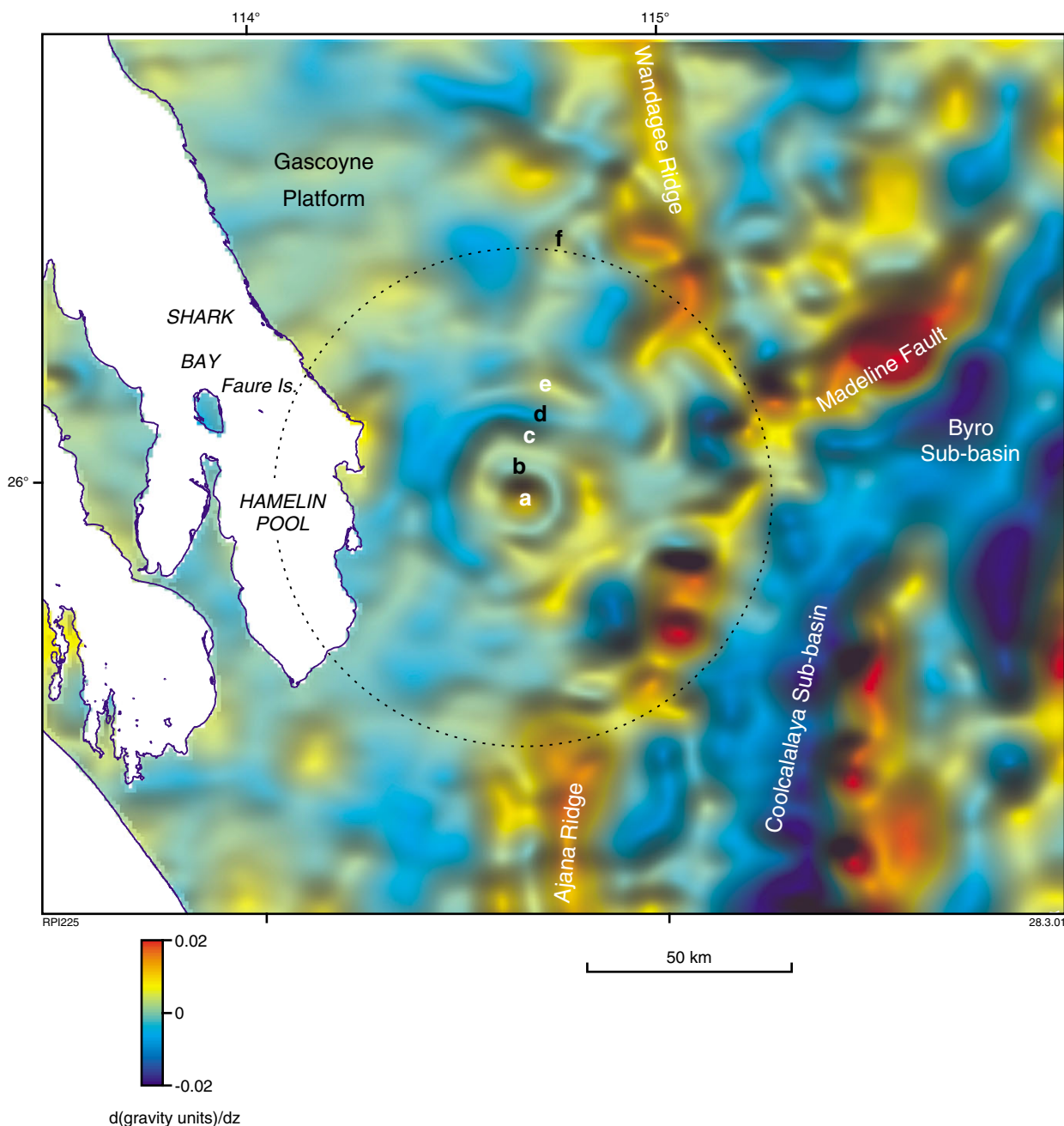


Figure 12. Bouguer gravity image of the Woodleigh impact structure, showing northwest-southwest gravity profile

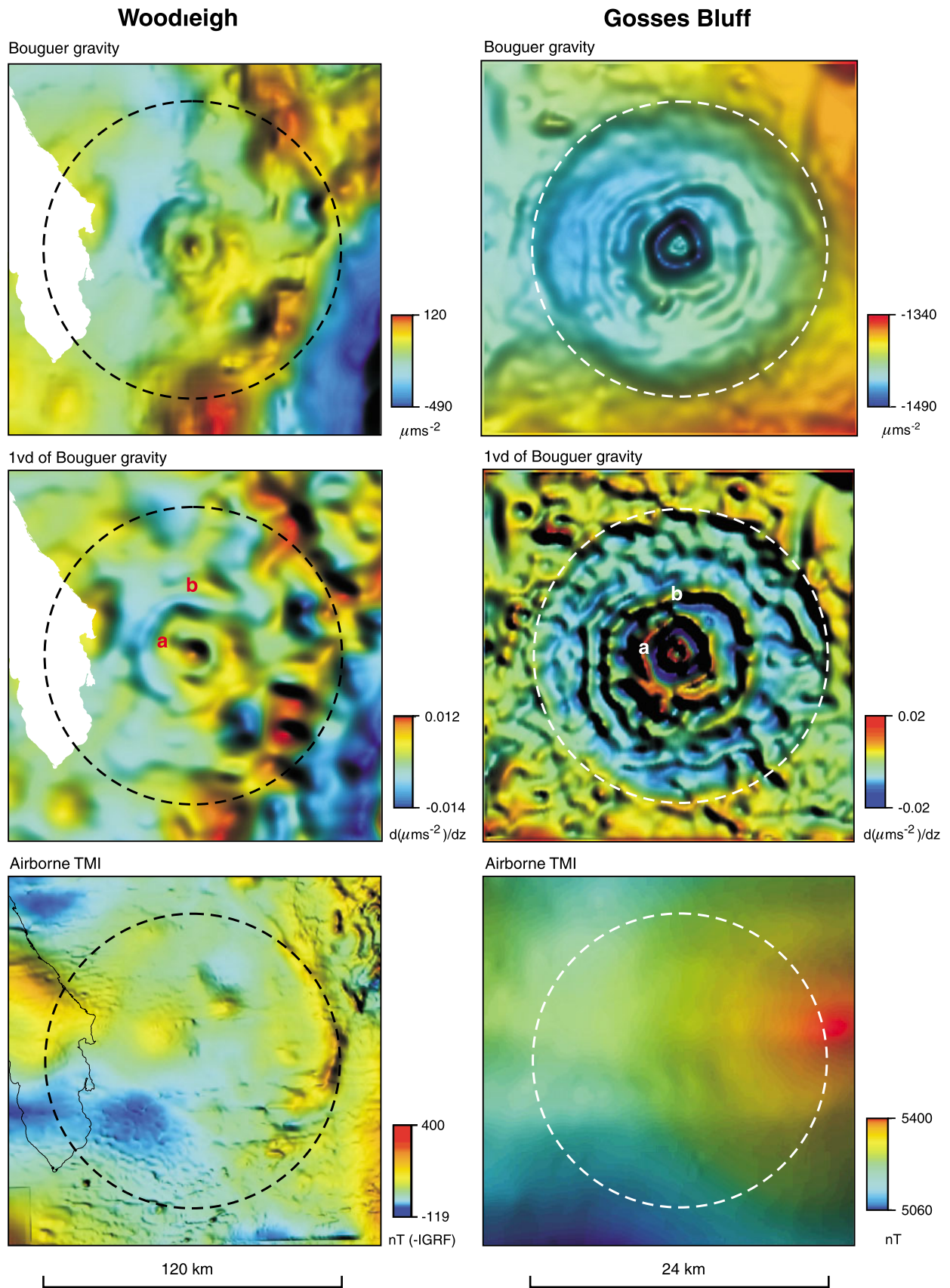


**Figure 13. Image of first vertical derivative of Bouguer gravity over the Woodleigh impact structure. Letters refer to subdivisions described in text**

ranges in thickness from 50 m on the eastern margin of the structure to 200 m on the western margin, as well as up to 400 m of Jurassic lacustrine deposits near the centre. Gravity images show the best developed circular features and in the absence of good-quality seismic data, gravity modelling is the best technique to analyse the internal morphology of the structure. This modelling was constrained by drillhole data and the structure evident on seismic sections. A series of two-and-a-half-dimensional (two-dimensional with an infinite strike length) gravity models were prepared (using Modelvision Pro software from Encom Technology Pty Ltd) on east–west (Fig. 15), north–south (Fig. 16), and northwest–southeast (Fig. 17) profiles.

As there are few constraints below the Phanerozoic section in this region, deep-crustal modelling was not attempted. Instead, the shallow crust was modelled from the residual gravity, which was calculated by subtracting the Bouguer gravity from the regional gravity curve. The regional curve was estimated by assuming zero residual over crystalline basement outcrop, and allowing for a regional increase in gravity towards the edge of the continental shelf to the west. A further constraint for the regional curve is the depth to basement of the Gascoyne Platform (Iasky and Mory, 1999).

The gravity models have been subdivided into density layers that broadly represent the stratigraphy of the



Bouguer gravity: 1000 m cell size (irregular 1 km grid)  
 TMI: ~200 m cell size (1600 m line spacing / 150 m height)  
 RPI233

Bouguer gravity: 200 m cell size (regular 500 m / 1 km grid)  
 TMI: ~400 m cell size (3200 m line spacing / 245 m height)

27.3.01

**Figure 14. Comparison of potential-field signature of the Woodleigh and Gosses Bluff impact structures (data used with the permission of AGSO; -IGRF = International Geophysical Reference Field removed)**



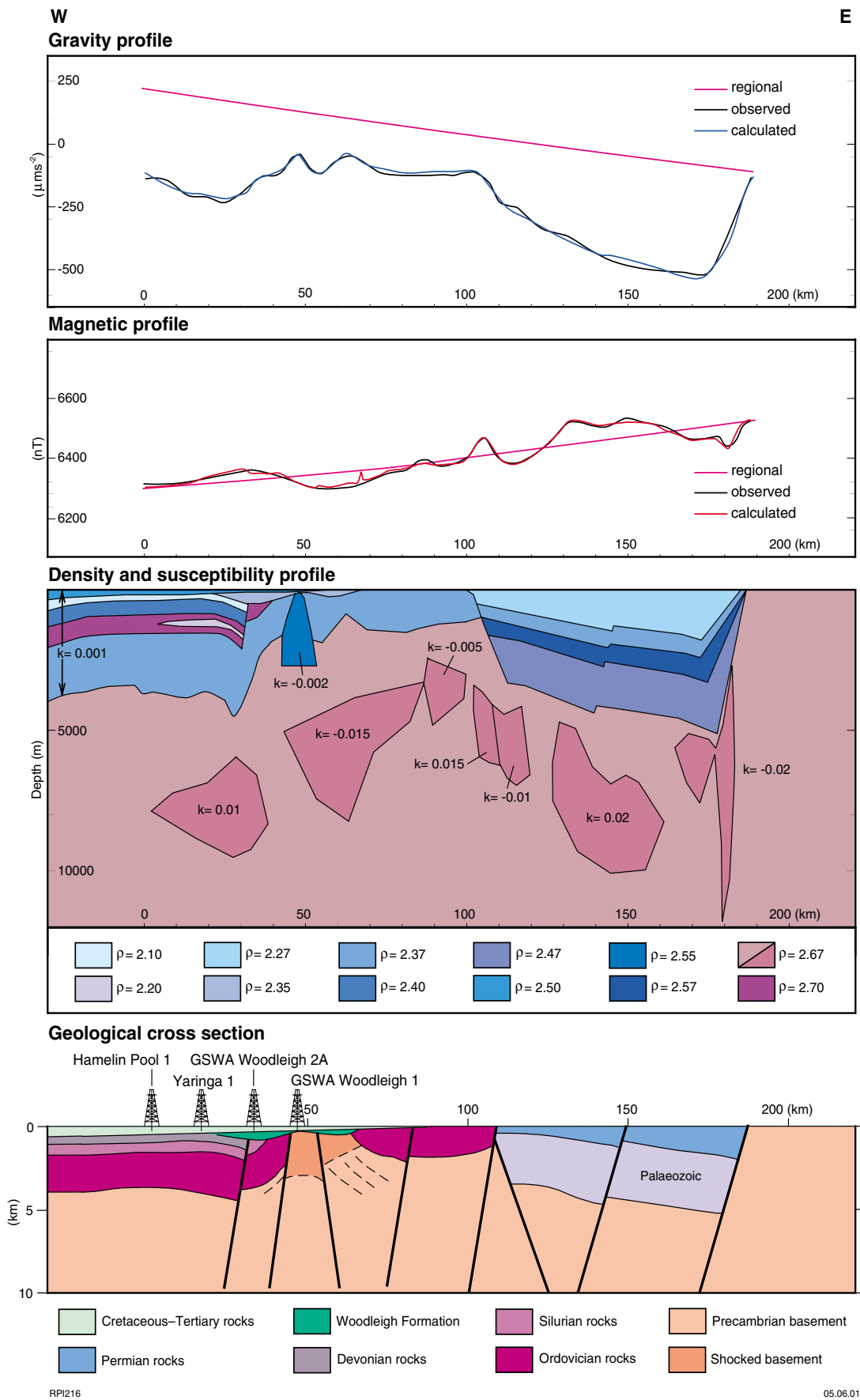


Figure 15. East-west two-dimensional gravity model and cross section of the Woodleigh impact structure. In the density and susceptibility profile, densities ( $\rho$ ) are in  $\text{g}/\text{cm}^3$  and susceptibilities ( $k$ ) are in SI units

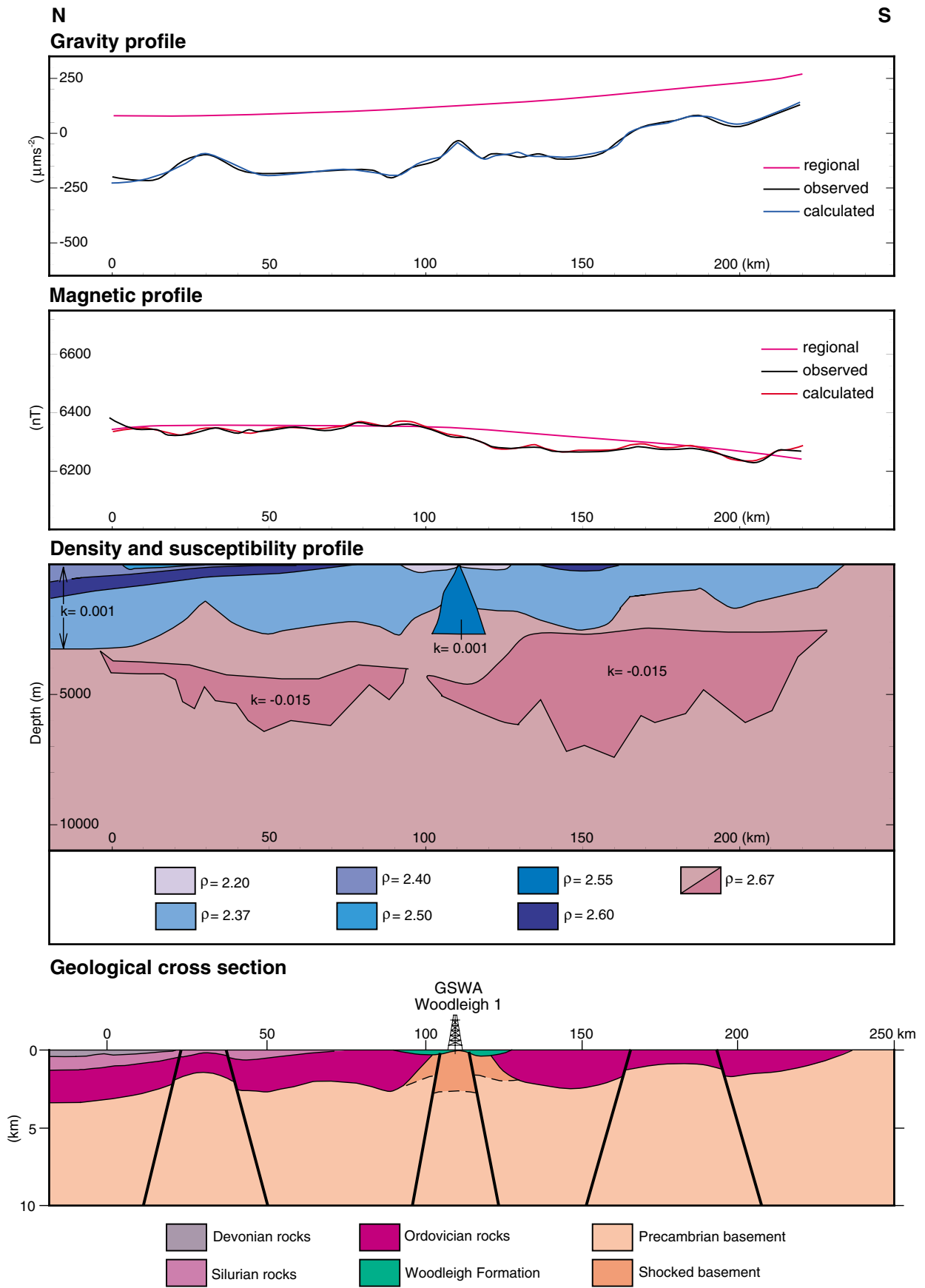


Figure 16. North-south two-dimensional gravity model and cross section of the Woodleigh impact structure. In the density and susceptibility profile, densities ( $\rho$ ) are in  $\text{g/cm}^3$  and susceptibilities ( $k$ ) are in SI units

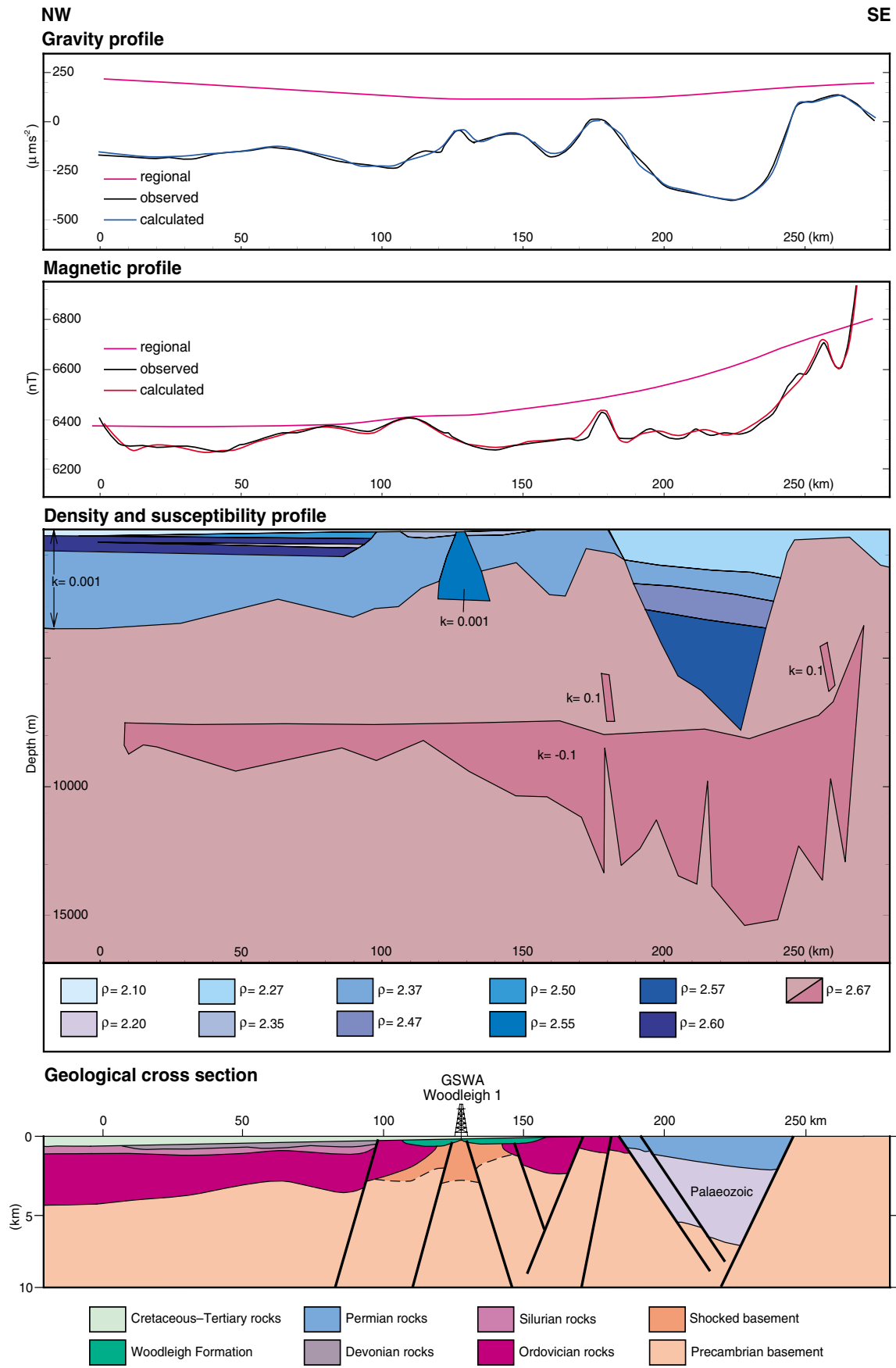


Figure 17. Northwest–southeast two-dimensional gravity model and cross section of the Woodleigh impact structure. In the density and susceptibility profile, densities ( $\rho$ ) are in  $\text{g}/\text{cm}^3$  and susceptibilities ( $k$ ) are in SI units

**Table 2. Density measurements of cores from GSWA Woodleigh 1 and 2A**

Depth (m)	Dry density (g/cm <sup>3</sup> )	Water-saturated density (g/cm <sup>3</sup> )	Lithology	Formation
<b>GSWA Woodleigh 1</b>				
192.10	2.43	2.45	granitoid	Precambrian basement
201.30	2.39	2.45	granitoid	Precambrian basement
225.90	2.34	2.42	granitoid	Precambrian basement
245.40	2.47	2.52	granitoid	Precambrian basement
266.70	2.72	2.76	biotite gneiss	Precambrian basement
289.30	2.46	2.52	granitoid	Precambrian basement
311.90	2.45	2.52	granitoid	Precambrian basement
333.00	2.43	2.50	granitoid	Precambrian basement
average	2.46	2.52		
<b>GSWA Woodleigh 2A</b>				
289.00	1.90	–	siltstone <sup>(a)</sup>	Woodleigh Formation
292.80	2.00	2.23	sandstone	Woodleigh Formation
317.09	2.53	2.57	sandstone	Woodleigh Formation
326.85	1.98	–	siltstone <sup>(a)</sup>	Woodleigh Formation
347.75	1.90	1.95	sandstone	Woodleigh Formation
387.26	1.88	2.13	sandstone	Woodleigh Formation
421.90	2.27	2.41	sandstone	Woodleigh Formation
456.94	2.01	2.23	sandstone	Woodleigh Formation
457.90	2.13	–	siltstone <sup>(a)</sup>	Woodleigh Formation
472.36	2.30	2.43	sandstone	Woodleigh Formation
486.00	1.99	–	siltstone <sup>(a)</sup>	Woodleigh Formation
496.05	2.02	2.23	sandstone	Woodleigh Formation
500.95	1.95	2.18	sandstone	Woodleigh Formation
521.96	2.01	2.23	diamictite	Unnamed paraconglomerate
529.93	2.08	2.27	diamictite	Unnamed paraconglomerate
544.05	2.07	2.27	diamictite	Unnamed paraconglomerate
563.15	2.11	2.30	diamictite	Unnamed paraconglomerate
582.49	2.14	2.32	diamictite	Unnamed paraconglomerate
589.00	2.13	2.38	dolomite breccia	Unnamed breccia
608.25	2.43	2.57	dolomite	Dirk Hartog Group
617.75	2.65	2.73	dolomite (gypsiferous)	Dirk Hartog Group

**NOTE:** (a) Siltstone samples disintegrated in water after several hours

Gascoyne Platform. These layers are constrained by geophysical log and core density measurements available from eight drillholes within or near the structure (Table 1, Fig. 1). The values in Table 1 represent weighted average densities for the formations penetrated by the respective drillholes. For GSWA Woodleigh 1 and 2A the values given in Table 1 are the averages of the core measurements in Table 2. The densities listed at the bottom of Table 1 are those used in the gravity model for the Gascoyne Platform. For the Byro Sub-basin to the east of the Woodleigh impact structure, where there are no available density data, density was increased with depth over four layers from 2.27 to 2.57 g/cm<sup>3</sup> in increments of 0.1 g/cm<sup>3</sup>. The thickness of each density layer was constrained by an interpreted depth to crystalline basement, interpreted from seismic data (Mory et al., 1998a).

Drillcore from GSWA Woodleigh 1 show that the impact has reduced the density of basement from 2.67 g/cm<sup>3</sup> (typical density for crystalline rocks) to about 2.52 g/cm<sup>3</sup> (Table 2), probably due to fracturing and shock vitrification with the associated introduction of volatile components. Within the central uplift, an inner core of lower density granite was modelled with a diameter of

2 km at its shallowest point and 10 km at a depth of about 2.5 km. The adjacent layer surrounding the inner core, represented by a density of 2.37 g/cm<sup>3</sup>, represents a highly brecciated, low-density crystalline basement (Fig. 15), making the central uplift 20–25 km wide. In the east–west gravity model there are broad flexures that decrease in amplitude with increasing distance from the centre – a style of deformation distinct from the fault-block structures in the Byro Sub-basin to the east (Figs 15 and 17). The Woodleigh impact structure is asymmetric in a northwesterly direction, with basement at a depth of 1–1.7 km to the east, and 3.1–3.6 km to the west (Figs 15 and 17). This asymmetry is interpreted as a structural dip to the northwest with an azimuth of 303°. A northerly trending regional dip is observed throughout the Southern Carnarvon Basin (Iasky and Mory, 1999) and is attributed to uplift and erosion along the eastern margin of the Gascoyne Platform, during the separation of Australia and Greater India in the Early Cretaceous. Near the Woodleigh impact structure, this tectonism is probably responsible for reactivation along the Madeline Fault.

Depth to crystalline basement in the north–south gravity model (Fig. 16) is shallower than in the western

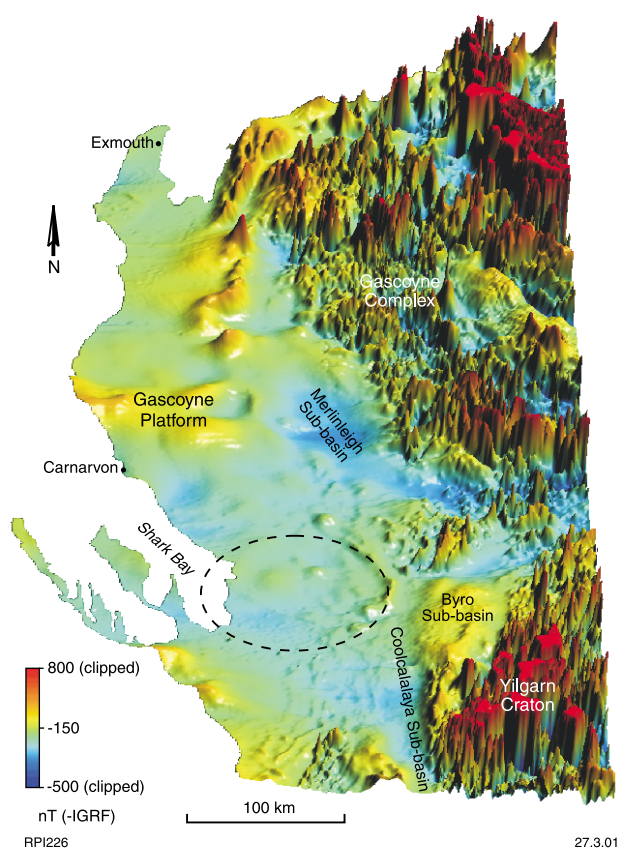


**Figure 18.** Oblique view from the south of the total magnetic intensity image of the Southern Carnarvon Basin (data from BMR/AGSO; -IGRF = International Geophysical Reference Field removed)

part of the east-west model because the profile traverses the western edge of the Wandagee-Ajana Ridge. The prominent symmetrical 'highs' 70–80 km from the centre of the Woodleigh impact structure are inferred to be gently folded basement rocks, probably pre-dating the impact. The regional northerly dip of the Gascoyne Platform (Iasky and Mory, 1999) is also evident in this model. In the centre of the structure, the low-density granite is modelled as a basement uplift of about 25 km in diameter, consistent with that interpreted in the east-west model.

## Magnetic surveys

### Airborne magnetic surveys

The magnetic signature of impact structures is less predictable than the gravity signature because of the much greater variation in the magnetic properties of rocks. It can vary depending on the composition of original rock types, degree of basement involvement, and post-impact hydrothermal effects (Pilkington and Grieve, 1992). A magnetic anomaly can be expected at the core of the central uplift due to magnetite crystallization from the high pressure and temperature produced by the impact. However, these anomalies may be too small to be resolved by airborne surveys and may not provide any distinguishable features, as shown, for example, by the aeromagnetic image of the Gosses Bluff impact structure (Fig. 14). Ground magnetic

surveys, however, show high-frequency anomalies not detected by the airborne magnetic survey (e.g. Gosses Bluff –Milton et al., 1996; and Manicouagan, Canada –Grieve and Pilkington, 1996). The predominant effect is a magnetic low (Clark, 1983; Hart et al., 1995; Scott et al., 1997), although a central dipolar anomaly is common in many impact structures with a diameter of more than 40 km (e.g. Tookoonooka, Fig. 10).

The Woodleigh impact structure is covered by a BMR regional airborne magnetic survey flown in 1956 over most of the onshore Southern Carnarvon Basin (Fig. 18). This survey was flown with a line spacing of one mile (~1600 m) at a height of 500 ft (~150 m). It is difficult to identify the impact structure from this dataset because high-frequency anomalies are not resolved and most of the southern Gascoyne Platform corresponds to a broad magnetic low (Figs 18 and 19). The most noticeable feature that may be associated with the eastern margin of the structure is an arcuate low-amplitude (about 130 nT), medium-frequency anomaly that covers an arc of almost 90° (Fig. 19). Similarly, the Shoemaker impact structure has an arcuate magnetic anomaly along its southeastern margin (Fig. 10). The arcuate magnetic anomaly along the eastern margin of the Woodleigh impact structure is probably related to the structure's eastern margin bounding fault. The restriction of this magnetic anomaly to the eastern margin may be due to the presence of magnetic material in the Ajana and Wandagee Ridges, but not in other basement features abutting the Woodleigh impact structure. Any tectonic activity along the ridges would have activated existing faults along the eastern margin of the structure. These ridges have been active at least up to the Late Miocene (Iasky et al., 1998a; Iasky et al., 1998b). Superimposing the drainage pattern over the total magnetic intensity image (Fig. 20) shows a drainage divide coincident with the eastern and southeastern margin and an overlapping creek system along the northwestern margin of the structure. This coincidence along the eastern margin of the structure implies that the margin-bounding fault may have been recently reactivated, probably in the Miocene when the region was subjected to east-west compression associated with the collision of the Australian and Indonesian Plates (Iasky and Mory, 1999).

Another prominent anomaly on the magnetic images (Figs 18 and 19) is a high-frequency northwesterly trending lineament, which traverses across the south-western quadrant of the Woodleigh impact structure. The lineament is probably the expression of a fault, which coincides with the northwesterly trending coastline, and is unrelated to the Woodleigh impact structure.

### Ground magnetic surveys

A small ground magnetic survey was carried out because the BMR regional aeromagnetic data were not at an appropriate spacing to reveal a central magnetic high. A central magnetic high is typical of many impact structures, for example, Chicxulub (Mexico), Vredefort (South Africa), Manicouagan (Canada), Saint Martin (Canada), and Dellen (Sweden; Pilkington et al., 1994; Grieve and Pilkington, 1996; Grieve and Pesonen, 1996). Magnetic data were acquired for five east-west traverses

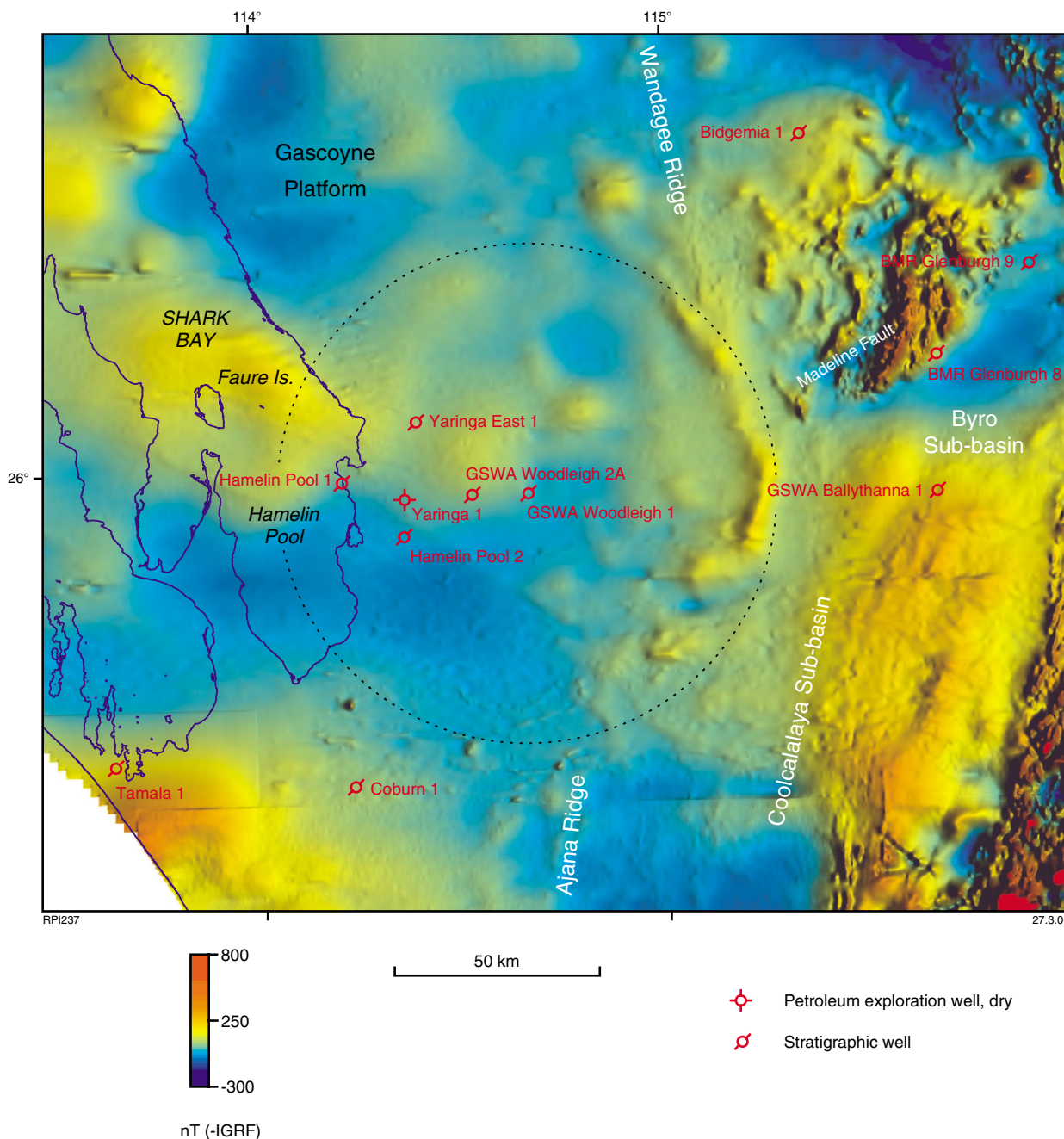


Figure 19. Total magnetic intensity image of the Woodleigh impact structure (data from BMR/AGSO; -IGRF = International Geophysical Reference Field removed)

and one north-south tie line over the centre of the Woodleigh impact structure (Fig. 21), and a regional east-west traverse from GSWA Woodleigh 2A to about 9 km east of GSWA Woodleigh 1 (Figs 22 and 23; Appendix 1).

The survey lines over the centre of the structure (Fig. 21) show a negative magnetic anomaly north of GSWA Woodleigh 1 and a positive anomaly to the southwest, forming what could be a dipole response with a 1500 m wavelength. A similar central magnetic signature is observed within the Acraman structure in South Australia (Williams et al., 1996), and is typical of impact structures with diameters of more than 40 km (Pilkington and Grieve, 1992). With such a small survey, however, the

relationship between the anomalies is ambiguous, and they could equally well be derived from a number of sources.

The regional east-west traverse (Fig. 22) shows a broad 10 nT negative anomaly near GSWA Woodleigh 1 at the centre of the impact structure. This traverse also shows a 15 nT high-frequency anomaly 4 km east of GSWA Woodleigh 2A that has no apparent man-made source and is not evident in the regional BMR data (Fig. 19). This traverse also indicates some low- and medium-wavelength anomalies over the centre of the structure not resolved in the regional BMR aeromagnetic data.

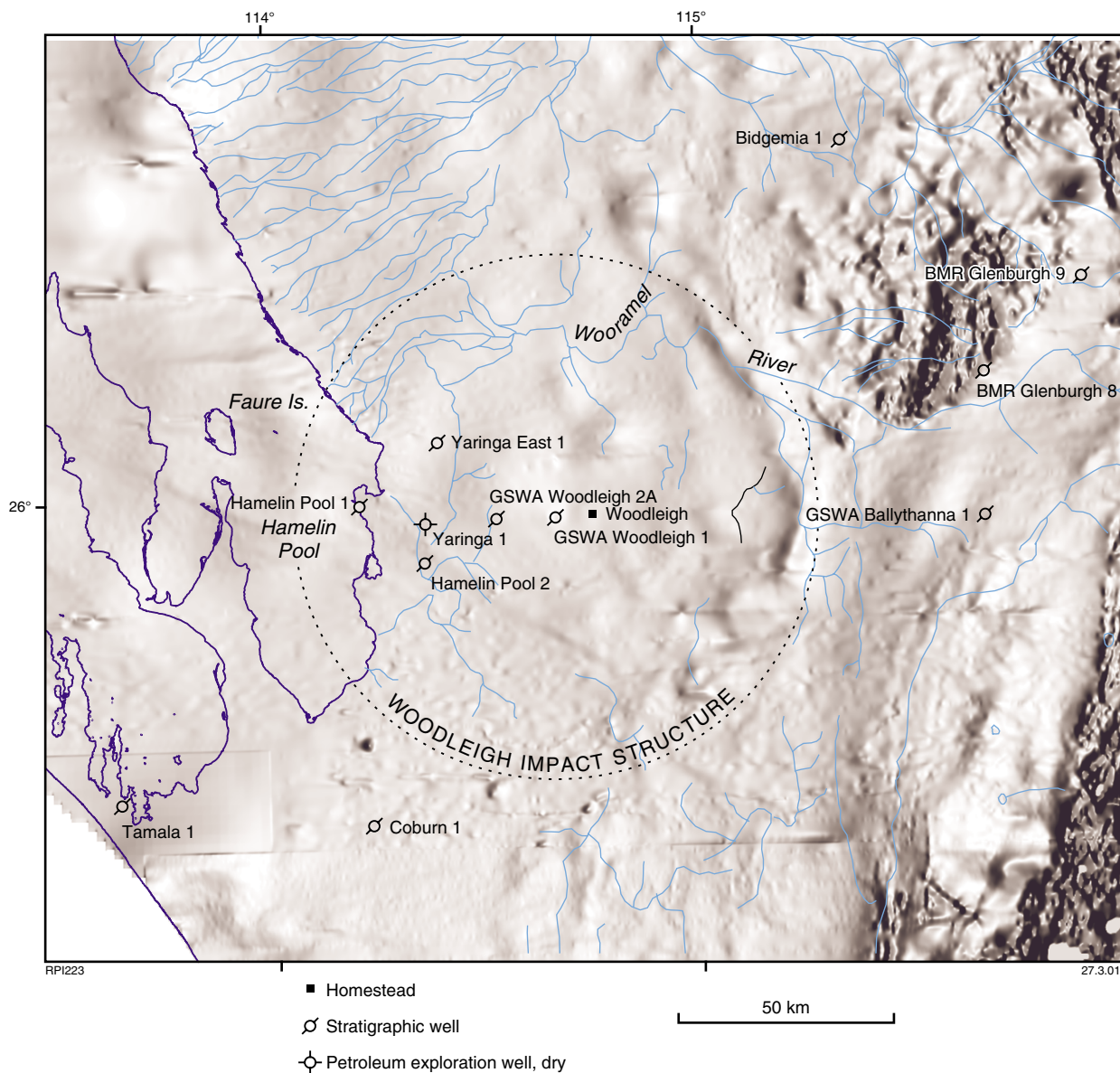


Figure 20. Drainage pattern superimposed on a grey-scale total magnetic intensity image of the Woodleigh impact structure (data from BMR/AGSO)

### Magnetic modelling

Two-and-a-half-dimensional magnetic models were produced (using Modelvision Pro software) for profiles across the Woodleigh impact structure along the same traverses as the gravity models (Figs 15-17). A regional magnetic curve was matched to the profile using a second-degree polynomial, and residual anomalies were modelled relative to a zero-background magnetic susceptibility. There are few constraints on the susceptibility contrast because there are no known measurements of susceptibility for crystalline basement rocks of the Southern Carnarvon Basin. Therefore, the magnetic susceptibility values used in the modelling were consistent with those of sedimentary and igneous rocks, which ranged from 0.001 to 0.1 SI (Telford et al., 1990). All models show that the source of the magnetic anomalies, which have long wavelengths, is deep within the basement.

The 100-120 nT magnetic anomaly at the eastern margin of the Woodleigh impact structure (Figs 15 and 17) corresponds to the arcuate anomaly on the magnetic image (Fig. 19). It can be modelled as an intrusive body along the margin fault. Three traverses, about 30 km in length, across the arcuate magnetic anomaly were used to model an intrusive body (Fig. 23). The traverse points were extracted from a grid of the BMR 1956 aeromagnetic data and a regional magnetic curve was fitted to the regional profile using a second-degree polynomial. The best fit was achieved with a tabular body at a depth of about 5 km, dipping at 58° to the west, and with a magnetic susceptibility contrast of 0.025 SI (Fig. 23). The dip of the body is consistent with a circular fault, bounding the crater margin, that dips towards the centre of the structure (cf. Grieve and Pilkington, 1996, fig. 2).

The east-west regional ground magnetic traverse, which extends from GSWA Woodleigh 2A to 9 km east of

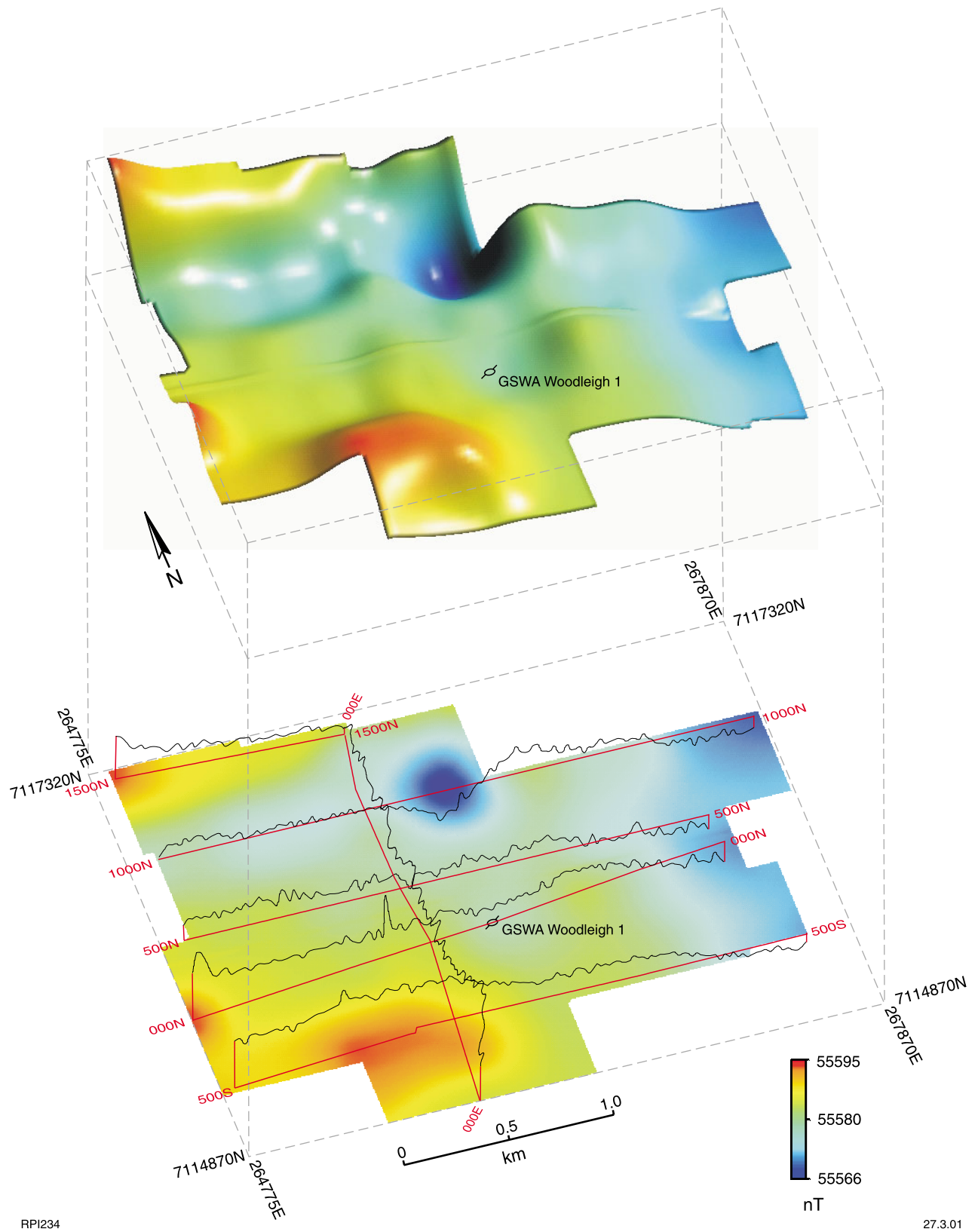


Figure 21. Image of the reconnaissance ground magnetic data over the centre of the Woodleigh impact structure



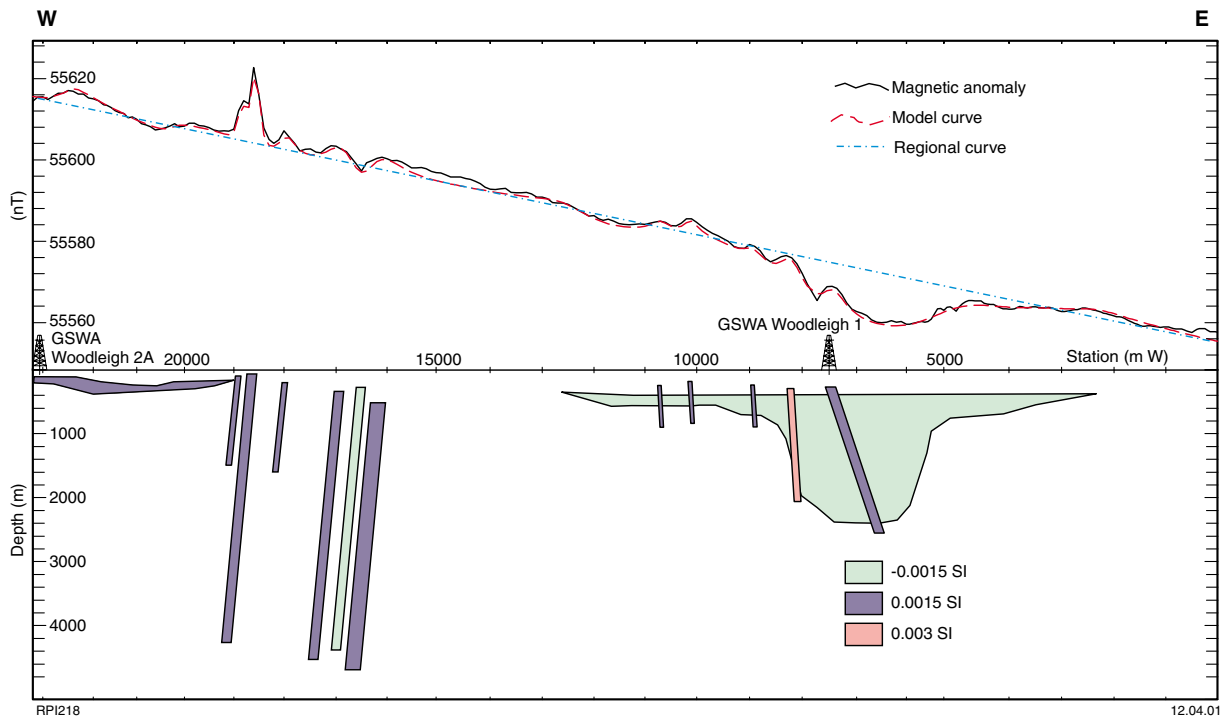


Figure 22. Regional ground magnetic traverse (top) and magnetic model (bottom) of the centre of the Woodleigh impact structure (see Figure 23 for location)

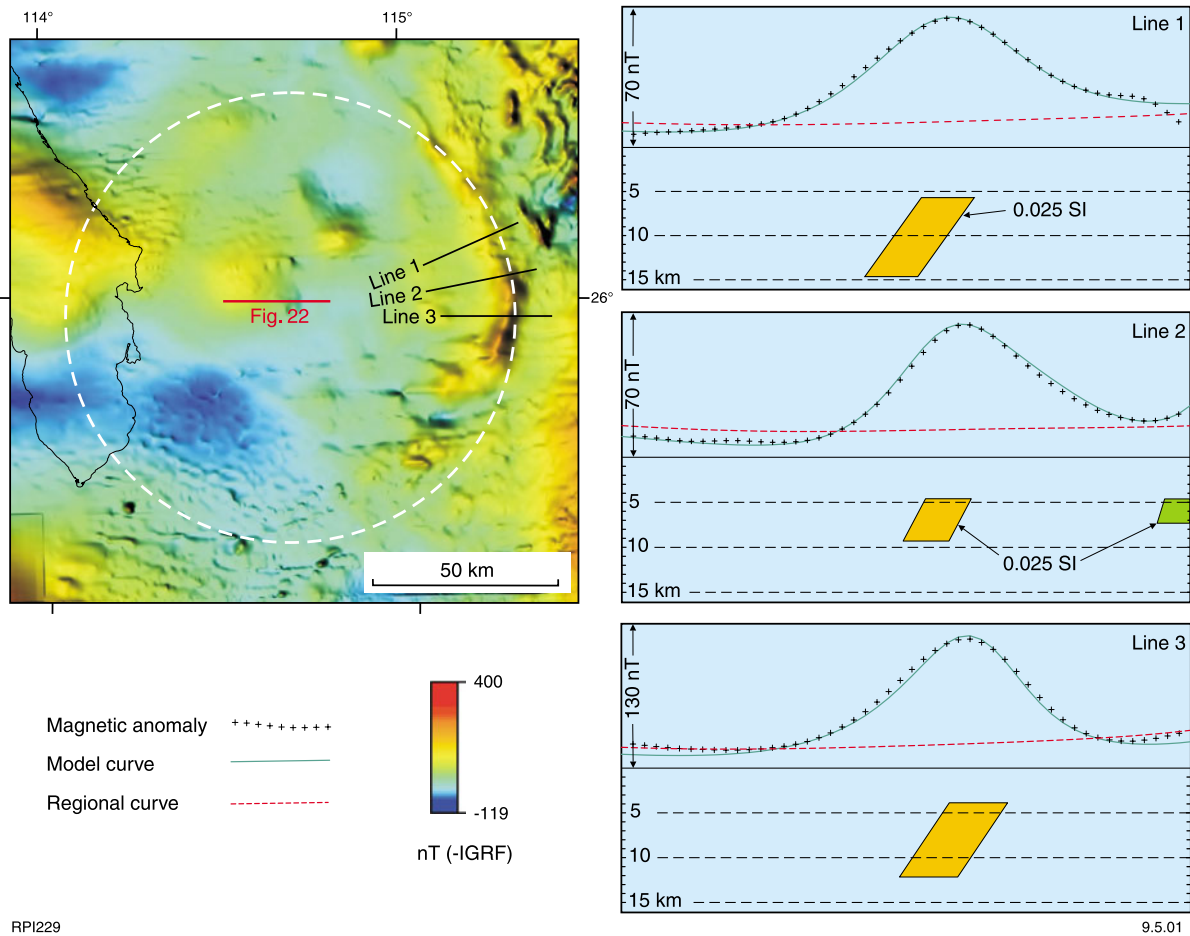
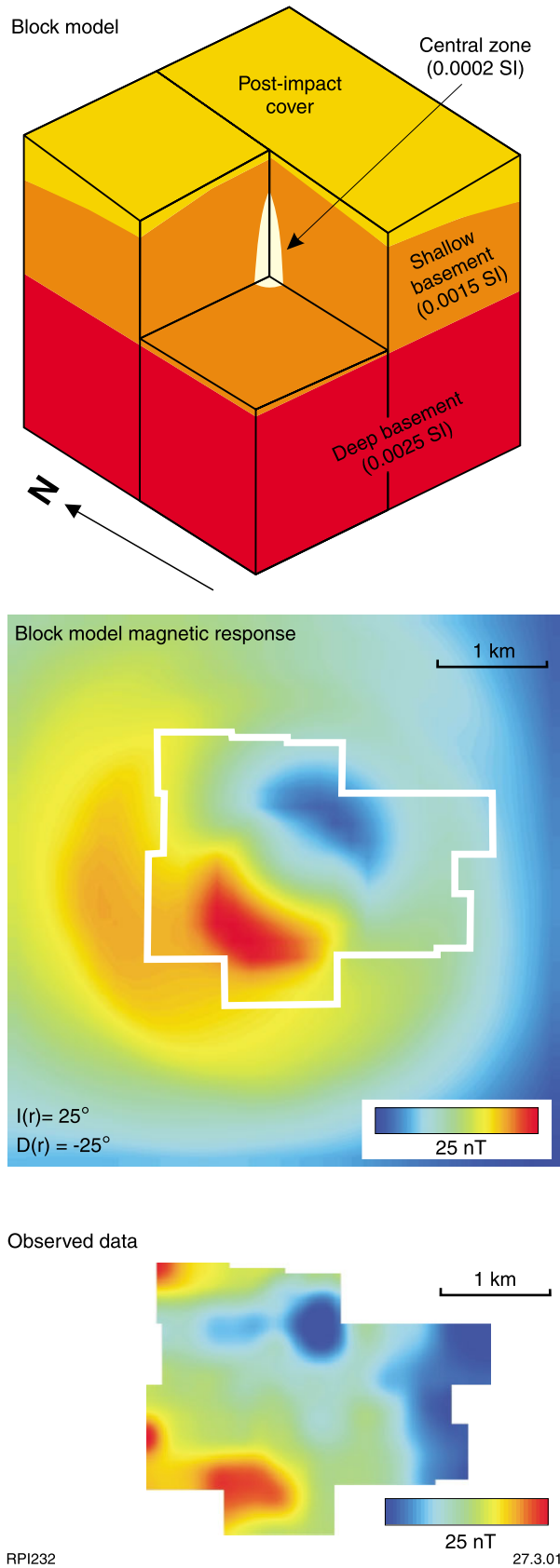


Figure 23. Magnetic model of arcuate anomaly on the eastern margin of the Woodleigh impact structure (-IGRF = International Geophysical Reference Field removed)



**Figure 24. Magnetic model for a central magnetic dipole anomaly of the Woodleigh impact structure**

GSWA Woodleigh 1 (Fig. 22), was modelled using a depth constraint of about 200 m to the granitic central uplift. The broad negative magnetic anomaly around the centre of the structure can be explained by a reduced magnetic susceptibility relative to the surrounding rocks. A negative magnetic response is typical of complex impact structures (Clark, 1983; Hart et al., 1995; Scott et al., 1997). At the point of impact, peak pressures of about 1 GPa can demagnetize and remove existing remanent magnetization, and pressures of more than 10 GPa can reduce levels of susceptibility (Cisowski and Fuller, 1978). For the Woodleigh impact structure, PDFs in drillcore samples from GSWA Woodleigh 1 indicate that pressures exceeded 14 GPa (Mory et al., in prep.). The observed magnetic profile in Figure 22 has short wavelength anomalies that have been modelled as dipping bodies with moderately low levels of magnetic susceptibility (0.0015–0.003 SI). These are interpreted as concentrations of magnetic material along fractured planes caused by the impact. The positive high-frequency anomaly at 19 000 m on this traverse (Fig. 22) is coincident with the inner annular gravity ridge at about 12 km radius from the centre of the structure (Fig. 3). This magnetic anomaly probably represents magnetic material intruding the ring fault at the western edge of the central uplift, which was previously interpreted (Iasky and Mory, 1999) as a northerly trending fault on the pre-Cretaceous subcrop geology map (Fig. 7).

Three-dimensional modelling (Fig. 24) was carried out to test whether the magnetic anomalies detected from the ground magnetic traverses (Fig. 21) could be generated by a single body (dipole response). Depth to basement, shape of the magnetic body, and regional tilt from the gravity modelling helped constrain the three-dimensional modelling (using Encom’s Noddy software). The best fit was obtained using a model in which the central basement uplift is divided into three distinct magnetic zones: deep basement (below 2300 m), shallow basement (200–2300 m), and a central narrow paraboloidal zone within shallow basement (800–2300 m). In addition, the central basement uplift is covered by 200 m of non-magnetic sedimentary rock. The entire model has been given a regional northwest tilt of 5° at an azimuth of 303° (Fig. 24), consistent with the gravity profiles. A remanent magnetization ( $I_{rem} = 25^\circ$ ,  $D_{rem} = -25^\circ$ ) for the central uplift region was required to obtain a fit to the observed data. In the model, the intensity of remanent magnetization decreases from the centre, consistent with central uplift regions (Grieve and Pilkington, 1996). This was done by applying a dominant remanent intensity to the central zone, weak remanent intensity to the shallow basement, and no remanence for the deeper basement (Fig. 24). The magnetic susceptibility was progressively reduced toward the centre of the model to reflect the zone of partial demagnetization that is typical in central uplift regions (Scott et al., 1997). This was done by assigning a value of 0.0025 SI to deep basement (based on the average susceptibility for granite; Telford et al., 1990), 0.0015 SI to the shallow basement, and 0.0002 SI to the central zone.

The best-fit model response (Fig. 24) has the same relative amplitude as the observed data and shows the

magnetic highs southwest and northwest of the ground survey, a circular magnetic low to the north, and a magnetic low along the eastern flank. The notable differences between the model response and observed data are the separation between the southwestern high and the circular low and the wavelength of the circular low. This may be a function of the simplicity of this model and probable anisotropy and variations in magnetic susceptibility within the central zone and surrounding basement. However, without extending the ground survey away from the central peak, it is difficult to determine whether the observed data represents a dipole or a multiple-body response.

The notion of a remanent magnetic field in the central uplift of the Woodleigh impact structure is confirmed by preliminary analyses of six drillcore samples of mafic gneiss from between 194.8 and 197.6 m in GSWA Woodleigh 1. These analyses show three remanence components: an unstable component demagnetized by 10 nT, an intermediate stability component preferentially demagnetized between 10 and 50 nT, and a steep downward component (Schmidt, P., CSIRO, North Ryde, written comm.). The analysis technique involved demagnetizing alternating fields using the least stable component to orient the core azimuthally, assuming it is the Earth's present magnetic field. With this technique the intermediate component appears to be directed shallowly down to the southeast, suggesting a Jurassic age for the remanent magnetic field. Analyses of additional samples, using thermal demagnetization, are yet to be undertaken. These preliminary results contrast with the Late Devonian K-Ar isotopic age of samples taken from clasts and matrix of the paraconglomerate near the base of the crater floor in GSWA Woodleigh 2A. If the impact was Late Devonian in age, the Jurassic palaeomagnetic result is puzzling because it is unlikely that the relatively undeformed rocks have been remagnetized after the impact event. Furthermore, vitrinite reflectance measurements, conodont colouration, and apatite fission-track analysis (Ghori, 1999) show that temperatures within the sedimentary section on the Gascoyne Platform did not exceed 150°C—well below the temperature necessary to remagnetize rock (550°C; Telford et al., 1990).

## Seismic interpretation

Seismic reflection data can provide detailed information on the subsurface geometry of impact structures. A diagnostic seismic character is the reduced coherency of reflections due to fracturing and fusion, particularly in the central uplift (Pilkington and Grieve, 1992; Milton et al., 1996; Dentith et al., 1999). The central uplift can commonly be distinguished by the presence of internal thrust faults and down faulting along its margin (Pilkington and Grieve, 1992). Away from the central uplift, the coherency of reflections increases and impact-generated flexures that extend outwards from the central peak die out before the crater rim, as exemplified by the Gosses Bluff (Milton et al., 1996, figs 7 and 8) and Chicxulub impact structures (Morgan and Warner, 1999b). With impacts on thick sedimentary successions, the coherency of reflectors increases with depth below the

central peak, indicating that much of the energy of the impact is absorbed in the top 3000–5000 m. Examples include the Yallalie structure in the Perth Basin (Dentith et al., 1999, fig. 7), Red Wing, USA (Pilkington and Grieve, 1992, fig. 16), and Gosses Bluff (Milton et al., 1996, figs 7 and 8). Crater rim faults are often more difficult to identify than the more obviously deformed central part of the structure because they are relatively shallow structures and therefore more readily eroded. However, depending on the quality of the seismic data, they can be detected if there has been only minor erosion (as seen in the offshore seismic data over the Chicxulub impact structure; Morgan et al., 1997).

The sparse seismic data over the Woodleigh impact structure (Fig. 9) are from 1965 and of average to poor quality. The best coverage is semi-detailed over the trough west of the central uplift where Conoco drilled Yaringa 1 (Fig. 9). The remainder of the structure has only regional coverage and includes an east-west line crossing the northwestern margin (YY65T-014; Fig. 25), a north-south line extending north from the centre (W65G-002; Fig. 26), and three adjacent east-west lines extending across the centre of the structure to the edge of Shark Bay (W65G-003, W65S-003, W65T-003; Plate 1, Fig. 27).

Stratigraphic control for the seismic interpretation is provided by the drillholes along the western part of lines W65G-003 and W65T-003. The most distinguishable feature along this line is a package of coherent high-amplitude reflectors representing the Silurian Dirk Hartog Group (Fig. 27, Plate 1). This package is also easily recognizable on line YY65T-015 (Fig. 28), but is not as obvious on line YY65T-014 (Fig. 25). Basement is interpreted at about 2 seconds on line YY65T-014, as the base of the high-amplitude reflectors, which probably correspond to the Tumblagooda Sandstone. On all sections, basement is characterized by incoherent low-amplitude reflectors, indicating its unlayered nature, although multiples emanating from the shallower part of the section can be misleading, particularly on line W65G-003 (Fig. 27). A further constraint to the depth of basement, albeit imprecise, is the depth determined from the gravity modelling. The two-way time to basement is entirely dependent on the stacked velocity of the seismic data, which may not represent the true velocity of the strata, therefore adding a degree of imprecision to depth conversions. The seismic horizon for the base of the Cretaceous was interpolated from well picks, assuming a 200 m-thick succession and subhorizontal dips. Similarly, the top of the Kopke Sandstone horizon was also interpolated from well picks, assuming a conformable relationship with the underlying Dirk Hartog Group. The horizon representing the base of the Woodleigh Formation is based on the thickness penetrated in Woodleigh 2A (Fig. 8) and its presence in nearby water bores (Fig. 9; Appendix 1).

Line YY65T-014 (Fig. 25), about 25 km north of line YY65T-015, is almost entirely positioned within the outer ring trough (Fig. 9). Little deformation is evident below the first 0.7 seconds of the section and, as in line YY65T-015, the upper part of the section was not imaged in the processing. The strata in the section have a regional westerly dip and three easterly dipping normal faults are

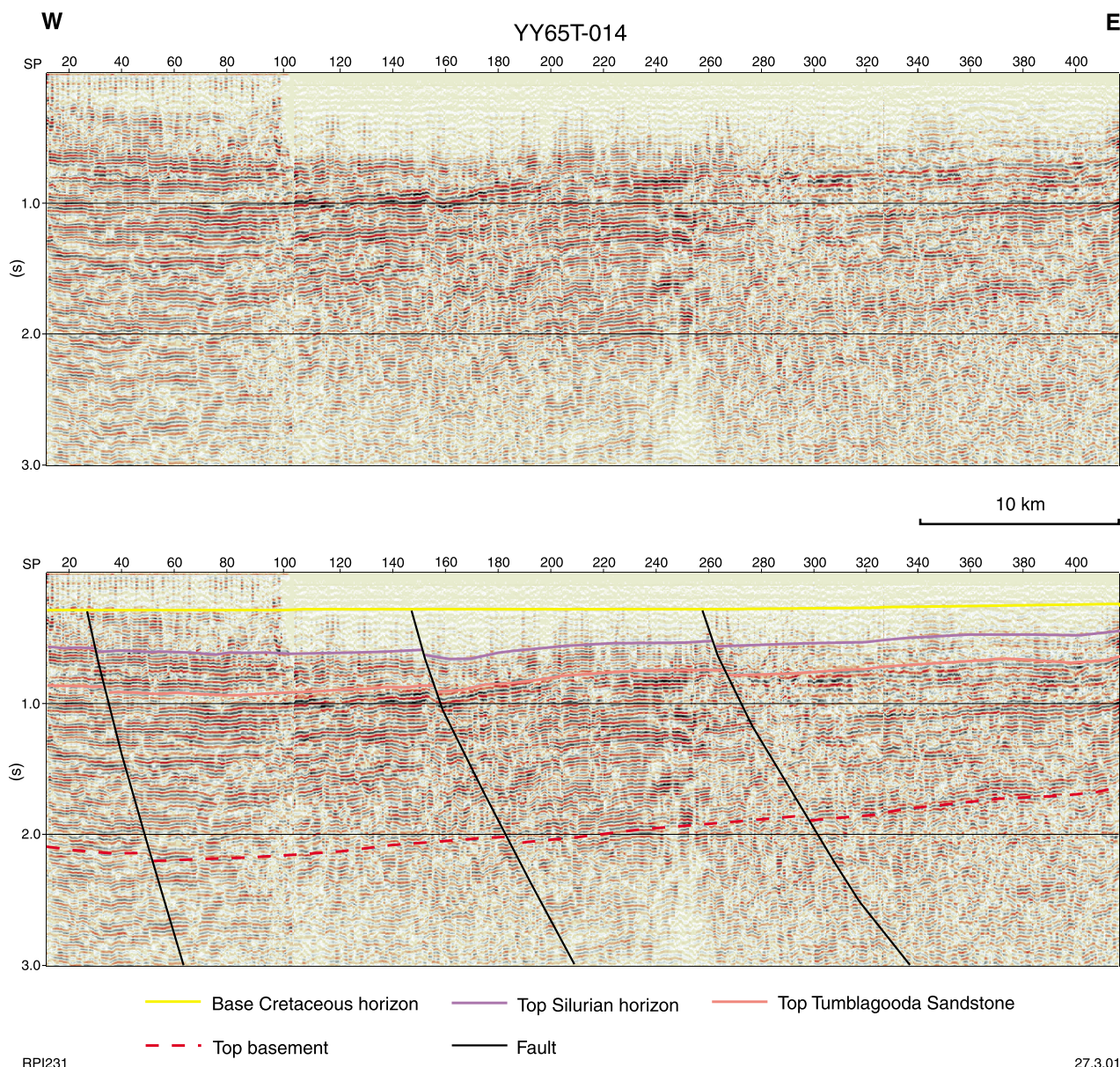


**Figure 25. East-west seismic section (line YY65T-014) across the northwestern margin of the Woodleigh impact structure (see Figure 9 for location)**

interpreted at SP 25, SP 145, and SP 255. At the Palaeozoic levels the most significant of these faults is at SP 145, but the SP 25 fault is most likely to represent the crater rim fault.

Line W65G-002A (Fig. 26) starts about 7 km west of the centre of the structure and extends north for about 35 km (Fig. 9). The southern part of the line (SP 1 to SP 80) shows incoherent reflectors over the central uplift. A flexure marking the edge of the central uplift is evident at SP 83 to SP 90, about 17-18 km from the centre of the structure. The fault at SP 87 is probably associated with the inner gravity ridge, and correlates with the fault interpreted on line W65G-003 at SP 410 (Fig. 27). Immediately outside this ring fault on line W65G-002 is a trough, also identified on line W65G-003, corresponding

to the annular gravity 'low' about 20 km from the centre of the structure. Gentle fault-bounded flexures continue north to about SP 108, about 34 km from the centre of the structure, coincident with the outer circular gravity ridge (Figs 9 and 13) and are imaged as the anticline into which Yaringa 1 was drilled on line W65G-003 (Fig. 27). Farther north on line W65G-002, cohesive reflectors become apparent with the degree of deformation decreasing into the outer ring trough.

The east-west section across the centre of the structure (Fig. 27, Plate 1) shows a series of easterly dipping reflectors on the eastern end, subhorizontal folded reflectors on the western end, and chaotic reflections in the central part of the seismic line. The easterly dipping Madeline Fault (Plate 1; immediately east of Fig. 27) is

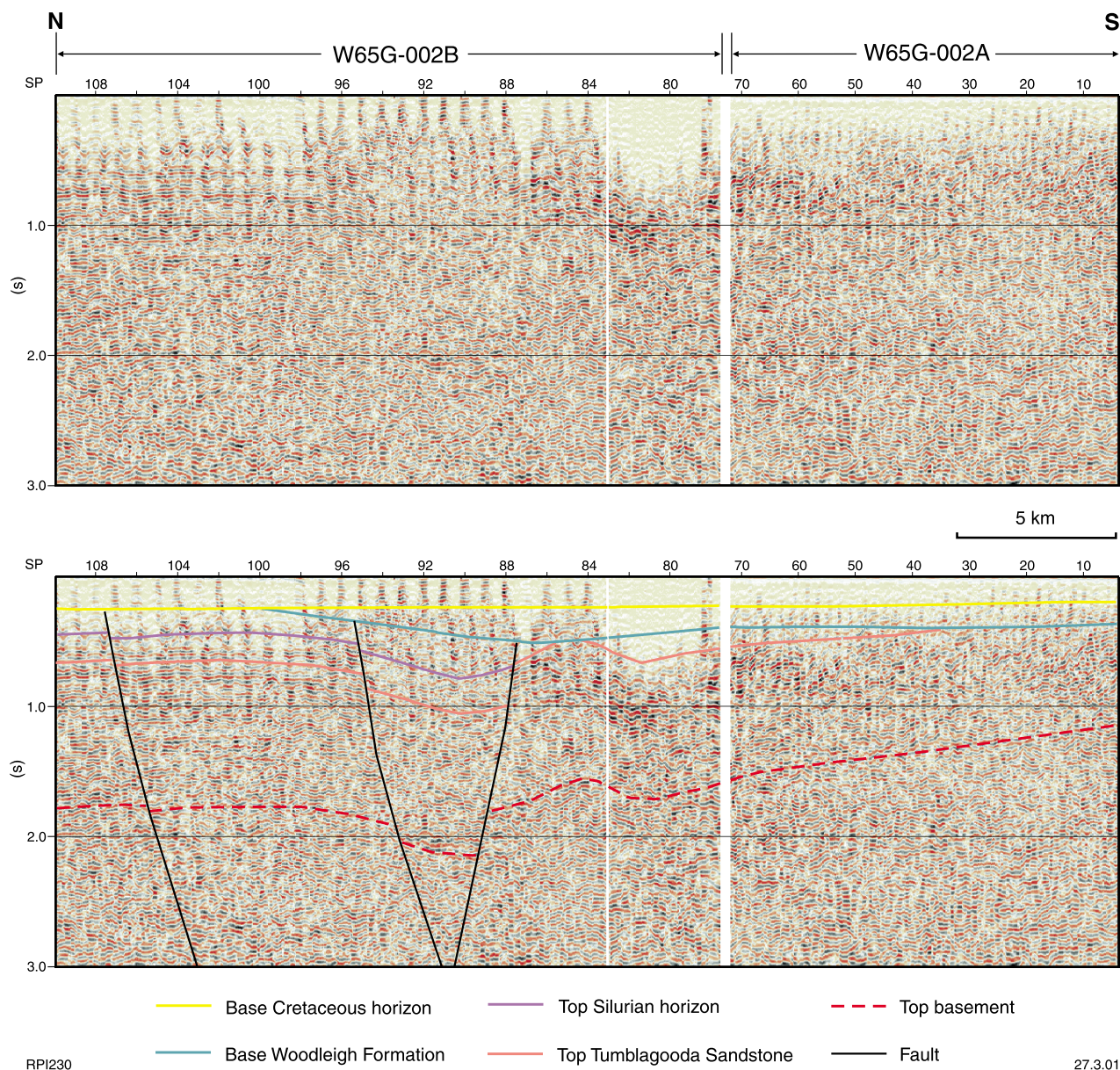


**Figure 26. North-south seismic section (line W65G-002), showing structural deformation across the northern half of the Woodleigh impact structure (see Figure 9 for location)**

interpreted immediately east of the interpreted crater rim, based on the extension of the fault from outcrop to the northwest and the dipping seismic character of the reflectors to the east. East of the Madeline Fault, the quality of data on line W65T-003, Fig. 27) varies depending on the coupling of seismic energy during acquisition, but westerly dipping faults antithetic to the Madeline Fault are evident in this area and differ from the style of deformation west of the Madeline Fault. Immediately east of the Madeline Fault, the section displays chaotic reflections, probably due to the unlayered nature of crystalline basement and fracturing caused by the impact. Based on the arcuate magnetic anomaly at the eastern crater rim (Fig. 23), a westerly dipping fault has been interpreted (Plate 1) at shot point (SP) 540-660 (line W65S-003 to W65T-003; Fig. 27). As there is no coherent reflector indicating the top of basement between SP 550

on line W65G-003 and SP 600 on line W65T-003, this level has been tentatively interpreted using the gravity model (Fig. 15) to rise and truncate at the base Cretaceous horizon (SP 890 on Fig. 27). Within this section there are some indications of steep dips towards the centre of the structure. Between SP 140 and SP 300 on line W65G-003, an anticline extends to about 34 km from the centre of the structure (Fig. 27). This impact-related flexure is coincident with the outer circular gravity ridge on the gravity image (Fig. 13).

Seismic line YY65T-015 (Fig. 28), north of and nearly parallel to line W65G-003 (Fig. 27), shows coherent reflections west of SP 145, about 23 km from the centre of the structure. East of this point, reflectors become less coherent as deformation is intense, but there are folded reflectors between SP 150 and SP 210 about 19 km from

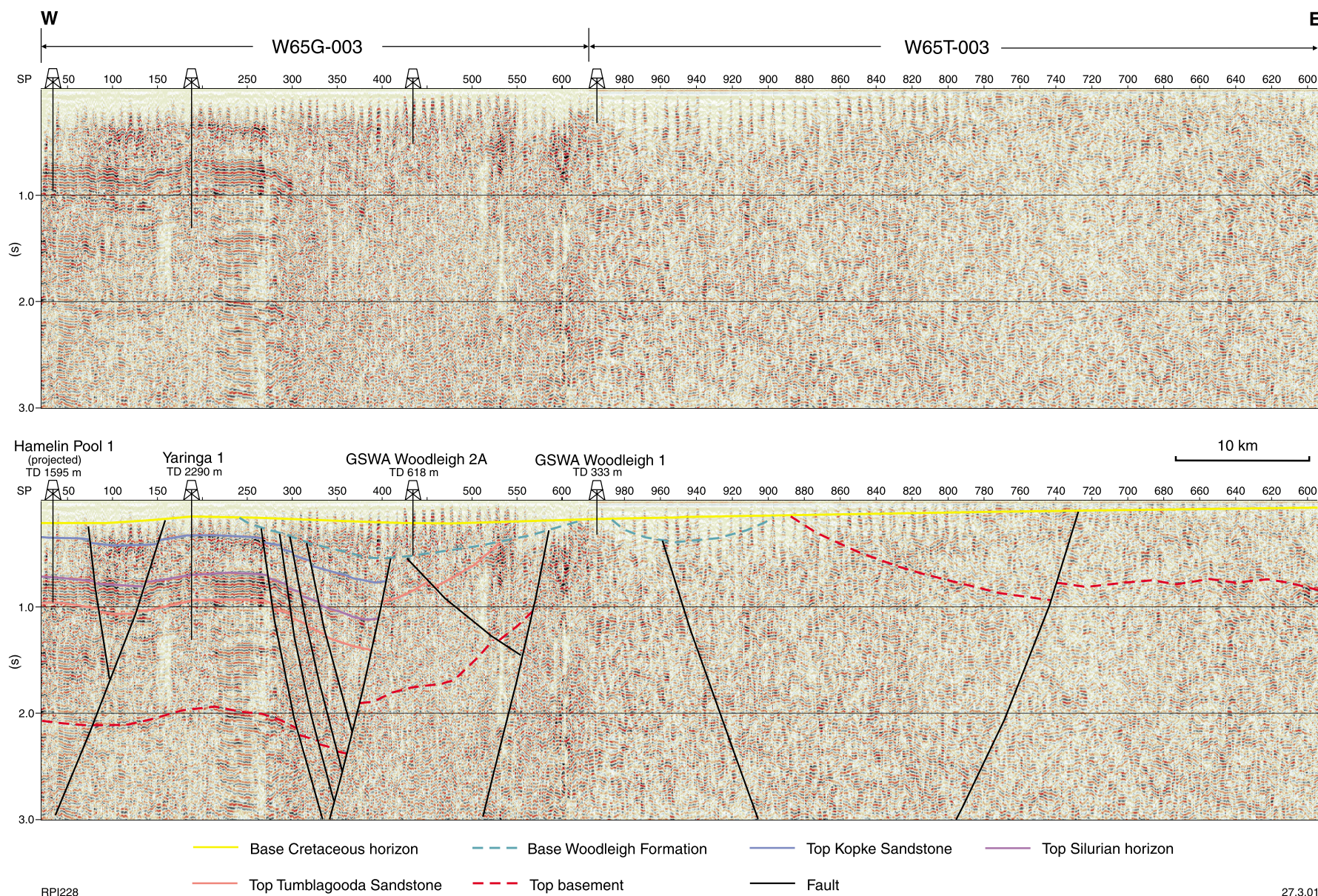
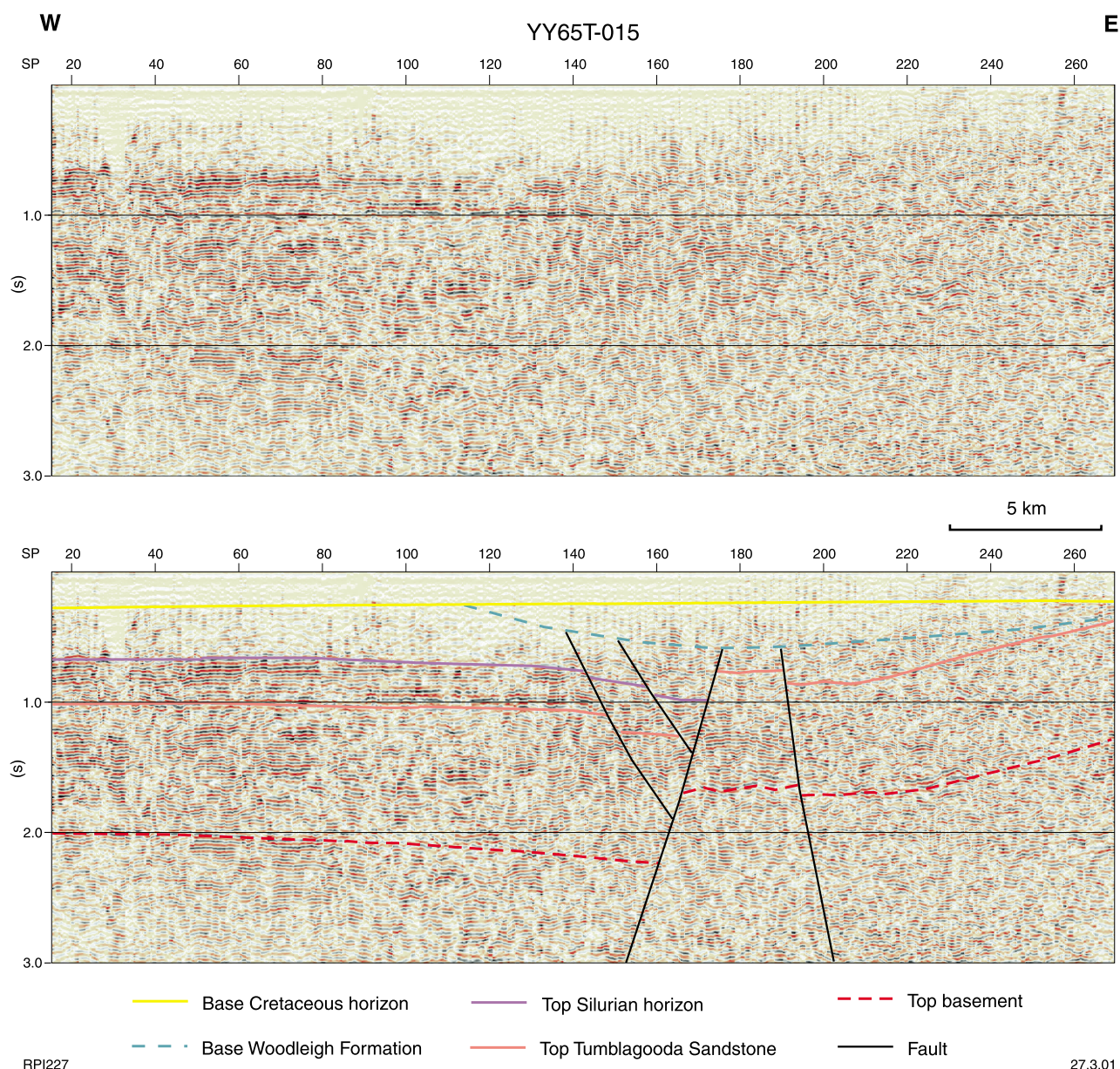


Figure 27. East-west seismic section (lines W65G-003 and W65T-003), showing the structure style across the Woodleigh impact structure (see Figure 9 for location)



**Figure 28. East-west seismic section (line YY65T-015), showing structural deformation in the western part of the Woodleigh impact structure (see Figure 9 for location)**

the centre of the structure, which correlate with the faulting down to the outer gravity trough also seen on line W65G-003 (Fig. 27). Between SP 10 and SP 140 on line YY65T-015, the package of reflectors representing the Silurian Dirk Hartog Group is recognizable and there is a small hint of the basement horizon. However, the first 0.7 seconds of the section was not imaged in the processing and it is not possible to recognize the base Cretaceous and base Woodleigh Formation horizons. These horizons have been extrapolated in this section.

## Discussion

The principal criterion used to delineate the diameter of the Woodleigh impact structure is the termination of regional structures, as defined by geophysics, in a zone

considered to mark the limits of impact deformation. This criterion is identical to that used in defining the size of the Chicxulub (Morgan and Warner, 1999a), Shoemaker (Pirajno and Glikson, 1998), and Lawn Hill (Shoemaker and Shoemaker, 1996) impact structures.

The 120-km diameter deduced for Woodleigh is based mainly on gravity data showing the terminations of the Ajana and Wandagee Ridges, as well as the arcuate positive magnetic anomaly coincident with a recent drainage, all about 60 km from the centre of the structure. The seismic data are not of sufficient quality to either prove or disprove the interpreted diameter, although zones of deformation are shown, consistent with the gravity image. The seismic data show intense deformation coincident with the central uplift, as inferred from the gravity data and structural highs and lows associated with

the annular gravity anomalies. The diffuse outermost annular gravity low corresponds to only minor faulting and folding on seismic line YY65T-014 (Fig. 25). This is consistent with seismic sections from other impact structures in sedimentary basins, such as Gosses Bluff (Milton et al., 1996) and Chicxulub (Morgan and Warner, 1999b), which show subhorizontal reflectors in the little-deformed outer annular zones.

The morphometric relationship between the rim-to-rim diameter of large craters and the diameter of their central uplift was estimated by Pike (1985) as  $D_{cp} = 0.199D^{1.058}$ , where  $D_{cp}$  is the diameter of the central peak, and  $D$  is the rim-to-rim diameter. Grieve and Pesonen (1992) produced a different relationship of  $D_{cp} = 0.31D^{1.02}$  based on measurements from a larger number of impact structures. The diameter of the central uplift region ( $D_{cp}$ ) for the Woodleigh impact structure is interpreted to extend to the inner annular gravity ridge (c on Fig. 13) at about 25 km diameter. Using this diameter, the diameter of the Woodleigh impact structure is calculated as 74 and 96 km using Grieve and Pesonen's (1992) and Pike's (1985) equations respectively, which are smaller than the interpreted diameter of 120 km. However, relationships between the central uplift region and diameter of the crater can vary considerably depending on the type of rocks involved in the collision and the amount of erosion of the original crater—the greater the erosion, the greater the apparent diameter of the conical central uplift. In particular, depth to crystalline basement and the rheology of both sedimentary and crystalline terranes are critical in determining the shape and elevation of the central uplift. The apparent depth ( $d_a$ ) of complex craters in crystalline terranes ( $d_a = 0.15 D^{0.43}$ ) is more than twice that for sedimentary basins ( $d_a = 0.12 D^{0.30}$ ; Grieve and Pilkington, 1996). Furthermore, it should also be noted that Grieve and Pesonen (1992) and Pike (1985) developed their empirical relationships from known complex craters, and there are few good-quality topographic data on the original dimensions of complex structures (Grieve and Pilkington, 1996). Most of these structures have had some degree of erosion, which produces a larger apparent diameter for the central uplift relative to the crater rim.

Using the Grieve and Pesonen (1992) relationship to determine the apparent depth of a crater in a sedimentary basin, the apparent depth for a crater 120 km in diameter is about 500 m. This depth is less than the 900–1100 m estimated by combining the thickness of the 379 m-thick infill section in GSWA Woodleigh 2A (Woodleigh Formation to the base of the unnamed breccia) and the estimated 500–700 m eroded from the top of this section (based on apatite fission-track analysis and geothermal history modelling by Gibson, 2000; Ghori in Mory et al., in prep.). The relationship for structural uplift ( $SU = 0.086D^{1.03}$ ; Grieve and Pilkington, 1996) indicates uplift in the order of 12 km for a structure with a diameter of 120 km. Unfortunately, this relationship cannot be used to prove or disprove the size of the Woodleigh impact structure because the original depth of the shock-metamorphosed granite at the centre of the structure (intersected in GSWA Woodleigh 1) is unknown.

The central gravity peak and the inner annular gravity trough about 10 km from the centre of the structure have

not been resolved satisfactorily by the seismic data, possibly because of the presence of shallow basement in this part of the structure. Within the inner annular gravity trough, brecciation probably increases along the circular fault bounding the basement plug thereby decreasing the density towards the margins of the central uplift. Seismic data reasonably delineate the profile of the western half of the Woodleigh impact structure, but the eastern half is more difficult to interpret because the images are poor over shallow basement. The western half has mostly coherent reflectors from the outer ring trough to the crater rim, whereas reflectors in the eastern half are chaotic to the edge of the structure, which is implied by an arcuate magnetic anomaly. The difference between the western and eastern halves of the structure may be a function of the thick sedimentary section on the western side of the structure compared to the shallow depth of crystalline rocks to the east, as inferred from the asymmetric gravity profile (Fig. 15).

The asymmetric gravity response of the structure is interpreted as a combination of low-density strata preserved by northwesterly tilting of the structure, and deeper heterogeneity within basement related to the Wandagee-Ajana Ridge. Early Cretaceous tectonism and the different styles of deformation in the adjacent terrains across the structurally elevated Wandagee-Ajana Ridge may explain the northwesterly tilt. Westward thickening of the Silurian succession across the Gascoyne Platform and the presence of Permian depocentres immediately to the east suggest that the Wandagee-Ajana Ridge had a long history as a basement high (Iasky and Mory, 1999). There is also evidence that the Wandagee Ridge was reactivated during the Early Cretaceous breakup of Australia from Greater India, and again in the Miocene (Crostella, 1995; Iasky et al., 1998a; Iasky and Mory, 1999). Breakup was a major event throughout the western margin of Western Australia and had a significant effect in the Southern Carnarvon Basin, particularly in the Merlinleigh and Byro Sub-basins. In the Gascoyne Platform, however, the effect of this deformation was relatively minor, and the Palaeozoic sedimentary succession now becomes progressively younger to the north (Fig. 7; Iasky and Mory, 1999).

## Conclusions

The Woodleigh impact structure is totally buried beneath 50–400 m of post-breakup Cretaceous to Holocene rocks, and can only be identified from geophysical and well data. The images of the gravity data (Figs 12 and 13) clearly show a series of concentric anomalies, suggesting a structure with an inner ring about 24 km in diameter that is interpreted as the central uplift portion of the impact structure. There is good coincidence between the concentric gravity lows and highs and the troughs and ridges identified on seismic sections within the Woodleigh impact structure. The gravity images indicate that the structure is at least 60–70 km in diameter based on an obvious circular gravity anomaly 30–35 km from the centre of the structure. However, a diameter of 120 km may be interpreted from the arcuate gravity anomaly in



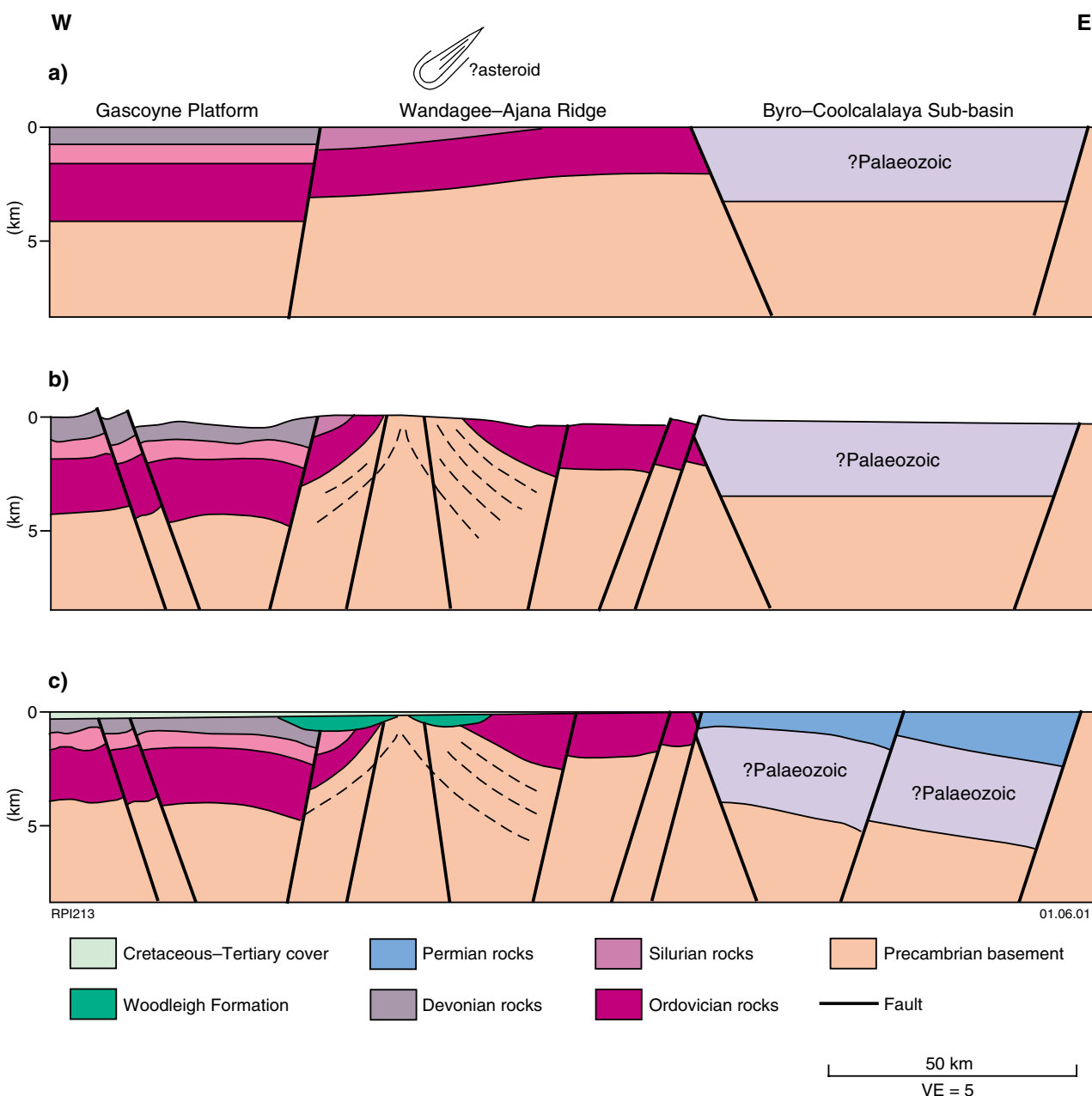


**Figure 29. Evolution of the Woodleigh impact structure, showing an east-west profile: a) pre-impact; b) shortly after impact; and c) at present**

the northwestern quadrant, the termination of the north-trending Wandagee and Ajana Ridges, and an arcuate magnetic anomaly (Fig. 19) on the eastern margin, all 60 km from the centre of the structure. The magnetic anomaly coincides with an arcuate drainage pattern, implying that the eastern margin fault has been reactivated recently. Gravity modelling indicates a central uplift area with basement rocks of lower density than average basement rocks, and away from the centre the undulating basement is interpreted as impact-related flexures. The ratio of the diameter of the inner gravity anomalies to the overall diameter of the Woodleigh impact structure is similar to that of Gosses Bluff, thereby indirectly supporting the 120-km diameter interpreted for Woodleigh.

The impact structure exhibits a subdued negative magnetic response, implying demagnetization due to the impact. Magnetic modelling across the structure is poorly constrained, but modelling indicates that magnetic sources are within basement and there is remanent magnetization at the centre of the structure. Seismic data show little deformation of the strata from the western half of the external ring trough, 30-35 km from the centre, to the edge of the structure. The eastern half of the structure has an incoherent seismic signature, implying that the nature of the terrain differs from the western half. It is possible that the impact occurred on the western edge of a continuous ridge (Wandagee-Ajana Ridge) and that the thicker sedimentary section to the west, being more ductile than the section with shallow crystalline basement

to the east, was deformed differently and produced an asymmetric gravity profile. However, a significant component of the asymmetric gravity profile is probably due to the post-impact tectonism, which reactivated faults along the Wandagee–Ajana Ridge and tilted the structure (and the rest of the Gascoyne Platform) to the northwest. Consequently, the ring synclines filled with low-density Jurassic sediments were preserved only on the western side of the structure, whereas the upthrown southeastern side of the structure was eroded, thereby diminishing the clarity of the gravity anomaly to the southeast.

Existing borehole data show that the Woodleigh Formation has an irregular distribution, which may be a function of erosion following long-term, post-impact isostatic adjustments of the low-density impacted aureole and regional tectonic episodes. However, most of these bores are within the southeastern quadrant of the structure and few samples are available. An apatite fission-track analysis of a sandstone from the base of the Woodleigh Formation in GSWA Woodleigh 2A shows that the base of the formation has been uplifted by about 700 m (Gibson, 2000). More analyses are necessary to confirm this estimate and to show which part of the structure underwent the greatest uplift.

The maximum likely age for the impact is Late Devonian, based on the regional stratigraphy and K–Ar isotope dating of samples from GSWA Woodleigh 1 and 2A. A minimum age is defined by the earliest Jurassic lacustrine infill (Woodleigh Formation). A more precise age for the impact cannot be determined from the regional stratigraphy because the youngest, clearly pre-impact strata preserved near the structure are Middle Devonian in age.

At the time of impact the Wandagee–Ajana Ridge was probably a continuous basement high (Fig. 29a). After impact (Fig. 29b) there would have been some isostatic adjustment due to the low density of the impact aureole. The period of adjustment is unclear, but there may have been several stages of uplift and subsidence, which must have ceased by the Early Jurassic when the crater was

infilled by lacustrine sediments (Woodleigh Formation). In the Early Cretaceous, the breakup of Australia from Greater India tilted the structure to the northwest, probably pivoted by tectonic movements along the Wandagee–Ajana Ridge. Geothermal history modelling together with apatite fission-track analysis data indicate that during this period the crater was uplifted and eroded by 500–700 m (Gibson, 2000; Ghori in Mory et al., in prep.), minimizing the distribution of the Lower Jurassic crater infill to mainly the central part of the structure. However, pockets of crater infill may be preserved farther from the centre of the structure. The final stage of the crater's evolution was shallow burial, commencing with the Early Cretaceous marine transgression (Fig. 29c).

The acquisition of more-detailed geophysical data than presently available and further drilling is required to obtain a better structural definition of the Woodleigh impact structure. More specifically, a high-resolution airborne magnetic survey would resolve high-frequency low-amplitude anomalies over the whole structure, including those identified in the centre of the structure by the ground magnetic survey. Modern seismic data over the structure could image the deformation to the margin, as could a marine gravity survey, and would confirm whether or not the structure extends into Hamelin Pool (where at present there are no seismic or gravity data). Further drilling is needed to confirm the distribution of the Woodleigh Formation, particularly south of the centre of the structure, and the extent and nature of the central uplift. In addition, new samples would allow further analyses to determine the age of the impact.

## Acknowledgements

We thank Alex Bevan (Western Australian Museum) and Andrew Glikson (Australian National University) for their useful comments on the manuscript, and Mick Claussen at Woodleigh Station who was particularly helpful during the fieldwork.

## References

- CISOWSKI, S. M., and FULLER, M., 1978, The effects of shock and magnetism of terrestrial rocks: *Journal of Geophysical Research*, v. 83, p. 3441–3458.
- CLARK, J. F., 1983, Magnetic survey data at meteoritic impact sites in North America: *Geomagnetic Services of Canada, Earth Physics Branch, Open Files*, 83-5, p. 1–32.
- CROSTELLA, A., 1995, Structural evolution and hydrocarbon potential of the Merlinleigh and Byro Sub-basins, Carnarvon Basin, Western Australia: *Western Australia Geological Survey, Report 45*, 36p.
- DENMAN, P. D., HOCKING, R. M., MOORE, P. S., WILLIAMS, I. R., and van de GRAAFF, W. J. E., 1985, Wooramel, W.A. Sheet SG 50-5: *Western Australia Geological Survey, 1:250 000 Geological Series*.
- DENTITH, M. C., BEVAN, A. W. R., BACKHOUSE, J., FEATHERSTONE, W. E., and KOEBERL, C., 1999, Yallalie: a buried structure of possible impact origin in the Perth Basin, Western Australia: *Geological magazine*, v. 136(6), p. 619–632.
- EDGAR, C. I., 1994, Nerren project, Carnarvon Basin, first and final surrender report E 09/576-588, E 09/597, 599-600; BHP Minerals Pty Ltd: *Western Australia Geological Survey, Statutory mineral exploration report, Item 7508 A40842* (unpublished).
- GHORI, K. A. R., 1999, Silurian–Devonian petroleum source-rock potential and thermal history, Carnarvon Basin, Western Australia: *Western Australia Geological Survey, Report 72*, 88p.
- GIBSON, H. J., 2000, Thermal history reconstruction in Carnarvon Basin wells Candace 1, Pendock 1, Wandagee 1, Woodleigh 2A and Echo Bluff 1 using apatite fission track analysis and vitrinite reflectance: *Western Australia Geological Survey, Statutory petroleum exploration report, S31450 A1* (unpublished).
- GLIKSON, A. Y., (editor), 1996, Australian impact structures: *Australian Geological Survey Organisation, Journal of Australian Geology and Geophysics, Thematic issue*, v. 16, no. 4, p. 371–625.
- GLIKSON, A. Y., MERNAGH, T. P., PIRAJNO, F., MORY, A. J., and IASKY, R. P., in prep., Woodleigh multi-ring impact structure, Western Australia: geochemical meteoritic signatures and differential volatilisation/condensation: *Meteoritics*.
- GORTER, J. D., NICOLL, R. S., and FOSTER, C. N., 1994, Lower Palaeozoic facies in the Carnarvon Basin, Western Australia: stratigraphy and hydrocarbon prospectivity, in *The sedimentary basins of Western Australia edited by P. G. PURCELL and R. R. PURCELL: Petroleum Exploration Society of Australia Symposium, Perth, W.A., 1994, Proceedings*, p. 569–588.
- GRIEVE, R. A. F., and PESONEN, L. J., 1992, The terrestrial impact cratering record: *Tectonophysics*, 216, p. 1–30.
- GRIEVE, R. A. F., and PESONEN, L. J., 1996, Terrestrial impact craters: their spatial and temporal distribution and impacting bodies: *Earth, Moon and Planets*, 72, p. 357–376.
- GRIEVE, R. A. F., and PILKINGTON, M., 1996, The signature of terrestrial impacts: *Australian Geological Survey Organisation, Journal 16/4*, p. 399–420.
- HART, R., HARGRAVES, R. B., ANDREOLI, M. A. G., and DOUCOUR, C. M., 1995, Magnetic anomaly near the center of the Vredefort structure: Implications for impact-related magnetic signatures: *Geology*, v. 23, p. 277–280.
- HENKEL, H., and REIMOLD, W. U., 1996, Integrated gravity and magnetic modelling of the Vredefort impact structure — reinterpretation of the Witwatersrand Basin as an erosional remnant of an impact basin: South Africa, University of Witwatersrand, *EGRU Information Circular 299*, 89p.
- HOCKING, R. M., 1991, The Silurian Tumbalagooda Sandstone, Western Australia: *Western Australia Geological Survey, Report 27*, 124p.
- HOCKING, R. M., MOORS, H. T., and van de GRAAFF, W. J. E., 1987, Geology of the Carnarvon Basin, Western Australia: *Western Australia Geological Survey, Bulletin 133*, 289p.
- IASKY, R. P., and MORY, A. J., 1999, Geology and petroleum potential of the Gascoyne Platform, Southern Carnarvon Basin, Western Australia: *Western Australia Geological Survey, Report 69*, 46p.
- IASKY, R. P., MORY, A. J., GHORI, K. A. R., and SHEVCHENKO, S. I., 1998a, Structure and petroleum potential of the southern Merlinleigh Sub-basin, Carnarvon Basin, Western Australia: *Western Australia Geological Survey, Report 61*, 63p.
- IASKY, R. P., MORY, A. J., and SHEVCHENKO, S. I., 1998b, A structural interpretation of the Gascoyne Platform, Southern Carnarvon Basin, Western Australia, in *The sedimentary basins of Western Australia 2 edited by P. G. PURCELL and R. R. PURCELL: Petroleum Exploration Society of Australia Symposium, Perth, W.A., 1998, Proceedings*, p. 589–598.
- LAYTON AND ASSOCIATES, 1981, Well completion report EP169: Woodleigh 1981/2 south Carnarvon Basin, W.A.: *Western Australia Geological Survey, Statutory petroleum exploration report, S2075 A1* (unpublished).
- LAYTON AND ASSOCIATES, 1982, TRs 7865H–7868H: Yaringa, south Carnarvon Basin, W.A., report on bore 1982/1: *Western Australia Geological Survey, Statutory mineral exploration report, Item 7425 A35956* (unpublished).
- McWHAE, J. R. H., PLAYFORD, P. E., LINDNER, A. W., GLENISTER, B. F., and BALME, B. E., 1958, The stratigraphy of Western Australia: *Geological Society of Australia, Journal*, v. 4, 162p.
- MILTON, D. J., BARLOW, B. C., BROWN, A. R., MOSS, F. J., MANWARING, E. A., SEDMIK, E. C. E., YOUNG, G. A., and VAN SON, J., 1996, Gosses Bluff — a latest Jurassic impact structure, central Australia. Part 2: seismic, magnetic and gravity studies: *Australian Geological Survey Organisation, Journal 16/4*, p. 487–527.
- MORGAN, J., WARNER, M., THE CHICXULUB WORKING GROUP, BRITTAN, J., BUFFLER, R., CAMARGO, A., CHRISTESON, G., DENTON, P., HILDEBRAND, A., HOBBS, R., MACINTYRE, H., MACKENZIE, G., MAGUIRE, P., MARIN, L., NAKAMURA, Y., PILKINGTON, M., SHARPTON, V., SNYDER, D., SUAREZ, G., and TREJO, A., 1997, Size and morphology of the Chicxulub impact crater: *Nature*, v. 390, no. 6659, p. 472–476.

- MORGAN, J., and WARNER, M., 1999a, Chicxulub: The third dimension of a multi-ring impact basin: *Geology*, v. 27, p. 407–410.
- MORGAN, J., and WARNER, M., 1999b, Morphology of the Chicxulub impact: peak-ring crater or multi-ring basin? *in* Large meteorite impacts and planetary evolution II *edited by* B. O. DRESSLER and V. L. SHARPTON: Geological Society of America, Special Paper 339, p. 281–290.
- MORY, A. J., IASKY, R. P., GLIKSON, A. Y., and PIRAJNO, F., 2000, Woodleigh, Carnarvon Basin, Western Australia: a new 120 km-diameter impact structure: *Earth and Planetary Science Letters*, v. 177(1–2), p. 119–128.
- MORY, A. J., IASKY, R. P., and SHEVCHENKO, S. I., 1998a, The Coolcalalaya Sub-basin: a forgotten frontier 'between' the Perth and Carnarvon Basins, W.A., *in* The sedimentary basins of Western Australia 2 *edited by* P. G. PURCELL and R. R. PURCELL: Petroleum Exploration Society of Australia Symposium, Perth, W.A., 1998, Proceedings, p. 613–622.
- MORY, A. J., NICOLL, R. S., and GORTER, J. D., 1998b, Lower Palaeozoic correlations and thermal maturity, Carnarvon Basin, W.A., *in* The sedimentary basins of Western Australia 2 *edited by* P. G. PURCELL and R. R. PURCELL: Petroleum Exploration Society of Australia Symposium, Perth, W.A., 1998, Proceedings, p. 599–611.
- MORY, A. J., PIRAJNO, F., GLIKSON, A. Y., and COKER, J. (compilers), *in prep.*, GSWA Woodleigh 1, 2, and 2A well completion report, Woodleigh impact structure, Southern Carnarvon Basin, Western Australia: Western Australia Geological Survey, Record 2001/6.
- PIKE, R. J., 1985, Some morphologic systematics of complex impact structures: *Meteoritics*, v. 20, p. 49–68.
- PILKINGTON, M., and GRIEVE, R. A. F., 1992, The geophysical signature of terrestrial impact structures: *Reviews of Geophysics*, 30, p. 161–181.
- PILKINGTON, M., HILDEBRAND, A. R., and ORTIZ-ALEMAN, C., 1994, Gravity and magnetic field modeling and structure of the Chicxulub crater, Mexico: *Journal of Geophysical Research*, v. 99, p. 13147–13162.
- PIRAJNO, F., and GLIKSON, A. Y., 1998, Shoemaker Impact Structure (formerly Teague Ring Structure), Western Australia: *The Australian Geologist*, v. 106, p. 16–18.
- PLADO, J., PERSONEN, L. J., and PUURA, V., 1999, Effects of erosion on gravity and magnetic signatures of complex impact structures: Geophysical modeling and applications, *in* Large meteorite impacts and planetary evolution II *edited by* B. O. DRESSLER and V. L. SHARPTON: Geological Society of America, Special Paper 339, p. 229–239.
- PLAYFORD, P. E., and CHASE, R. E., 1955, Carnarvon Basin waterbores: Western Australia Geological Survey, Statutory petroleum exploration report, S126 A1 (unpublished).
- SCOTT, R. G., PILKINGTON, M., and TANCZYK, E. I., 1997, Magnetic investigations of the West Hawk, Deep Bay and Clearwater impact structures, Canada: *Meteoritics and Planetary Science*, v. 32, p. 293–308.
- SHARPTON, V. L., MARIN, L. E., CARNEY, J. L., LEE, S., RYDER, G., SCHURAYTZ, B. C., SIKORA, O., and SPUDIS, P. D., 1996, A model of the Chicxulub impact basin based on evaluation of geophysical data, well logs and drill core samples: Geological Society of America. Special Paper 307, p. 55–74.
- SHOEMAKER, E. M., and SHOEMAKER, C. S., 1996, The Proterozoic impact record of Australia: Australian Geological Survey Organisation, *Journal* 16/4, p. 379–398.
- TELFORD, W. M., GELDART, L. P., and SHERIFF, R. E., 1990, *Applied geophysics*, 2nd edition: Cambridge University Press, 770p.
- TREWIN, N. H., 1993a, Mixed aeolian sandsheet and fluvial deposits in the Tumblagooda Sandstone (Late Silurian) of Western Australia: Geological Society of London, Special Publication, v. 73, p. 219–230.
- TREWIN, N. H., 1993b, Controls on fluvial deposition in mixed fluvial and aeolian facies within the Tumblagooda Sandstone (?Late Silurian) of Kalbarri, Western Australia: *Sedimentary Geology*, v. 85, p. 387–400.
- van de GRAAFF, W. J. E., HOCKING, R. M., and BUTCHER, B. P., 1983, Yaringa, W.A. Sheet SG 50-9: Western Australia Geological Survey, 1:250 000 Geological Series.
- WILLIAMS, G. E., SCMIDT, P. W., and BOYD, D. M., 1996, Magnetic signature and morphology of the Acraman impact structure, South Australia: Australian Geological Survey Organisation, *Journal* 16/4, p. 431–442.
- YASIN, A. R., and MORY, A. J., 1999a, Coburn 1 well completion report, Gascoyne Platform, Carnarvon Basin, Western Australia: Western Australia Geological Survey, Record 1999/5, 99p.
- YASIN, A. R., and MORY, A. J., 1999b, Yaringa East 1 well completion report, Gascoyne Platform, Carnarvon Basin, Western Australia: Western Australia Geological Survey, Record 1999/7, 53p.

## Appendix 1

## Summary of wells and bores that penetrated below the Cretaceous horizon in the Woodleigh area

No. <sup>(a)</sup>	Well or bore	Latitude (S)	Longitude (E)	Total depth (m)	Stratigraphy	Reference <sup>(b)</sup>
1	BHP ND1	26°19'00"	114°51'00"	375.5	K/S/Ot	Item 7508
2	BHP ND2	26°23'40"	114°41'45"	438.6	K/S/Ot	Item 7508
3	CRAE GRH1	25°40'32"	114°49'29"	224	K/Dk	Item 7465 A36058
4	Carpentaria CB2	26°29'55"	114°39'30"	160	K/?Jw or S/Ot	Item 11083 A58930
5	Carpentaria CB3	26°29'05"	114°47'10"	170	K/?Jw or S/Ot	Item 11083 A58930
6	Carpentaria CB4	26°03'35"	114°31'30"	286	K/Jw	Item 11083 A58930
7	GSWA Woodleigh 1	26°03'24"	114°39'51"	333	K/p €	S20565
8	GSWA Woodleigh 2A	26°03'28"	114°31'34"	618	K/Jw/?S	S20565
9	Hamelin Pool 1	26°01'35"	114°12'23"	1 595	K/Ds/Dk/Df/S/Ot	S440 V1
10	Hamelin Pool 2	26°08'55"	114°21'24"	1 219	K/Ds/Dk/Df/S	S440 V2
11	SEC SB1	26°38'30"	114°38'55"	184	K/Ot	Rockwater Pty Ltd (1982) <sup>(c)</sup>
12	SEC SB3A	26°12'25"	114°56'50"	240	K /?Ot	Rockwater Pty Ltd (1982) <sup>(c)</sup>
13	Utah G1	25°52'45"	115°03'15"	85	Q/?	Item 7405 A35905
14	Utah SP218	26°39'25"	114°50'15"	122	K /?Ot	Item 7405 A35904
15	Utah TN2	26°10'40"	115°14'40"	234	Cz/?Ot	Item 7405 A35907
16	Utah TN3	26°10'40"	115°11'50"	205	Cz/?Ot	Item 7405 A35907
17	Utah TN4	26°10'40"	115°07'50"	171	Cz/?Ot	Item 7405 A35907
18	Utah TN5	26°10'45"	115°02'50"	203	Cz/?Ot	Item 7405 A35907
19	Utah TN6	26°10'45"	115°00'45"	144	Cz/?Ot	Item 7405 A35907
20	Utah TS11	26°17'15"	115°00'35"	252	Q /?Ot	Item 7405 A35906
21	Utah TS14	26°27'15"	114°57'05"	192	Cz/?Ot	Item 7405 A35906
22	Utah W1	26°27'15"	114°58'55"	160	Q/K/?	Item 7405 A35906
23	Utah W2	26°02'40"	115°03'05"	91	Q /?Ot	Item 7405 A35906
24	Utah W3	26°01'40"	115°12'30"	171	Q/?P	Item 7405 A35906
25	Western Colliers YR11B	26°27'55"	115°00'10"	150	C z/?P	Item 7472 A36075
26	Woodleigh 1981/2	26°03'22"	114°40'02"	189	K/p €	S6169 A2
27	Woodleigh 1982/1	26°15'01"	114°51'12"	207	K/?Jw/S	Item 7425 A35956
28	Woodleigh water bore 1	26°03'30"	114°39'00"	279	K/Jw/?S	S126 A1
29	Woodleigh water bore 2	26°03'15"	114°42'45"	298	K/Jw	Woodleigh Station records
30	Woodleigh water bore 4A	26°12'10"	114°46'30"	244	K/Jw	Woodleigh Station records
31	Woodleigh water bore 7	26°07'45"	114°45'05"	235	K/Jw	S126 A1
32	Woodleigh water bore 9	26°10'05"	114°52'35"	183	K/Jw	S126 A1
33	Woodleigh water bore 10A	26°12'	114°40'	126	K/Jw	Woodleigh Station records
34	Yaringa 1	26°03'58"	114°21'35"	2 288	K/Ds/Dk/Df/S/Ot	S305
35	Yaringa East 1	25°53'41"	114°23'27"	829	K/Dn/Ds/Dk	S20339

**NOTES:** (a) No.: Numbers refer to drillholes on Figure 9  
 (b) Item and A numbers refer to open-file statutory mineral exploration reports held in the Western Australian Department of Minerals and Energy library, Perth  
 S numbers refer to open-file statutory petroleum exploration reports held in the Western Australian Department of Minerals and Energy library, Perth  
 (c) ROCKWATER PTY LTD, 1982, Dampier to Perth natural gas pipeline hydrostatic testing water supply, completion report for borefield BF 1 –BF 12: State Energy Commission of Western Australia (unpublished)

K:	undifferentiated Cretaceous	Df:	Lower Devonian Faure Formation
Jw:	Lower Jurassic Woodleigh Formation	S:	Silurian Dirk Hartog Group
P:	Permian	Ot:	Ordovician Tumbagoooda Sandstone
Dn:	Upper-Middle Devonian Nannyarra Sandstone	p €:	Precambrian
Ds:	Lower Devonian Sweeney Mia Formation	Q:	Quaternary
Dk:	Lower Devonian Kopke Sandstone	Cz:	Cainozoic

## Appendix 2

# Acquisition and processing of ground magnetic data

## Acquisition

A small reconnaissance survey was conducted over the centre of the structure with the objective of delineating any high-frequency anomalies associated with the impact. Gravity stations located by differential global positioning system (DGPS) were used as control points. Off-road, control points were determined using a Garmin handheld GPS unit.

Two Scintrex MP-3 magnetometers were used –one for field readings and the other for base-station measurements. Field readings were taken with the sensor at a constant height of 2 m.

For the regional traverse (Fig. 22) readings were taken at 100 m intervals. The location of readings between control points along this traverse was measured with both a vehicle odometer and a handheld GPS unit in order to minimize the error. The high-frequency 40 nT anomaly, 4 km east of GSWA Woodleigh 2A, was verified by re-measuring the anomaly with a 25 m station interval. A 2.5 km part of the regional traverse, centred on GSWA Woodleigh 1, was also re-measured with a 25 m station interval (Fig. 21).

Data along the off-road traverses were located only with the aid of handheld GPS units. Control points were recorded at 1 km intervals, and readings were taken at approximately 25 m intervals. Although the 25 m intervals were measured by pacing, tests had proved that, over 100 m intervals, this method was accurate to within 5 m. Hence, over the 1 km distance between GPS control points, an error of up to 50 m is expected. The positions of the magnetic field measurements were interpolated between control points to evenly spread any positional error over the length of the traverse. Taking into account the errors associated with locations and bearings measured with the handheld GPS unit, we estimate a maximum error of 10% for the location of magnetic field measurements.

All magnetic field measurements were monitored and apparent high gradients in the field were always verified to eliminate noise.

## Processing

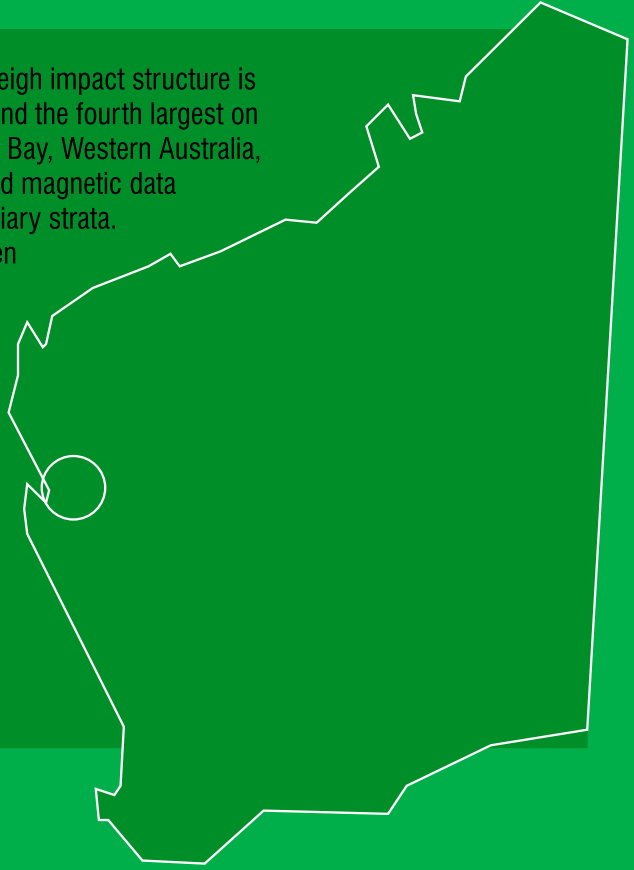
The following processing steps were carried out:

1. The data were downloaded from the Scintrex MP-3 magnetometers.
2. The files were edited using a text editor to ensure that they were organized in a format that could be easily processed using inhouse software and Microsoft Excel.
3. The base-station data were plotted and despiked.
4. A 3rd or 4th order polynomial curve was fitted to the despiked base-station data to mathematically represent the diurnal variation.
5. The diurnal-variation equation was used to correct the field data.
6. Station locations of the field data were interpolated between control points.
7. Data were adjusted to correct miss-ties at line intersections –because of the positional error the adjustment is only approximate.

At an estimated diameter of 120 km, the multi-ring Woodleigh impact structure is arguably the largest proven impact structure in Australia and the fourth largest on Earth. Centred about 50 km east of Hamelin Pool in Shark Bay, Western Australia, the impact structure is best shown by gravity, seismic, and magnetic data because it is buried beneath up to 600 m of Jurassic–Tertiary strata.

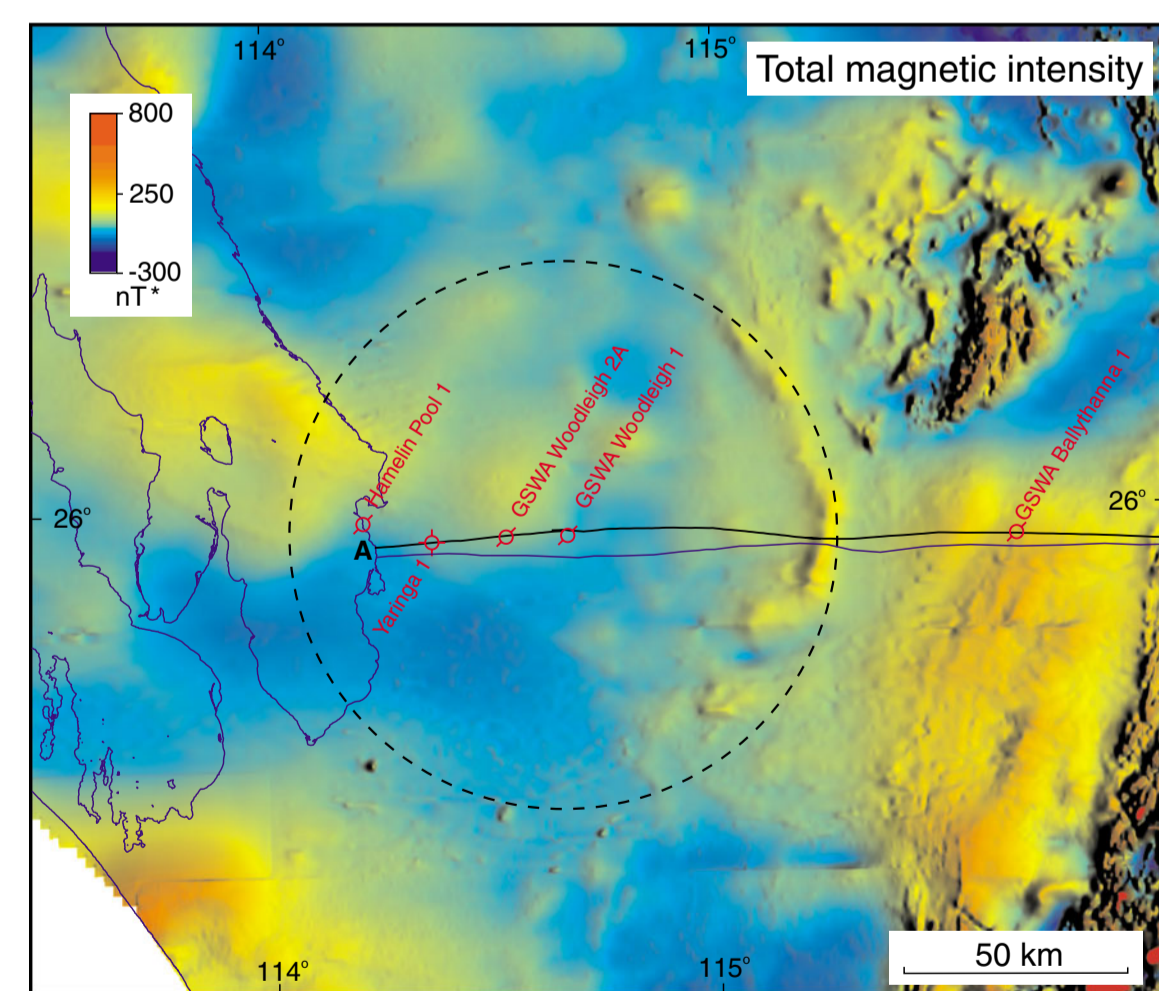
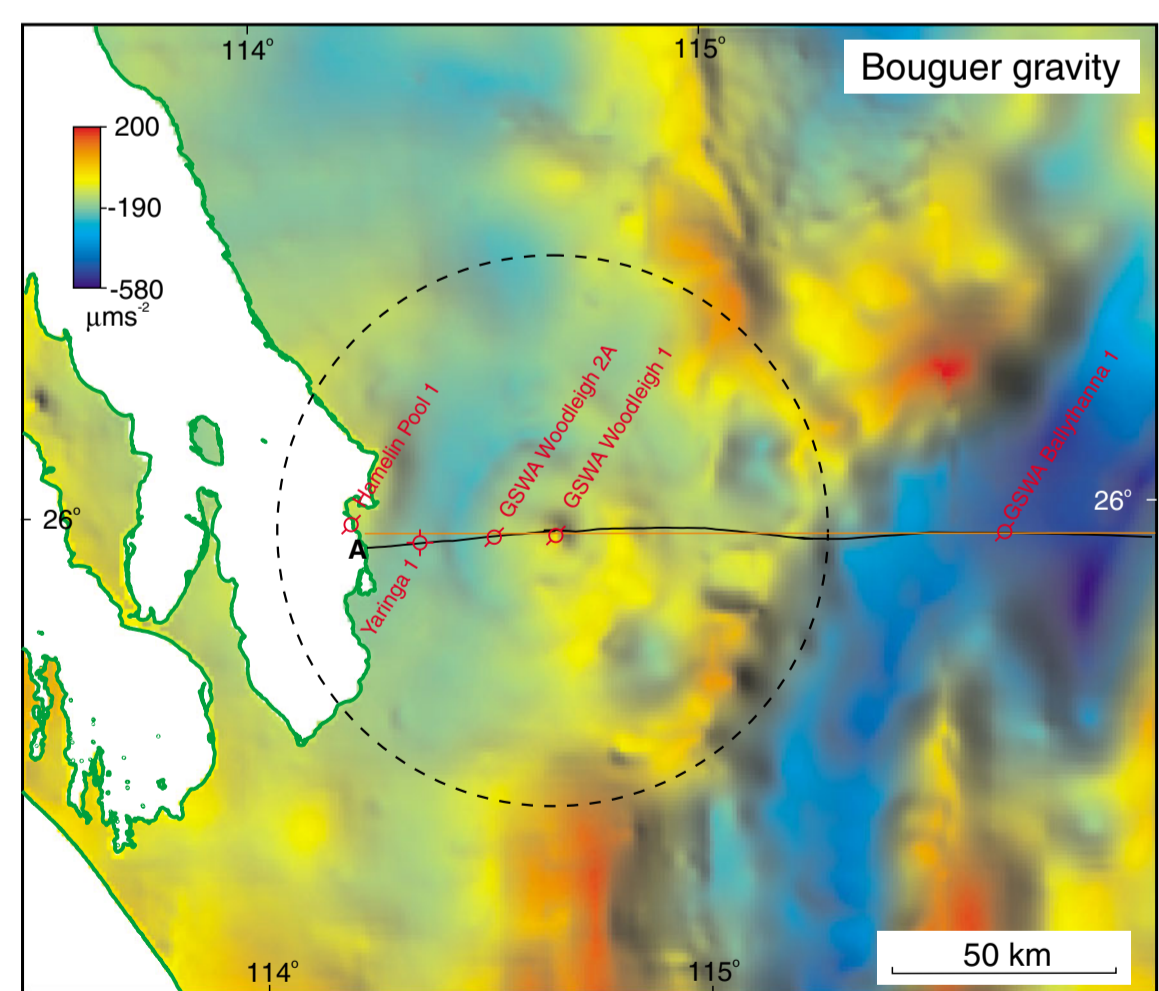
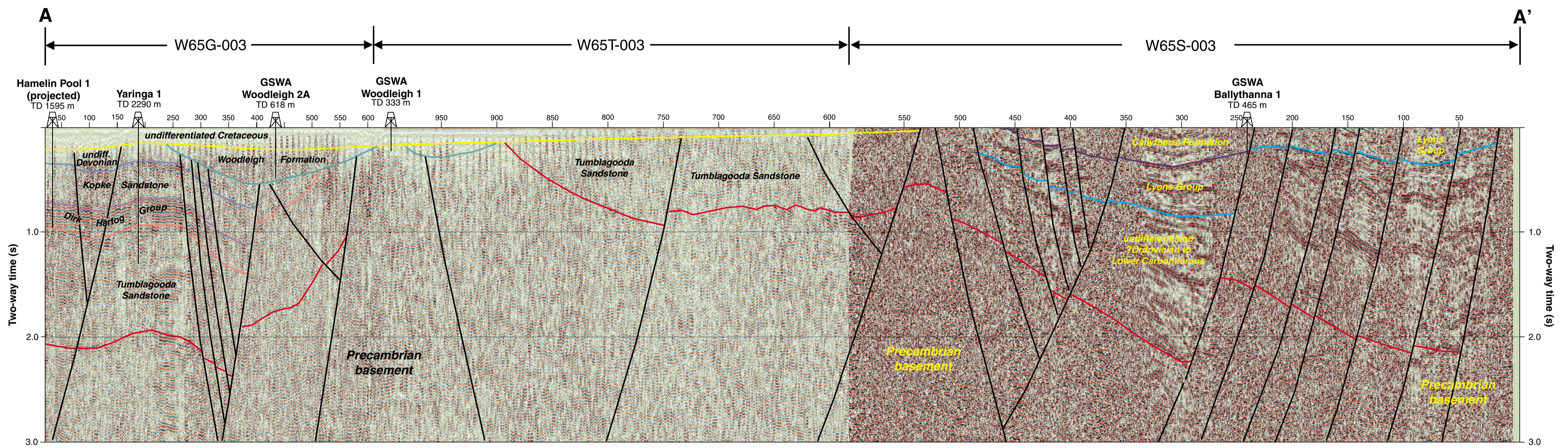
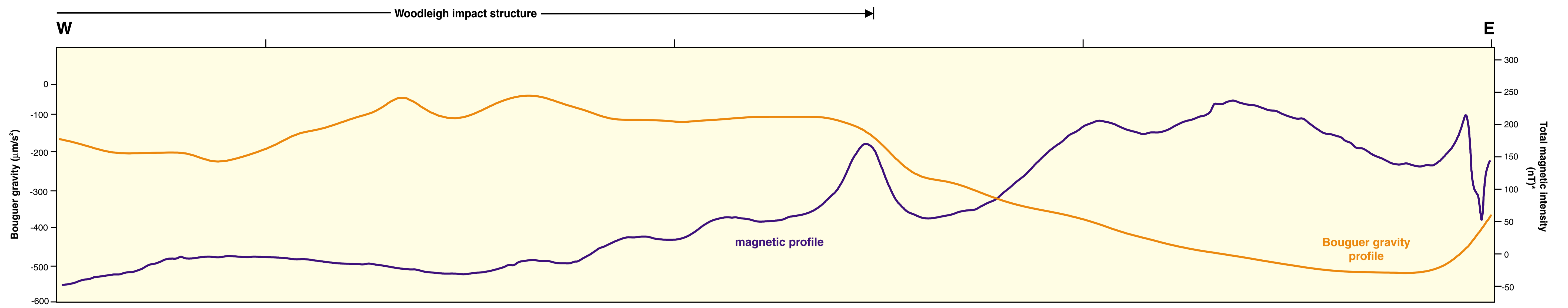
Regional stratigraphy constrains the age of impact between the Middle Devonian and Early Jurassic.

This Report focuses on the interpretation of the gravity, seismic, and magnetic data to determine the morphology of the structure. Concentric gravity highs and lows within the structure correspond to troughs and ridges on seismic data. As in other impact structures, the most intense deformation is in the inner third of the structure with only minor deformation to the outer rim. The outer limit of the structure is shown by the abrupt truncation of the northerly trending Wandagee and Ajana Ridges, an arcuate magnetic anomaly to the east, and minor drainage features.



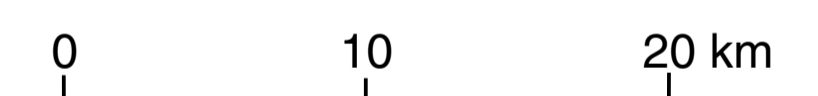
**Further details of geological publications and maps produced by the Geological Survey of Western Australia can be obtained by contacting:**

**Information Centre  
Department of Minerals and Energy  
100 Plain Street  
East Perth WA 6004  
Phone: (08) 9222 3459 Fax: (08) 9222 3444  
[www.dme.wa.gov.au](http://www.dme.wa.gov.au)**

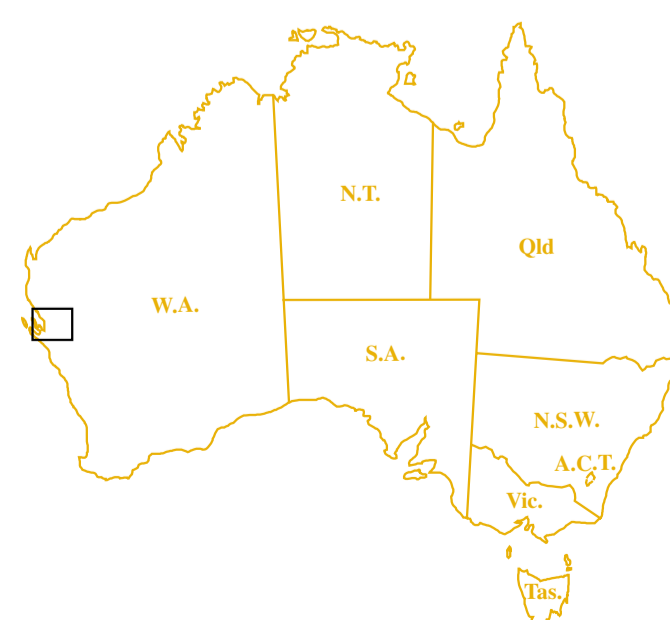


**Stratigraphy**

Undifferentiated Cretaceous	
Woodleigh Formation	
Callytharra Formation	
Lyons Group	
undifferentiated Devonian	undifferentiated
Kopke Sandstone	?Ordovician
Dirk Hartog Group	to Lower
Tumblagooda Sandstone	Carboniferous
Precambrian basement	



- Inferred outer limit of Woodleigh impact structure
- Seismic line location
- Gravity profile
- Airborne magnetic survey flight line
- Stratigraphic well
- Petroleum exploration well, dry

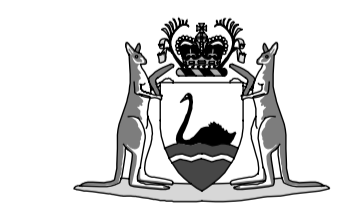


Compiled by R. P. Iasky, A. J. Mory, and K. A. Blundell, 2001

Published by the Geological Survey of Western Australia. Digital copies of this map are available from the Information Centre, Department of Minerals and Energy, 100 Plain Street, East Perth, W.A. 6004. Phone (08) 9222 3459, Fax (08) 9222 3444

The recommended reference for this plate is: IASKY, R. P., MORY, A. J., and BLUNDELL, K. A., 2001. Geophysical profiles across the Woodleigh impact structure, in The geophysical interpretation of the Woodleigh impact structure, Southern Carnarvon Basin, Western Australia. Western Australia Geological Survey, Report 79, Plate 1

© Western Australia 2001



GOVERNMENT OF WESTERN AUSTRALIA  
HON. OLIVE GROOM M.L.A.  
MINISTER FOR STATE DEVELOPMENT, TOURISM,  
SMALL BUSINESS, GOLDFIELDS-ESPERANCE



DEPARTMENT OF MINERALS AND ENERGY  
L.C. RANFORD, DIRECTOR GENERAL



GEOLOGICAL SURVEY OF WESTERN AUSTRALIA  
T.M. GRIFFIN, DIRECTOR

GEOLOGICAL SURVEY OF WESTERN AUSTRALIA  
REPORT 79 PLATE 1

**GEOLOGICAL PROFILES  
ACROSS THE  
WOODLEIGH IMPACT STRUCTURE**